

FILTERING AND MULTI-PORT DIRECTIONAL COUPLERS

CHEW HOO BENG

**A project report submitted in partial fulfilment of the
requirements for the award of the degree of
Bachelor (Hons) of Electronic and Communications Engineering**

**Faculty of Engineering and Science
Universiti Tunku Abdul Rahman**

MAY 2012

DECLARATION

I hereby declare that this project report is based on my original work except for citations and quotations which have been duly acknowledged. I also declare that it has not been previously and concurrently submitted for any other degree or award at UTAR or other institutions.

Signature : _____

Name : Chew Hoo Beng

ID No. : 08UEB04682

Date : _____

APPROVAL FOR SUBMISSION

I certify that this project report entitled “**FILTERING AND MULTI-PORT DIRECTIONAL COUPLERS**” was prepared by **Chew Hoo Beng** has met the required standard for submission in partial fulfilment of the requirements for the award of Bachelor of Electronic and Communications Engineering (Hons.) at Universiti Tunku Abdul Rahman.

Approved by,

Signature : _____

Supervisor: Dr. Lim Eng Hock

Date : _____

The copyright of this report belongs to the author under the terms of the copyright Act 1987 as qualified by Intellectual Property Policy of University Tunku Abdul Rahman. Due acknowledgement shall always be made of the use of any material contained in, or derived from, this report.

© 2012, Chew Hoo Beng. All right reserved.

Specially dedicated to
my beloved parents and friends.

ACKNOWLEDGEMENTS

First of all, I would like to thank my supervisor, Dr Lim Eng Hock, for his valuable guidance and advice throughout all the stages of this research project. His stimulating conversation and discussion have been a constant source of valuable ideas in the development of these new devices. He is always ready to give consultation all the time.

Besides that, I would like to acknowledge to my seniors and friends who are and have been doing their research under the supervision of my project supervisor. They have shared their knowledge and experience with me and are willing to render a helping hand whenever I faced problems.

I would like to thank UTAR for preparing such a good environment for me. Finally, I am thankful to the laboratory assistants who helped me throughout the research project.

FILTERING AND MULTI-PORT DIRECTIONAL COUPLERS

ABSTRACT

Directional coupler is a four-port device that couples the input power at Port 1 to Port 2 (Through Port) and Port 3 (Coupled Port), but not to Port 4 (Isolation Port). Nowadays, these components are essential to all communication systems as they play an important role in the monitoring and measurement of signal samples within an assigned operating frequency. The first part of project is to propose a wideband directional coupler with high roll-off performance. A multi-port directional coupler with two coupled ports is presented in the second part. Microwave Office and High Frequency Structure Simulator (HFSS) have been used to simulate and optimize the amplitude and phase responses of the directional coupler. Finally, the proposed directional couplers are fabricated and measured using the Vector Network Analyzer (VNA) in the laboratory. The simulation and experimental results are compared, showing good agreement. Case studies have been conducted on the proposed directional couplers in order to study the effects of different design parameters. Discussion and recommendations have been made after each case study. The proposed directional couplers are novel and intended to be published in the international top journals.

TABLE OF CONTENTS

| | |
|--|--------------|
| DECLARATION | ii |
| APPROVAL FOR SUBMISSION | iii |
| ACKNOWLEDGEMENTS | vi |
| ABSTRACT | vii |
| TABLE OF CONTENTS | viii |
| LIST OF TABLES | xi |
| LIST OF FIGURES | xii |
| LIST OF SYMBOLS / ABBREVIATIONS | xviii |

CHAPTER

| | | |
|----------|--|----------|
| 1 | INTRODUCTION | 1 |
| | 1.1 Background | 1 |
| | 1.2 Issues | 3 |
| | 1.3 Research Aim and Objectives | 5 |
| | 1.4 Project Motivation | 6 |
| | 1.5 Thesis Overview | 6 |
| 2 | LITERATURE REVIEW | 8 |
| | 2.1 Background | 8 |
| | 2.2 Directional Coupler | 8 |
| | 2.2.1 Coupled-line Directional Coupler | 13 |
| | 2.2.2 Theory | 13 |
| | 2.3 Recent Developments | 15 |

| | | |
|----------|---|-----------|
| 2.3.1 | Directional Coupler Loaded With Shunt Inductors | 16 |
| 2.3.2 | Branch line coupler with $\lambda/4$ open circuited coupled-lines | 18 |
| 2.3.3 | Wilkinson power divider incorporating quasi-elliptic filters | 21 |
| 2.4 | Introduction of Simulation Tools | 23 |
| 2.4.1 | High Frequency Structure Simulator | 23 |
| 2.4.2 | Microwave Office | 24 |
| 3 | FILTERING DIRECTIONAL COUPLER | 25 |
| 3.1 | Background | 25 |
| 3.2 | Bandpass-filtering Directional Coupler | 25 |
| 3.2.1 | Configuration | 28 |
| 3.2.2 | Transmission Line Model | 30 |
| 3.2.3 | Results | 31 |
| 3.2.4 | Parametric Analysis | 35 |
| 3.3 | Five-mode Filtering Directional Coupler | 54 |
| 3.3.1 | Configuration | 54 |
| 3.3.2 | Results | 55 |
| 3.4 | Discussion | 56 |
| 4 | MULTI-PORT DIRECTIONAL COUPLER | 59 |
| 4.1 | Background | 59 |
| 4.2 | Four-port Directional Coupler | 59 |
| 4.2.1 | Configuration | 60 |
| 4.2.2 | Transmission Line Model | 61 |
| 4.2.3 | Results | 62 |
| 4.3 | Six-port Directional Coupler | 63 |
| 4.3.1 | Configuration | 64 |
| 4.3.2 | Transmission Line Model | 66 |
| 4.3.3 | Results | 67 |

| | | |
|----------|--|-----------|
| 4.3.4 | Parametric Analysis | 70 |
| 4.4 | Discussion | 90 |
| 5 | FUTURE WORK AND RECOMMENDATIONS | 92 |
| 5.1 | Achievements | 92 |
| 5.2 | Future Work | 93 |
| 5.3 | Conclusion | 93 |
| | REFERENCES | 94 |

LIST OF TABLES

| TABLE | TITLE | PAGE |
|--------------|---|-------------|
| 1.1 | Frequency band designation. | 1 |
| 1.2 | Microwave frequency band designation. | 2 |
| 2.1 | Port definition of directional coupler. | 11 |
| 3.1 | Comparison of the experiment, HFSS simulation, and TLM modelling results. | 33 |
| 4.1 | Comparison of HFSS simulation and TLM modelling. | 63 |
| 4.2 | Comparison of the experiment, HFSS simulation, and TLM modelling. | 68 |

LIST OF FIGURES

| FIGURE | TITLE | PAGE |
|--------|---|------|
| 1.1 | General microstrip structure. | 4 |
| 2.1 | Power flows in conventional directional coupler. | 10 |
| 2.2 | Directional coupler with port 2 as input port. | 10 |
| 2.3 | Conventional coupled line directional coupler. | 13 |
| 2.4 | Even- and odd-mode characteristic impedance design data for the coupled microstrip lines. | 15 |
| 2.5 | Schematics of a conventional microstrip directional coupler. | 16 |
| 2.6 | Schematics of the proposed microstrip directional coupler with shunt inductors. | 16 |
| 2.7 | Fabricated 20-dB directional coupler with shunt inductors. | 17 |
| 2.8 | S-parameters of the directional coupler with shunt inductors. | 17 |
| 2.9 | Directivity and coupling levels of directional coupler with shunt inductors. | 18 |
| 2.10 | Circuit configuration for branch line coupler with $\lambda/4$ open circuited lines. | 19 |
| 2.11 | Structure and dimensions for the branch line coupler with $\lambda/4$ open circuited lines. | 19 |
| 2.12 | Return loss and isolation characteristics of the branch line coupler with $\lambda/4$ open circuited lines. | 20 |

| | | |
|------|---|----|
| 2.13 | Insertion loss, coupling characteristics, and phase differences of the branch line coupler with $\lambda/4$ open circuited lines. | 20 |
| 2.14 | Layout configuration for Wilkinson power divider incorporating quasi-elliptic filters. | 21 |
| 2.15 | Fabricated Wilkinson power divider incorporating quasi-elliptic filters. | 22 |
| 2.16 | Simulated and measured S-parameters of Wilkinson power divider incorporating quasi-elliptic filters. | 22 |
| 3.1 | Top-down view of proposed wideband bandpass filter. | 26 |
| 3.2 | S-parameter of the proposed bandpass filter. | 27 |
| 3.3 | Configuration of the proposed microstrip bandpass filtering directional coupler. | 29 |
| 3.4 | Prototype of the proposed bandpass filtering directional coupler. | 29 |
| 3.5 | Transmission line model of the proposed filtering directional coupler. | 30 |
| 3.6 | Simulated and measured amplitude responses of the filtering directional coupler. | 32 |
| 3.7 | Simulated and measured phase responses of the filtering directional coupler. | 32 |
| 3.8 | Amplitude responses of the experimental and TLM model. | 34 |
| 3.9 | Phase responses of the experimental and TLM model. | 34 |
| 3.10 | Effect of width w_1 on the filtering directional coupler. | 36 |
| 3.11 | Effect of width w_2 on the filtering directional coupler. | 37 |
| 3.12 | Effect of width w_3 on the filtering directional coupler. | 38 |

| | | |
|------|---|----|
| 3.13 | Effect of width w_4 on the filtering directional coupler. | 39 |
| 3.14 | Effect of width w_5 on the filtering directional coupler. | 40 |
| 3.15 | Effect of width w_6 on the filtering directional coupler. | 41 |
| 3.16 | Effect of width w_7 on the filtering directional coupler. | 42 |
| 3.17 | Effect of gap g_2 on the filtering directional coupler. | 43 |
| 3.18 | Effect of gap g_3 on the filtering directional coupler. | 44 |
| 3.19 | Effect of gap g_4 on the filtering directional coupler. | 45 |
| 3.20 | Effect of gap g_5 on the filtering directional coupler. | 46 |
| 3.21 | Effect of gap g_6 on the filtering directional coupler. | 47 |
| 3.22 | Effect of length l_1 on the filtering directional coupler. | 48 |
| 3.23 | Effect of length l_2 on the filtering directional coupler. | 49 |
| 3.24 | Effect of length l_3 on the filtering directional coupler. | 50 |
| 3.25 | Effect of length l_4 on the filtering directional coupler. | 51 |
| 3.26 | Effect of length l_5 on the filtering directional coupler. | 52 |
| 3.27 | Effect of length l_9 on the filtering directional coupler. | 53 |
| 3.28 | Top-down view of the five-mode filtering directional coupler | 54 |
| 3.29 | Amplitude responses of five-mode filtering directional coupler. | 56 |
| 3.30 | Cascading a multimode bandpass filter with a directional coupler. | 57 |

| | | |
|------|--|----|
| 3.31 | The proposed idea of the multimode filtering directional coupler. | 57 |
| 3.32 | Amplitude responses of the three- and five-mode filtering directional couplers. | 57 |
| 4.1 | Top-down view of the four-port directional coupler. | 60 |
| 4.2 | Transmission line model of the four-port directional coupler. | 61 |
| 4.3 | S-parameters of the four-port directional coupler. | 62 |
| 4.4 | Phase response of the four-port directional coupler. | 62 |
| 4.5 | Top-down view of the proposed six-port directional coupler. | 65 |
| 4.6 | Prototype of the proposed six-port directional coupler. | 65 |
| 4.7 | Transmission line model of the six-port directional coupler. | 66 |
| 4.8 | Amplitude responses of the HFSS simulation and experiment for the proposed six-port directional coupler. | 67 |
| 4.9 | Amplitude responses of the experiment and TLN model for the proposed six-port directional coupler. | 67 |
| 4.10 | Phase responses of the HFSS simulation and experiment for the six-port directional coupler. | 69 |
| 4.11 | Phase responses of the experiment and TLM model for the six- port directional coupler. | 69 |
| 4.12 | Effects of width w_1 on the reflection coefficient and isolation. | 70 |
| 4.13 | Effects of width w_1 on the insertion loss and coupling. | 71 |
| 4.14 | Effects of width w_2 on the reflection coefficient and isolation. | 72 |

| | | |
|------|--|----|
| 4.15 | Effects of width w_2 on the insertion loss and coupling. | 73 |
| 4.16 | Effects of width w_3 on the reflection coefficient and isolation. | 74 |
| 4.17 | Effects of width w_3 on the insertion loss and coupling. | 75 |
| 4.18 | Effects of gap g_1 on the reflection coefficient and isolation. | 76 |
| 4.19 | Effects of gap g_1 on the insertion loss and coupling. | 77 |
| 4.20 | Effects of gap g_2 on the reflection coefficient and isolation. | 78 |
| 4.21 | Effects of gap g_2 on the insertion loss and coupling. | 79 |
| 4.22 | Effects of length l_1 on the reflection coefficient and isolation. | 80 |
| 4.23 | Effects of length l_1 on the insertion loss and coupling. | 81 |
| 4.24 | Effects of length l_2 on the reflection coefficient and isolation. | 82 |
| 4.25 | Effects of length l_2 on the insertion loss and coupling. | 83 |
| 4.26 | Effects of length l_3 on the reflection coefficient and isolation. | 84 |
| 4.27 | Effects of length l_3 on the insertion loss and coupling. | 85 |
| 4.28 | Effects of length l_4 on the reflection coefficient and isolation. | 86 |
| 4.29 | Effects of length l_4 on the insertion loss and coupling. | 87 |
| 4.30 | Effects of length l_5 on the reflection coefficient and isolation. | 88 |

| | | |
|------|---|----|
| 4.31 | Effects of length l_5 on the insertion loss and coupling. | 89 |
| 4.32 | Two independent conventional directional couplers. | 90 |
| 4.33 | The proposed six-port directional coupler. | 90 |

LIST OF SYMBOLS / ABBREVIATIONS

| | |
|------------------|------------------------------------|
| λ | Wavelength, m |
| f | Frequency, Hz |
| c | Speed of light, m/s |
| ϵ_r | Dielectric constant |
| ϵ_{eff} | Effective dielectric constant |
| h | Thickness of substrate, mm |
| w | Width of microstrip lines, mm |
| Z_o | Characteristic impedance, Ω |
| Z_{in} | Input impedance, Ω |
| S_{11} | Reflection coefficient, dB |
| S_{21} | Insertion loss, dB |
| S_{31} | Insertion loss, dB |
| S_{41} | Isolation, dB |

CHAPTER 1

INTRODUCTION

1.1 Background

Microwave and RF wireless technologies have been extensively used in the modern world. They have many commercial and military applications, which include communications, radar, navigation, remote sensing, RF identification, broadcasting, automobiles, and so on. In general, microwave spectrum spreads from 300MHz to 30 GHz, which corresponds to a wavelength ranging from 1cm to 100cm. (Kai Chang, 2000). With the rapid advancement of mobile and wireless communications, nowadays, microwave components are highly demanded. Some of the important passive components are filter, power divider, coupler, balun, transformer, circulator, and so on. Table 1.1 and 1.2 below show the frequency band designation and microwave frequency band designation.

Table 1.1: Frequency band designation.

| Frequency Band | Designation | Typical Services |
|----------------|-----------------------------|--|
| 3-30 KHz | Very Low Frequency (VLF) | Navigation, sonar |
| 30-300 KHz | Low Frequency (LF) | Radio beacons, navigational aids |
| 300-3000 KHz | Medium Frequency (MF) | AM broadcasting, directional finding, maritime radio |

| | | |
|-------------|------------------------------|--|
| 3-30 MHz | High Frequency (HF) | Telephone, telegraph, facsimile |
| 30-300 MHz | Very High Frequency (VHF) | Television, FM Broadcast, air-traffic control |
| 300-3000MHz | Ultra High Frequency (UHF) | Television, satellite communications |
| 3- 30 GHz | Super High Frequency (SHF) | Airborne radar, microwave links, common-carrier land mobile communication, satellite communication |
| 30-300GHz | Extreme High Frequency (EHF) | Radar, experimental |

Obtained from: http://media.wiley.com/product_data/excerpt/11/07803603/0780360311.pdf

Table 1.2: Microwave frequency band designation.

| Frequency | Microwave band designation | |
|----------------|----------------------------|-----|
| | Old | New |
| 500 – 1000 MHz | VHF | C |
| 1-2 GHz | L | D |
| 2-3 GHz | S | E |
| 3-4 GHz | S | F |
| 4-6 GHz | C | G |
| 6-8 GHz | C | H |
| 8-10 GHz | X | I |
| 10-12.4 GHz | X | J |
| 12.4-18 GHz | Ku | J |
| 18-20 GHz | K | J |
| 20-26.5 GHz | K | K |
| 26.5-40 GHz | Ka | K |

Obtained from: http://media.wiley.com/product_data/excerpt/11/07803603/0780360311.pdf

The great interest in microwave engineering arises for a variety of reasons. During the World War II, microwave engineering was also known as radar (Radio Detection and Ranging) engineering because of the great stimulus given to the development of microwave systems. High resolution radars are capable of detecting and locating enemy planes and ships. (Geoffrey Hyde, 1998). However, in the recent years, microwave frequencies have also come into widespread use in communication link.

In addition, various types of designs and specifications of microwave components are available and can be found on IEEE Xplore database. These publications continue to increase widely. Meanwhile, research and implementation on directional couplers are done in this project.

1.2 Issues

Generally, couplers are components that are used to combine or divide signals. They are widely used in antenna feeds, frequency discriminators, balanced mixers, modulators, balanced amplifiers, phase shifters, automatic signal level control, signal monitoring and many other applications. (Kai Chang, 2000). Various types of directional couplers have been designed according to different operating frequencies. It includes dual-band and multi-band directional couplers. There are applications in which wide bandwidth is preferable because it allows more components to share the same spectrum simultaneously.

In the 40s, variety of directional couplers were invented and characterized at the MIT Radiation Laboratory (Pozar, 1998). These include Bethe-hole coupler, multi-hole directional coupler, and various types of couplers using coaxial probes. In the mid-50s to 60s, many of these directional couplers were reinvented using stripline and microstrip technologies due to its easy implementation and integration. Microstrip technology is used in this project because it has many advantages such as

low in cost, small in size, the absence of critical matching and cut-off frequency and the ease of active device integration. Moreover, it consists of a thin-film strip in intimate contact with one side of a flat dielectric substrate with a similar thin-firm ground-plane conductor on the other side of the substrate. It can be fabricated by photolithographic processes.

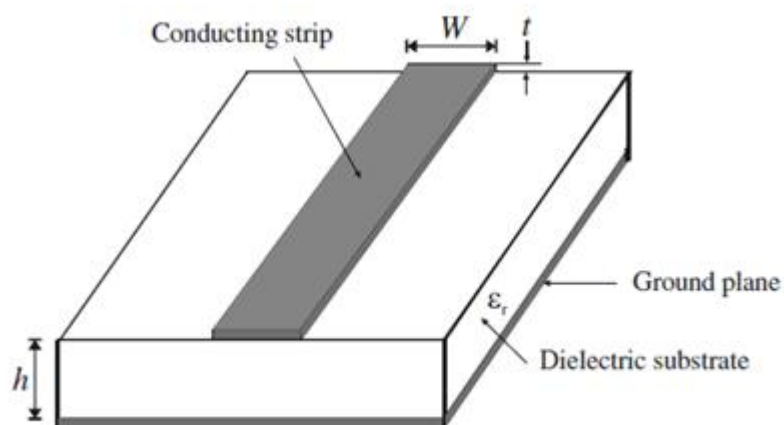


Figure 1.1: General microstrip structure.

Figure 1.1 shows the cross section view of a microstrip. It consists of a conductive microstrip line and a ground plane that are separated by a substrate. W , t and h represent the width, thickness and, height respectively. ϵ_r is the dielectric constant of the substrate. In fact, microstrip has major advantages over stripline and waveguide where all the active components can be mounted on top of the substrate. Hence, it is a convenient form of transmission line structure that is used for probe measurement of voltage, current, and waves.

Besides that, most microwave and RF systems were designed to operate with characteristic impedance of 50Ω . Characteristic impedance is the ratio of the amplitude of a single pair of voltage and current waves propagating along the microstrip line without reflections. It is important as it affects the reflection coefficient, S_{11} , which is also known as return loss - signal loss due to reflection at a discontinuity or impedance mismatch of a device. In order to minimize return loss, the characteristic impedance of a designed microstrip must be equal to the input impedance of the system which is usually 50Ω .

1.3 Research Aim and Objectives

The main objective of this project is to propose and construct a new microstrip directional coupler that offers better performances. Stable, flat and wide bandwidth, as well as high selectivity, are among the targets to be achieved in a directional coupler.

The first proposed idea is to design a multimode single-layered microstrip directional coupler with high selectivity. Basically, this is one of the latest techniques to design a microwave component where filtering effect is embedded into the coupled-line directional coupler itself. The number of coupled-lines is used to determine the number of modes of a device. Obviously, the more modes a directional coupler has, the wider the bandwidth is. In this project, three- and five-mode directional couplers have been designed, analyzed, and demonstrated.

In the second part, a multiport directional coupler has been designed to generate two desired coupling levels. Two independent directional couplers have been analyzed and merged to become a single multiport directional coupler. In this project, the author has analyzed a directional coupler that has 10 dB and 20 dB coupling levels.

Throughout this project, the author have gained better understanding of some of the passive microwave components such as directional couplers, filters and power dividers. In addition, both of the proposed multimode filtering and multiport directional couplers are considered a breakthrough. The two ideas are intended to be submitted to the IEEE transaction Microwave Theory and Techniques and IEEE Microwave and Wireless Components Letters, respectively.

1.4 Project Motivation

With the advancement of microwave and RF wireless technologies, various types of microwave components can be designed according to the needs of industries. It is a good achievement to come up with a new prototype of directional coupler with good matching, high selectivity and wide bandwidth. In this project, the author has contributed to the further understanding of microwave components and design topologies.

Many problem-solving skills have been acquired throughout the whole project. Hence, it generates momentum for the author to explore and solve problems whenever they occur. In addition, with the intention to publish in IEEE Transactions on Microwave Theory and Techniques and IEEE Microwave and Wireless Components Letters, it gives the author extra motivation to explore more related on the directional coupler.

1.5 Thesis Overview

In this thesis, the necessary theory pertaining to different microwave components will be presented in Chapter 2, including that for the coupled-line directional coupler. It consists of theory, issues, design considerations and recent developments of various types of microwave components. Apart from that, some of the simulation softwares were introduced in this chapter as well.

In Chapter 3 and Chapter 4, a multimode filtering directional coupler and multiport directional coupler will be discussed separately. The design considerations and configuration are further analyzed in these two chapters. Here, the transmission line model of the respective directional coupler has been simulated using Microwave Office. Some of the important parameters were also analyzed in these two chapters. The results and performances of the directional couplers were discussed and

compared to those for the conventional directional coupler. Based on the results obtained, the author can confirm that the multimode and multi-port directional couplers have been successfully realized.

Lastly, the conclusion and the recommendations for the further studies as well as the improvements on the design of directional coupler are given in Chapter 5.

CHAPTER 2

LITERATURE REVIEW

2.1 Background

Firstly, the theory of the conventional directional coupler will be analyzed in this chapter. Also, the design methodology of the new components, the design considerations as well as some of the issues will be discussed, following by the recent developments. Lastly, the basic simulation tools that have been used to carry out this project will be introduced.

2.2 Directional Coupler

Directional couplers are passive microwave components that are commonly used for power division or power combining. Basically, directional couplers is a four-port device that contains four ports where a wave incident at port 1 (input port) couples power into port 2 (direct port) and port 3 (coupled port) but not into port 4 (isolation port).

In general, a lossless, reciprocal, matched four-port directional coupler will have a scattering matrix as in the following:

$$\bar{S} = \begin{bmatrix} 0 & \alpha & j\beta & 0 \\ \alpha & 0 & 0 & j\beta \\ j\beta & 0 & 0 & \alpha \\ 0 & j\beta & \alpha & 0 \end{bmatrix}$$

Whereas, this ideal coupler is completely characterized by the coupling coefficient c , where we find:

$$\bar{S} = \begin{bmatrix} 0 & \sqrt{1-c^2} & jc & 0 \\ \sqrt{1-c^2} & 0 & 0 & jc \\ jc & 0 & 0 & \sqrt{1-c^2} \\ 0 & jc & \sqrt{1-c^2} & 0 \end{bmatrix}$$

In other words:

$$\beta = c \quad \text{and} \quad \alpha = \sqrt{1-\beta^2} = \sqrt{1-c^2}$$

Moreover, for directional coupler, the coupling coefficient, c will be less than $1/\sqrt{2}$ always. Therefore, we find that:

$$0 \leq c \leq \frac{1}{\sqrt{2}} \quad \text{and} \quad \frac{1}{\sqrt{2}} \leq \sqrt{1-c^2} \leq 1$$

The physical behaviour of a directional coupler can be analyzed when a signal is given to port 1, with power P_1^+ . Firstly, if all other ports are matched, we find out that the power flowing out of port 1 is:

$$P_1^- = |S_{11}|^2 P_1^+ = 0$$

While the power coming out of port 2 is:

$$P_2^- = |S_{21}|^2 P_1^+ = (1-c^2)P_1^+$$

And the power coming out of port 3 is:

$$P_3^- = |S_{31}|^2 P_1^+ = c^2 P_1^+$$

Finally, we find there is no power flowing out of port 4:

$$p_4^- = |S_{41}|^2 p_1^+ = 0$$

Hence, in the terminology of the directional coupler, we define port 1 as input port, port 2 as the through port, port 3 as the coupled port, and port 4 as the isolation port.

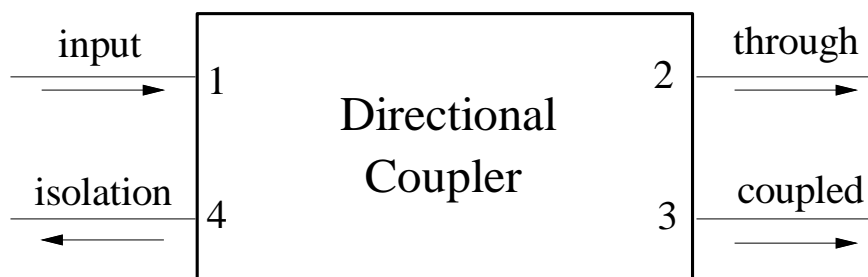


Figure 2.1: Power flows in conventional directional coupler.

However, for an ideal directional coupler, any of the coupler ports can function as input with different through port, coupled port and isolation port for each case. Figure 2.1 below shows example of a signal is incident on port 2, while all other ports are matched.

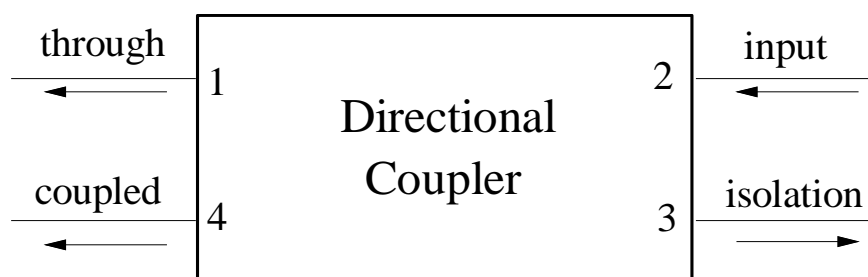


Figure 2.2: Directional coupler with port 2 as input port.

Thus, we can summarize from the scattering matrix of directional coupler to obtain the table below:

Table 2.1: Port definition of directional coupler.

| <i>Input</i> | <i>Through</i> | <i>Coupled</i> | <i>Isolation</i> |
|--------------|----------------|----------------|------------------|
| Port 1 | Port 2 | Port 3 | Port 4 |
| Port 2 | Port 1 | Port 4 | Port 3 |
| Port 3 | Port 4 | Port 1 | Port 2 |
| Port 4 | Port 3 | Port 2 | Port 1 |

Generally, the coupling coefficients for directional coupler are in the range of approximately:

$$0.25 > c^2 > 0.0001$$

As a result, we find that $\sqrt{1-c^2} \approx 1$, which means the power output from the through port is just slightly smaller than power incident on the input port. Meanwhile, the power output of the coupling port is typically a small fraction of the power incident of the input port.

Unfortunately, it is difficult to realise an ideal directional coupler. For example, the input matching is hardly perfect, so that the diagonal elements of the scattering matrix are not zero although they are very small. Likewise, the isolation port is never perfectly isolated. There will be small amount of power leakage to other ports. Therefore, the through port will be slightly less than the value $\sqrt{1-c^2}$. The scattering matrix for a non-ideal directional coupler is:

$$\bar{S} = \begin{bmatrix} S_{11} & S_{21} & jc & S_{41} \\ S_{21} & S_{11} & S_{41} & jc \\ jc & S_{41} & S_{11} & S_{21} \\ S_{41} & jc & S_{21} & S_{11} \end{bmatrix}$$

Based on the scattering matrix above, there are some important parameters in describing the performance of the coupler which are coupling factor, directivity, and isolation. (David M. Pozar, 2005).

- Coupling factor (in dB): The ratio of input power to the coupled power.

$$C = 10 \log \frac{P_1}{P_3}$$

- Directivity (in dB): The ratio of coupled power to the power at the isolated port.

$$D = 10 \log \frac{P_3}{P_4}$$

- Isolation (in dB): The ratio of input power to power flowing out of the isolated port. Isolation is also known as the sum of coupling factor and directivity of the directional coupler.

$$I = 10 \log \frac{P_1}{P_4} = 10 \log \frac{P_1}{P_3} \frac{P_3}{P_4} = 10 \log \frac{P_1}{P_3} + 10 \log \frac{P_3}{P_4}$$

$$I = C + D$$

An ideal directional coupler has infinite directivity and isolation. Hence, maintaining a symmetric structure is an important factor since an ideal coupler with ideal isolation and matching performance can be realized if and only if the structure is symmetric. (Michael Dydyk, 1999).

2.2.1 Coupled-line Directional Coupler

Generally, there are several methods to design a directional coupler. One of the common methods to design directional coupler is using coupled-line theory. Figure 2.3 shows the conventional coupled-line directional coupler. In this structure, the coupling level between the ports is due to the interaction of the electromagnetic fields along transmission lines which have been placed in close proximity. In addition, it can be named as TEM-mode quarter-wavelength directional coupler. (Leo Young, M.A., Dr. Eng., 1963).

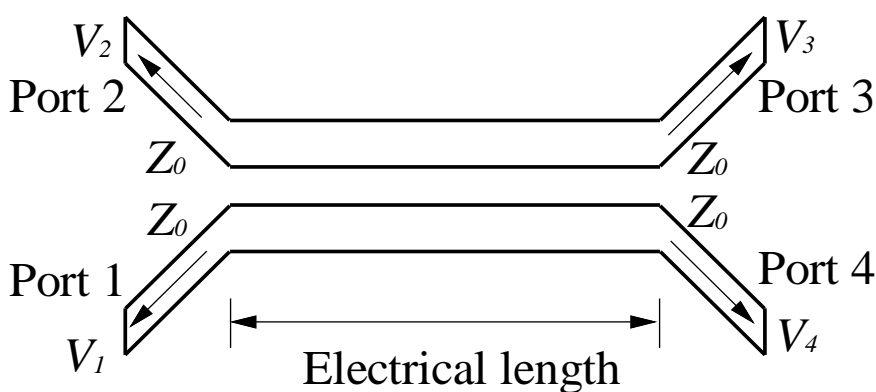


Figure 2.3: Conventional coupled line directional coupler.

2.2.2 Theory

According to Shimizu and Jones (J.K. Shimizu, E. M. T. Jones, 1958), all the ports of the directional coupler were terminated in its characteristic impedance Z_0 . Based on Figure 2.3, the coupled voltage V_2 at port 2 produced by the applied voltage V_1 at port 1 is equal to:

$$\frac{V_2}{V_1} = \frac{jc \sin \theta}{\sqrt{1-c^2} \cos \theta + j \sin \theta}$$

While the voltage, V_4 at port 4 is equal to:

$$\frac{V_4}{V_1} = \frac{\sqrt{1-c^2}}{\sqrt{1-c^2} \cos \theta + j \sin \theta}$$

Meanwhile, the voltage, V_3 at port 3 is zero for all frequencies. The midband amplitude coupling factor, c is given in terms of the even mode characteristic impedance, Z_{0e} and odd mode characteristic impedance, Z_{0o} as:

$$c = \frac{Z_{0e} - Z_{0o}}{Z_{0e} + Z_{0o}}$$

While the characteristic impedance Z_0 is expressed in terms as:

$$Z_0 = \sqrt{Z_{0e} Z_{0o}}$$

According to all the equations above, the even and odd mode impedances can be written as :

$$Z_{0e} = Z_0 \sqrt{\frac{1+c}{1-c}}$$

and

$$Z_{0o} = Z_0 \sqrt{\frac{1-c}{1+c}}$$

With these equations, they allow us to use the even- and odd-mode characteristic impedances to determine the width and separation of the lines for a given coupling coefficient. Figure 2.4 below shows an even- and odd-mode characteristic impedance of coupled-line microstrip directional coupler with dielectric constant, ϵ_r equal to 10 (David M. Pozar, 1998). The parameters used in the graph are represented as below:

S = Separation

W = Width of Microstrip lines

D = Dielectric thickness

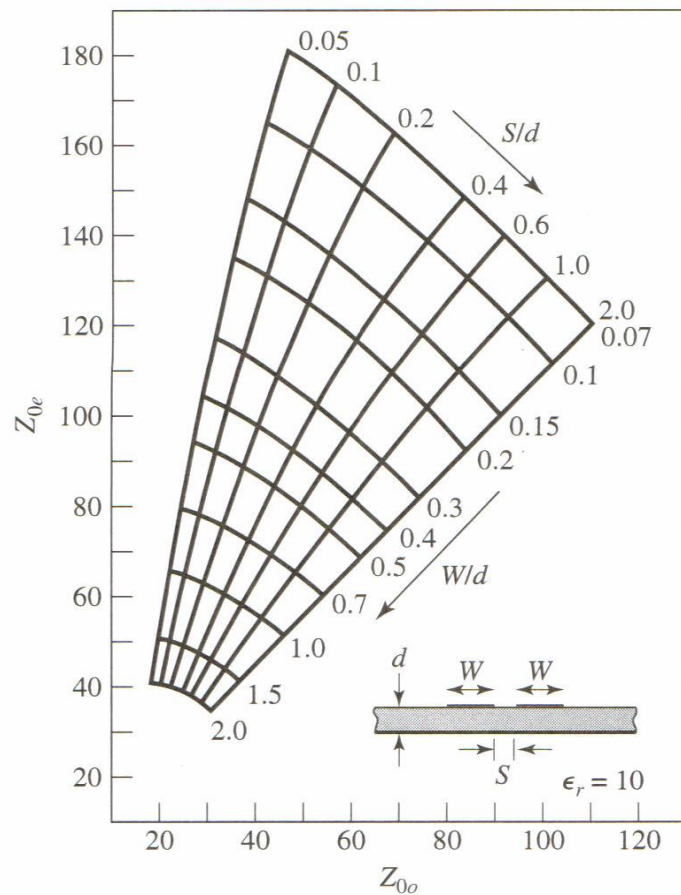


Figure 2.4: Even- and odd-mode characteristic impedance design data for the coupled microstrip lines.

2.3 Recent Developments

In order to design directional couplers with good performance, different methods have been developed to improve the performances such as bandwidth, isolation, and directivity. In this section, several techniques being commonly used by the industry are reviewed.

2.3.1 Directional Coupler Loaded With Shunt Inductors

In general, the parasitic effects of junction discontinuities in various parts of microstrip directional couplers have critical effects especially on the directivity. Without a proper modeling of these parasitic effects, directivity enhancement becomes extremely difficult especially for weak coupling levels. (Seungku Lee, Yongshik Lee, April 2010). Several methods such as designing a directional coupler using single-element compensation (Dydyk, 1999) or using the quadrupled inductive-compensated technique (Ravee Phromloungsri, Mitchai Chongcheawchamnan, Ian D. Robertson, 2006) were done in the past to improve the directivity. In April 2010, Seungku Lee and Yongshik Lee suggested that the issue of parasitic effects related to junction discontinuities have never been investigated. The effects on the directivity of such directional couplers may be detrimental especially for weak coupling levels at high frequencies. Therefore, these have been taken into account in the design equation through proper modeling. As a result, Seungku Lee and Yongshik Lee proposed a microstrip directional coupler loaded with shunt inductors. Here shows the schematics of a conventional directional coupler and the proposed microstrip directional coupler. (Seungku Lee, Yongshik Lee, April 2010).

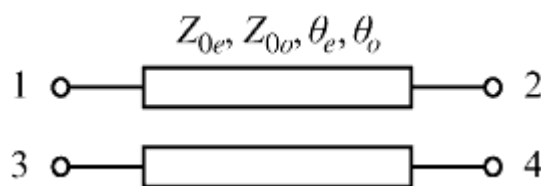


Figure 2.5: Schematics of a conventional microstrip directional coupler.

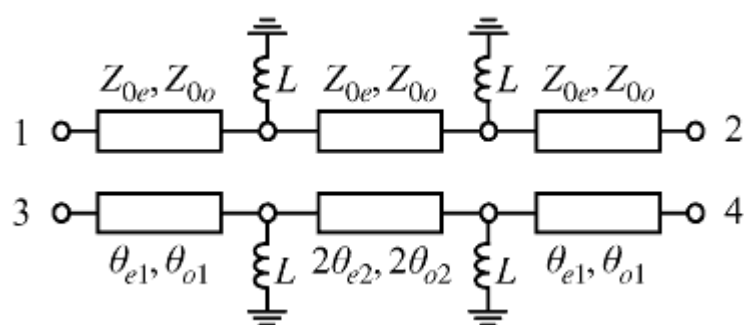


Figure 2.6: Schematics of the proposed microstrip directional coupler with shunt inductors.

With the proposed microstrip directional coupler, a 20-dB directional coupler was designed at 2.4 GHz. A maximum directivity of 56 dB has been measured by the author, which has an improvement of 48 dB over a conventional directional coupler. In addition, a total of 16.3 % bandwidth at 2.4 GHz has been measured in which the directivity remains above 20 dB. (Seungku Lee, Yongshik Lee, April 2010).

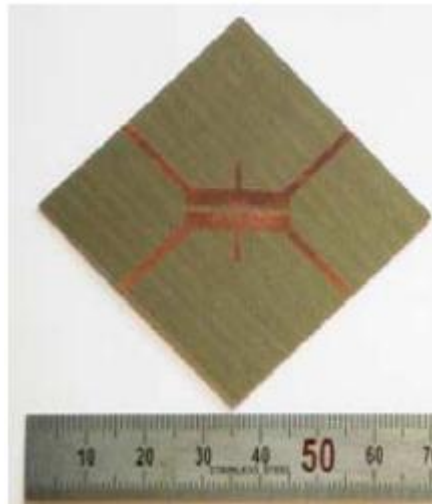


Figure 2.7: Fabricated 20-dB directional coupler with shunt inductors.

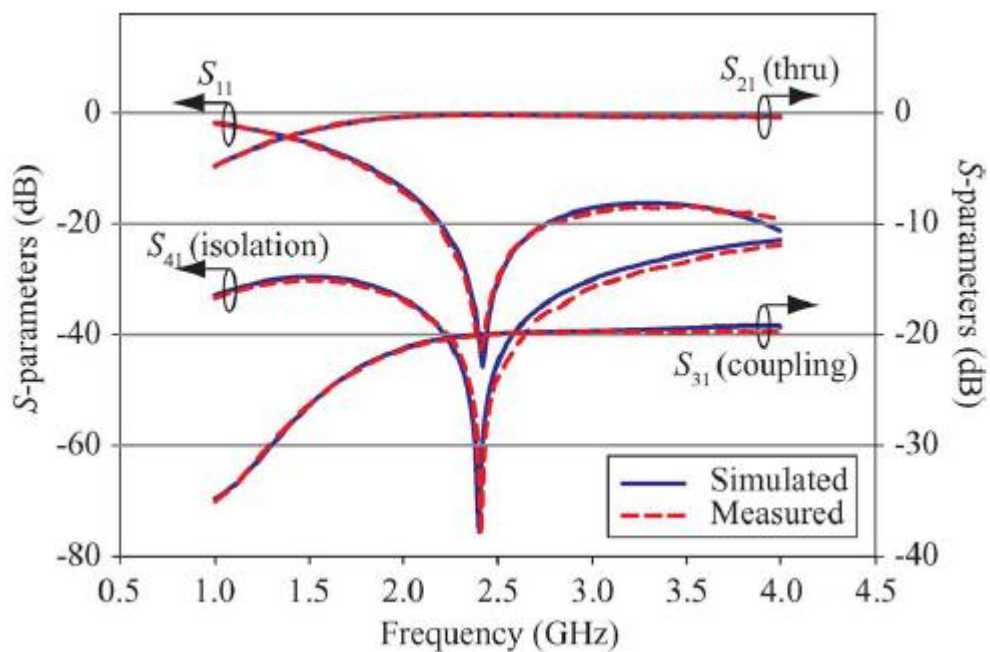


Figure 2.8: S-parameters of the directional coupler with shunt inductors.

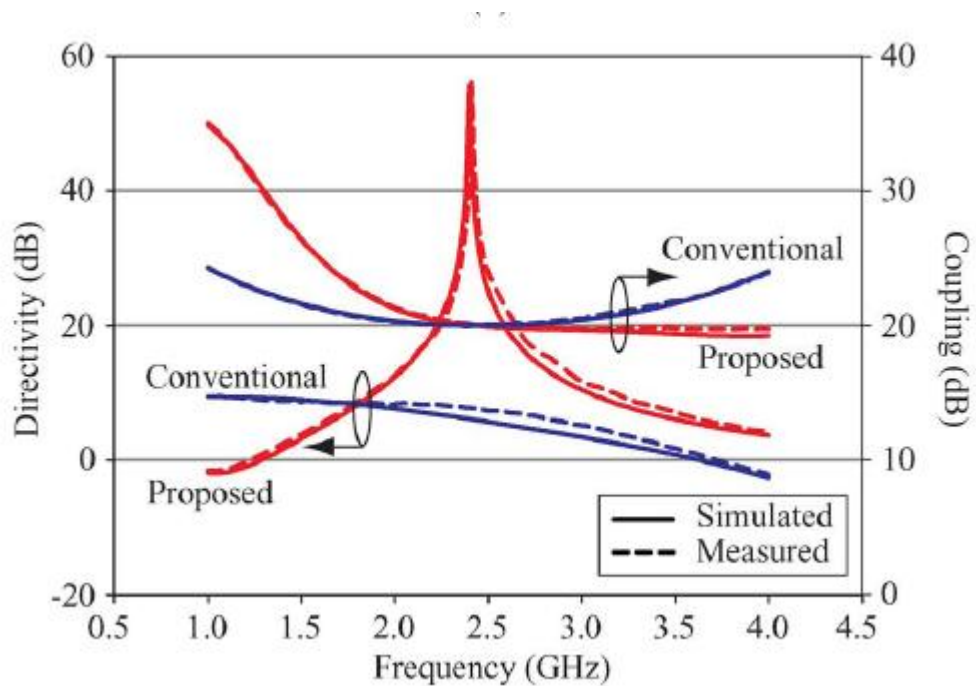


Figure 2.9: Directivity and coupling levels of directional coupler with shunt inductors.

2.3.2 Branch line coupler with $\lambda/4$ open circuited coupled-lines

Branch line couplers with equal power division or combination are the basic circuit components for balanced mixers, power amplifiers, array antennas, modulators, matched attenuators and filters. However, the conventional branch line coupler using $\lambda/4$ transmission line length only provides a narrowband characteristic, which is the major limitation of the coupler. Here, Werner A. Arriola, Jae Young Lee, and Ihn Seok Kim proposed a new wideband 3 dB branch line coupler by implementing four additional $\lambda/4$ open circuited coupled-lines. The $\lambda/4$ open circuited coupled-lines are used to provide wideband matching condition, inherent dc blocking capability, and band pass filter function. (T. Jensen, V. Zhurbenko, V. Krozer, and P. Meincke, Dec. 2007). Figure 2.10 shows the circuit configuration of the proposed wideband branch line coupler.

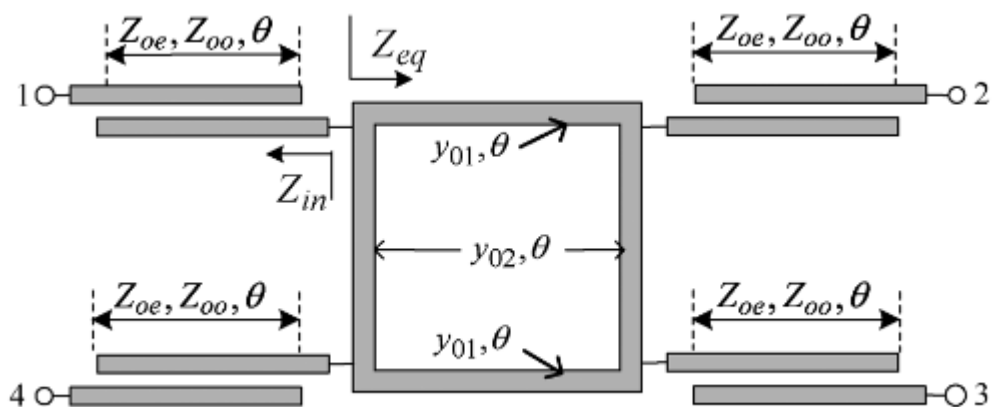


Figure 2.10: Circuit configuration for branch line coupler with $\lambda/4$ open circuited lines.

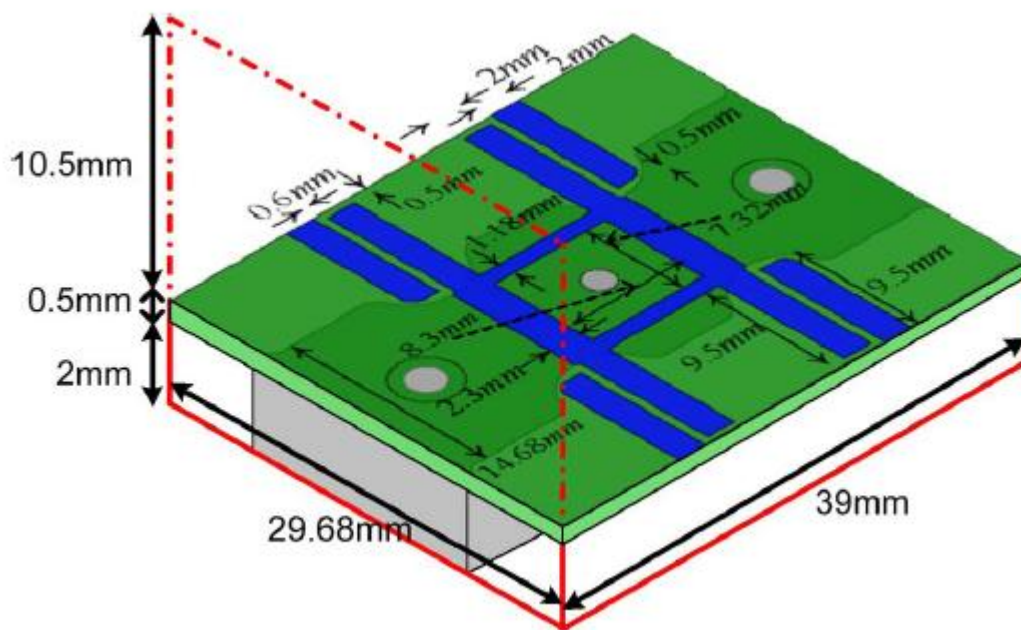


Figure 2.11: Structure and dimensions for the branch line coupler with $\lambda/4$ open circuited lines.

The proposed branch line coupler was designed to operate from 4.54 GHz to 7.21 GHz. Based on the results, the return loss and isolation characteristics are both below -20 dB over 49% fractional bandwidth. Besides that, it has high roll-off skirts for S_{21} and S_{31} at out of band frequencies.

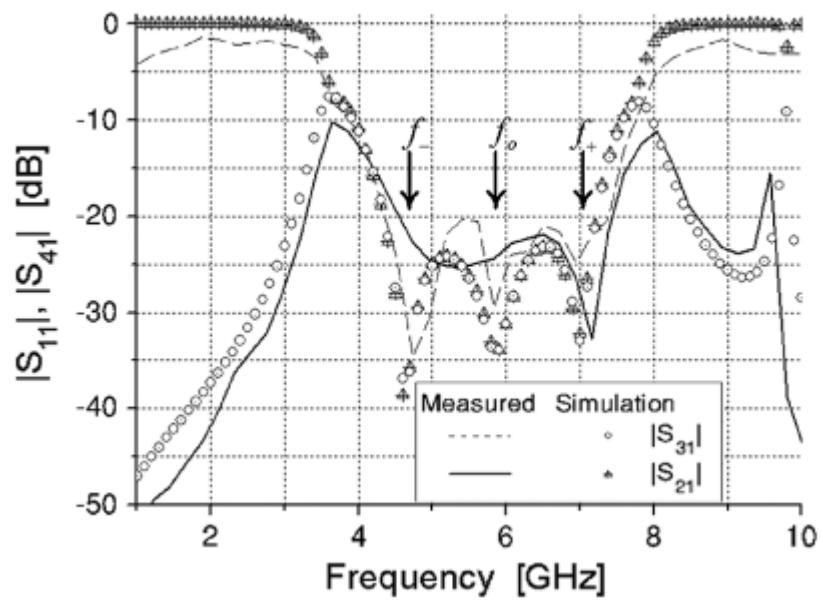


Figure 2.12: Return loss and isolation characteristics of the branch line coupler with $\lambda/4$ open circuited lines.

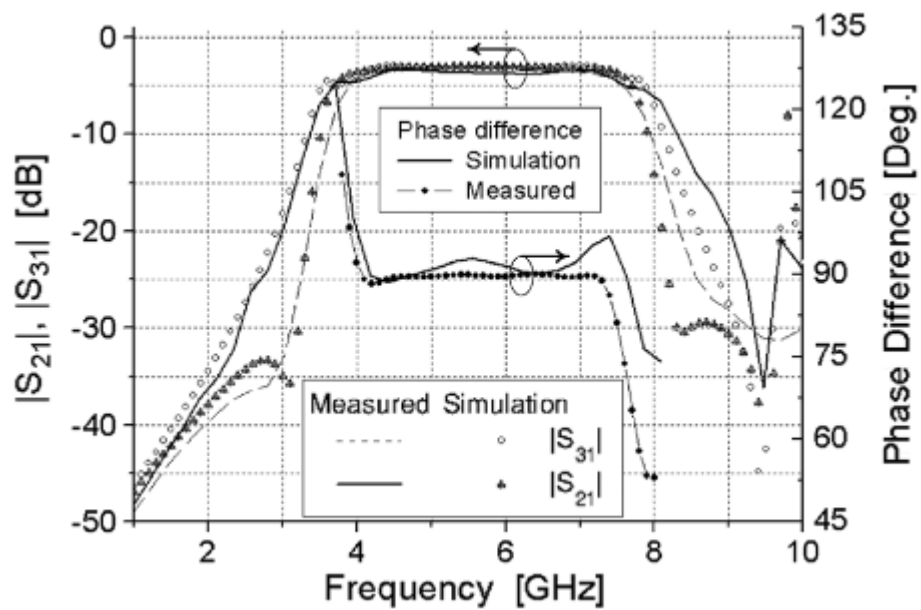


Figure 2.13: Insertion loss, coupling characteristics, and phase differences of the branch line coupler with $\lambda/4$ open circuited lines.

2.3.3 Wilkinson power divider incorporating quasi-elliptic filters

Wilkinson power divider plays an important role in microwave circuits, such as balanced amplifiers and feeding networks of antenna arrays. One of the drawbacks of the conventional Wilkinson power divider is its poor out of band rejection. Therefore, a Wilkinson power divider with improved out of band rejection is proposed by J. Y. Shao, S. C. Huang and Y. H. Pang. They suggested that the quarter wavelength transformer of the Wilkinson power divider is to be replaced by a fourth-order quasi elliptic filter to obtain good passband selectivity. In addition, transmission zeros were created by using 0° feeding structure to enhance the out of band rejection. (J. Y. Shao, S. C. Huang and Y. H. Pang, November 2011). Figure 2.14 shows the circuit layout of the Wilkinson power divider where the quasi-elliptic filters were arranged into U-shaped unit impedance resonators to make circuit compact.

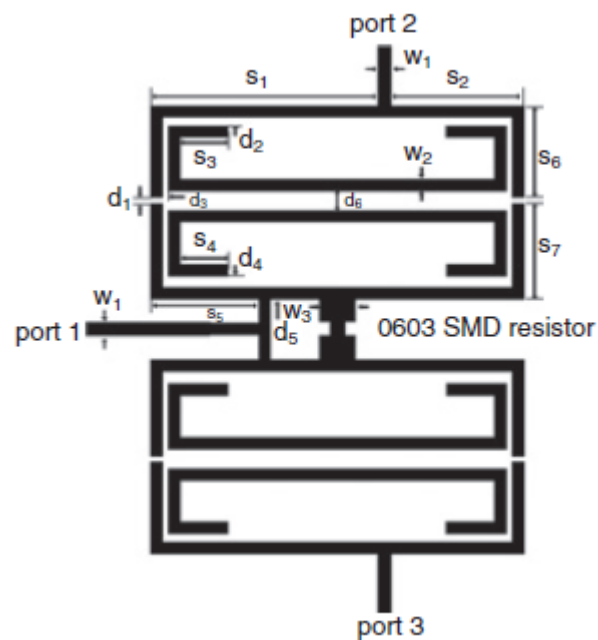


Figure 2.14: Layout configuration for Wilkinson power divider incorporating quasi-elliptic filters.

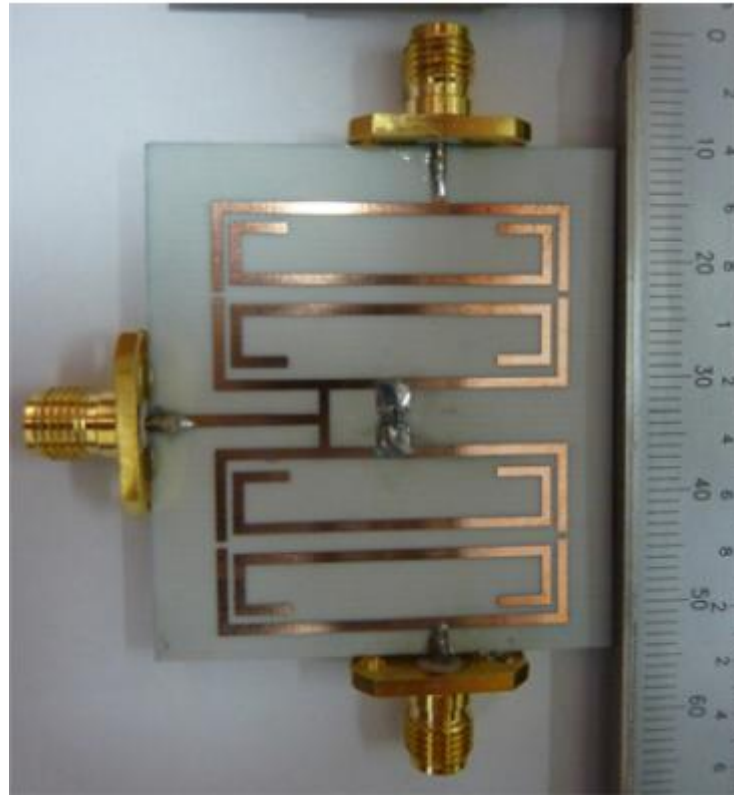


Figure 2.15: Fabricated Wilkinson power divider incorporating quasi-elliptic filters.

With the proposed designs shown in figure 2.14 and 2.15, a 2 GHz Wilkinson power divider incorporating quasi-elliptic filters with a fractional bandwidth of 5% was obtained. From the measured amplitude response curve, 40 dB roll-off skirt is obtained at 2 ± 0.12 GHz, which validates the design concept.

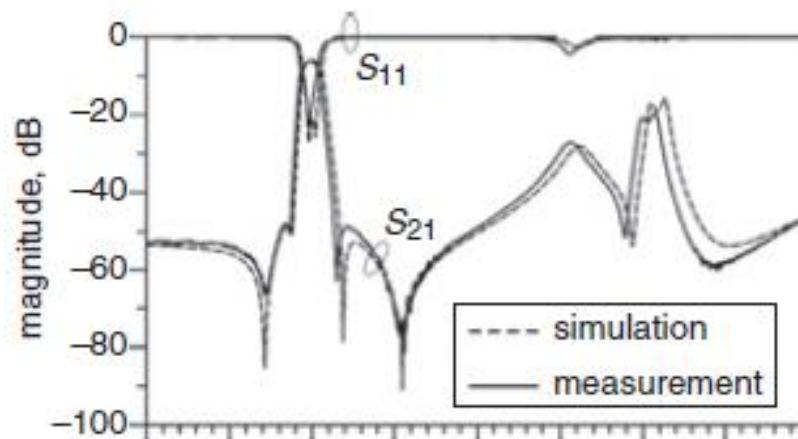


Figure 2.16: Simulated and measured S-parameters of Wilkinson power divider incorporating quasi-elliptic filters.

2.4 Introduction of Simulation Tools

In order to carry out the experiments of this project, several tools and software were used. They include ANSOFT HFSS (High Frequency Structure Simulator), Microwave Office, TXLine, CST Design Environment, Eagle, Freelance Graphics, and so on. In the following sections, background on both HFSS and Microwave Office will be introduced.

2.4.1 High Frequency Structure Simulator

High Frequency Structure Simulator (HFSS) is a registered trademark of Ansoft Corporation. HFSS is a high performance full-wave electromagnetic (EM) field simulator for arbitrary 3D volumetric passive device modeling that has a great graphical user interface (GUI). Ansoft HFSS employs the Finite Element Method (FEM) with adaptive meshing to give unparalleled performance and insight to all three dimension (3D) EM problems. In addition, Ansoft HFSS has evolved over a period of years with the industries. It is the tool of choice for high productivity research, development, and virtual prototyping.

With the rapid advancement of HFSS, the analysis of the scattering matrix parameters (S, Y, Z parameters) and the visualization of the 3-D electromagnetic fields (near field and far field) can be done easily. It helps to determine the signal quality, transmission path losses, and reflection coefficients due to impedance mismatch, parasitic coupling, and radiation.

2.4.2 Microwave Office

Microwave Office was used to perform transmission line modeling to represent the equivalent circuit of the proposed design. Registered under the trademark of the AWR Corporation, Microwave Office is also known as AWR. The software is user friendly because it incorporates plenty of Free Online Training Courses and AWR User Forum. Users can browse through the courses and tutorial to get familiar with the software.

Besides that, one of the hot functions that make Microwave Office impressive is the Variable Tuner. It helps the optimization process. Users are required to input the Max values, Min values and Step settings and control the resolution when sliding the tuner. With the advancement of this software, the transmission line models of any designs can be easily modeled.

CHAPTER 3

FILTERING DIRECTIONAL COUPLER

3.1 Background

A bandpass-filtering directional coupler is a coupling device that possesses high roll-off skirts so that it can remove the out-of-band frequency components more efficiently. Zeros are usually placed adjacent to the cut-off frequencies of the passbands. In this chapter, a bandpass-filtering directional coupler was analyzed. Simulations, measurements, and the transmission line models have been studied. To further improve the performance, a five-mode directional coupler with high selectivity is proposed and discussed.

3.2 Bandpass-filtering Directional Coupler

As discussed earlier, a directional coupler should have good VSWR, high isolation, good directivity, sharp roll-off, and constant coupling over a wide bandwidth. Various techniques have been proposed to overcome the inherent problems of the microstrip directional couplers, such as low selectivity and limited bandwidth. In this section, a bandpass filter and a directional coupler are combined to achieve high selectivity.

First and foremost, a bandpass filter is designed by using parallel coupled-line theory. The proposed design was drawn by using Ansoft HFSS. Figure 3.1 shows the top-down view of the proposed bandpass filter.

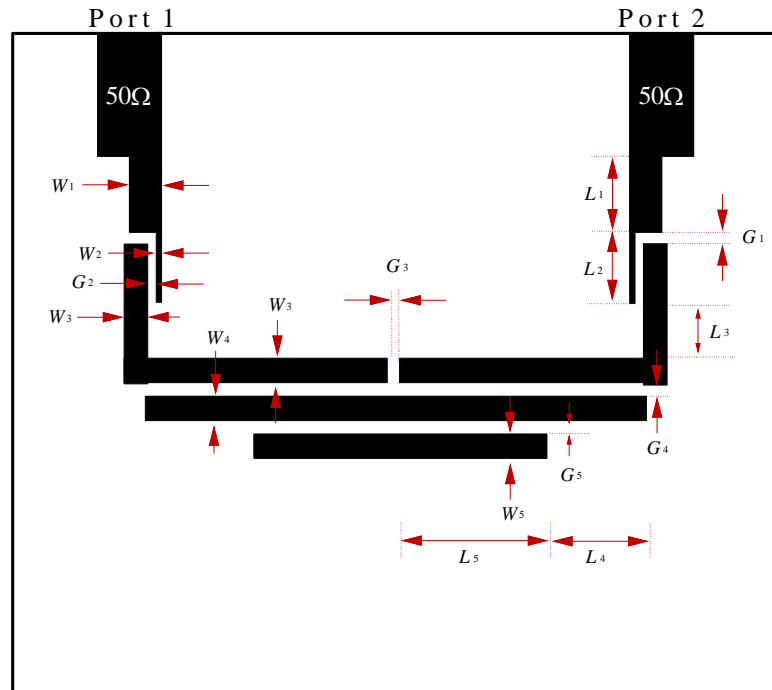


Figure 3.1: Top-down view of proposed wideband bandpass filter.

The detailed design parameters are given by: $w_1 = 1.4$ mm, $w_2 = 0.3$ mm, $w_3 = 1.12$ mm, $w_4 = 1.14$ mm, $w_5 = 1.14$ mm, $l_1 = 5.4$ mm, $l_2 = 8.75$ mm, $l_3 = 2.93$ mm, $l_4 = 3.0$ mm, $l_5 = 6.88$ mm, $g_1 = 0.19$ mm, $g_2 = 0.20$ mm, $g_3 = 0.24$ mm, $g_4 = 0.30$ mm and $g_5 = 0.54$ mm.

The configuration was simulated using Ansoft HFSS with all the parameters above. Figure 3.2 shows the performance of the proposed bandpass filter. As can be seen from the amplitude response of the bandpass filter, the operating frequencies of the bandpass filter are ranging from 3.88 GHz to 5.85 GHz with a total operating bandwidth of 1.97 GHz. It is a three-mode bandpass filter where the first pole locates at 4.32 GHz, and the second and third poles combine at the frequency of 5.39 GHz. Besides that, the fractional bandwidth of the bandpass filter can be calculated as the following:

Center Frequency

$$\begin{aligned}
 &= \frac{\text{LowerFrequency} + \text{HighFrequency}}{2} \\
 &= \frac{3.88 \text{ GHz} + 5.84 \text{ GHz}}{2} \\
 &= 4.86 \text{ GHz}
 \end{aligned}$$

Fractional Bandwidth

$$\begin{aligned}
 &= \frac{\text{HighFrequency} - \text{LowerFrequency}}{\text{CenterFrequency}} \times 100\% \\
 &= \frac{5.84 \text{ GHz} - 3.88 \text{ GHz}}{4.86 \text{ GHz}} \times 100\% \\
 &= 40.32\%
 \end{aligned}$$

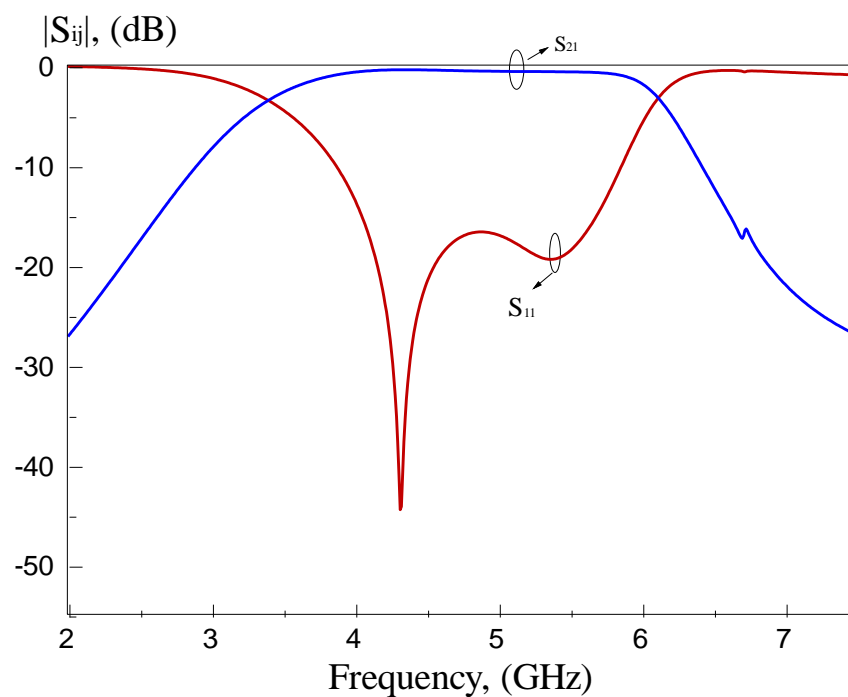


Figure 3.2: S-parameter of the proposed bandpass filter.

Next, the configuration of the bandpass filter is further improved to become a directional coupler. A fraction of input power signal is coupled to port 3, which is

also defined as coupled port. The final configuration of this bandpass-filtering directional coupler will be discussed in Section 3.2.1.

3.2.1 Configuration

Multimode bandpass directional couplers have been successfully proposed and constructed in this research project. Basically, this proposed design was fabricated on the RT Duroid 5870 substrate (with a dielectric constants of $\epsilon_r = 2.33$ and a thickness of 1.57mm). It is a three-port directional coupler where Port 1 functions as an input Port, Port 2 as a direct port, and Port 3 as a coupled port. No isolation port is needed by this design as Port 4 can be eliminated without affecting the results.

All microstrip feedlines have the characteristic impedance of 50Ω . The proposed directional coupler is designed to be symmetric and the feedlines are connected such that thinner strip lines with lengths, l_1 and l_2 , can be used to control the impedance matching. The length of the coupled lines increases when the frequency of the device decreases. Two 90° bends are added to the coupled lines to reduce the size of the directional coupler. The middle portion of the proposed directional coupler is designed with the parallel coupled-line theory and it makes the directional coupler to have high selectivity performance.

Figure 3.3 shows the top-down view of the proposed directional coupler. The detailed design parameters are given by: $w_1 = 1.4$ mm, $w_2 = 0.3$ mm, $w_3 = 1.12$ mm, $w_4 = 1.14$ mm, $w_5 = 1.14$ mm, $w_6 = 0.3$ mm, $w_7 = 1.0$ mm, $l_1 = 5.4$ mm, $l_2 = 8.75$ mm, $l_3 = 2.93$ mm, $l_4 = 3.0$ mm, $l_5 = 6.88$ mm, $l_6 = 0.24$ mm, $l_7 = 0.53$ mm, $l_8 = 2.19$ mm, $l_9 = 5.79$ mm, $g_1 = 0.19$ mm, $g_2 = 0.20$ mm, $g_3 = 0.24$ mm, $g_4 = 0.30$ mm, $g_5 = 0.54$ mm, and $g_6 = 0.5$ mm. The prototype of the proposed bandpass-filtering directional is shown in Figure 3.4.

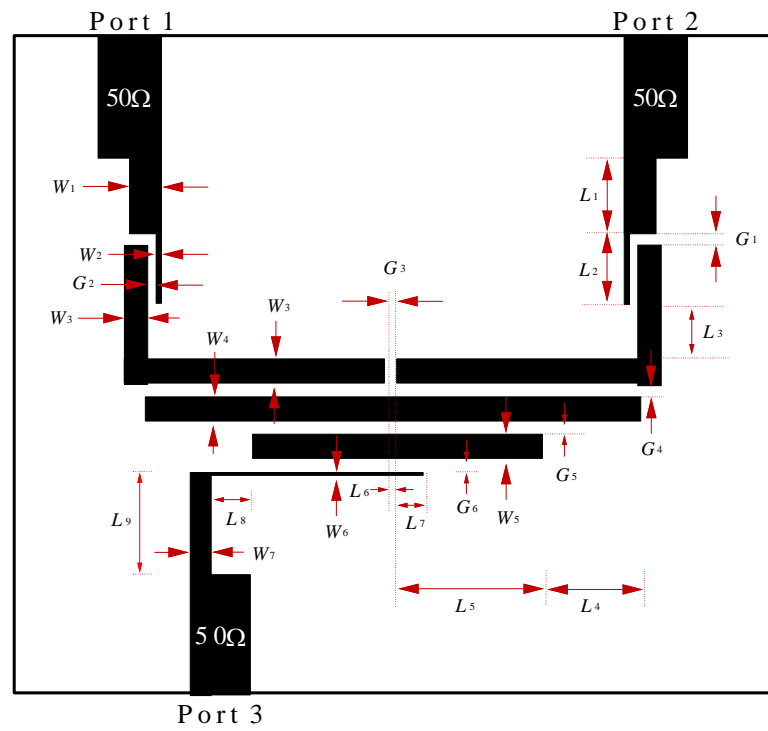


Figure 3.3: Configuration of the proposed microstrip bandpass filtering directional coupler.

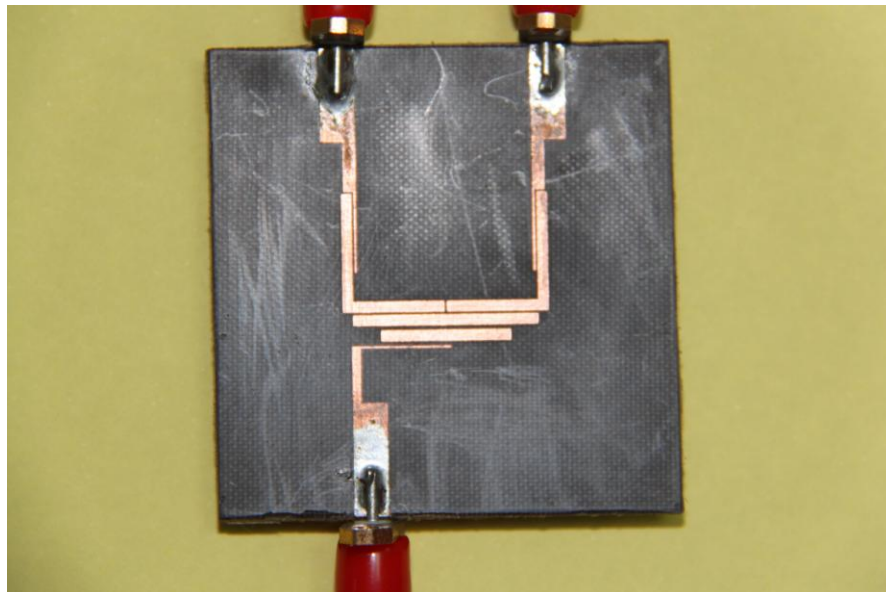


Figure 3.4: Prototype of the proposed bandpass filtering directional coupler.

3.2.2 Transmission Line Model

In order to simulate the effect of the multiple sections of coupled lines, a transmission line model is derived by combining the equivalent circuit with capacitors. Figure 3.5 shows the corresponding equivalent circuit of the proposed directional coupler, which is simulated using Microwave Office.

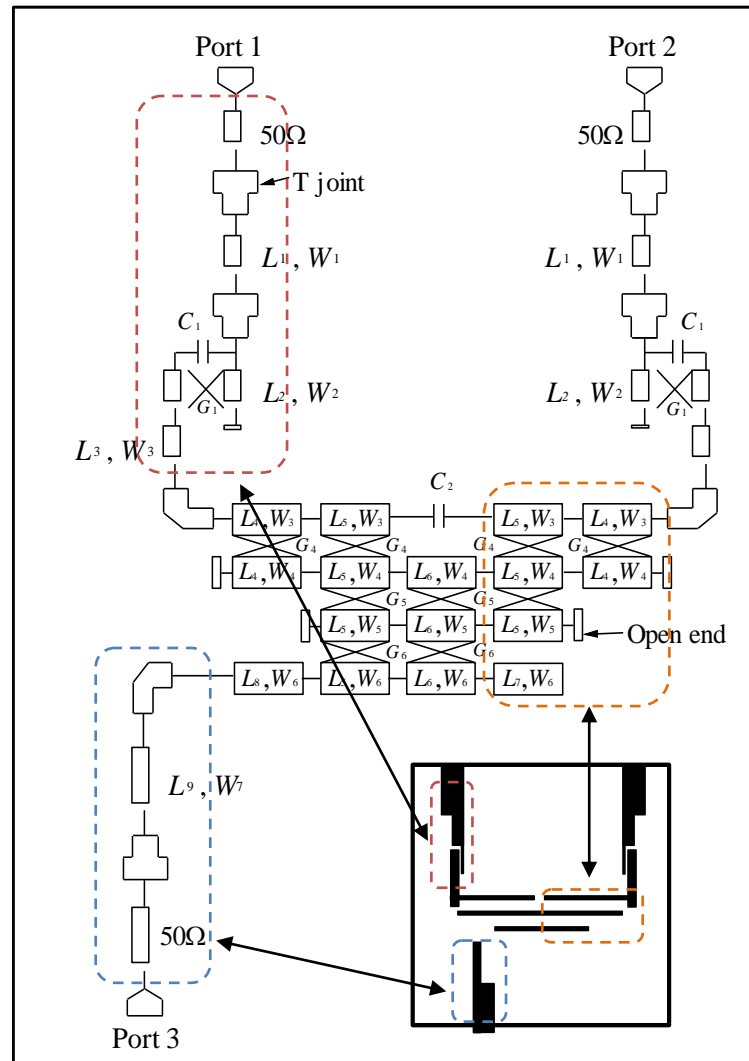


Figure 3.5: Transmission line model of the proposed filtering directional coupler.

As can be seen from the model, the gap g_3 is represented by a capacitor c_3 . It is used to control the electrical signal passing through the model. In Microwave Office, the MSTEPX (Microstrip Step in Width Offset) model is used to represent

the impedance conversion in between coupled lines. It is a step that allows two sections of transmission lines to join up at an asymmetric junction with a relative offset. Besides that, MOPEN (Microstrip Open Circuit with End Effect) is used to represent the open-circuited edges. The gap g_2 is represented by the capacitor c_1 or c_2 , which represents the leaked electric field. The parallel-coupled lines at the middle of the proposed directional coupler are represented by Coupled-Microstrip-Section with a gap. By using the transmission line model in Figure 3.5, the design of the directional coupler can be easily modelled.

The detailed design parameters are given by: $w_1 = 1.4$ mm, $w_2 = 0.3$ mm, $w_3 = 1.12$ mm, $w_4 = 1.14$ mm, $w_5 = 1.14$ mm, $w_6 = 0.3$ mm, $w_7 = 1.0$ mm, $l_1 = 5.4$ mm, $l_2 = 8.75$ mm, $l_3 = 2.93$ mm, $l_4 = 3.0$ mm, $l_5 = 6.88$ mm, $l_6 = 0.24$ mm, $l_7 = 0.53$ mm, $l_8 = 2.19$ mm, $l_9 = 5.79$ mm, $g_2 = 0.20$ mm, $g_4 = 0.30$ mm, $g_5 = 0.54$ mm, $g_6 = 0.5$ mm, $c_1 = 2.5 \times 10^{-13}$ F, $c_2 = 2.5 \times 10^{-13}$ F, and $c_3 = 3.35 \times 10^{-13}$ F.

3.2.3 Results

The configuration of the directional coupler was simulated by using Ansoft HFSS. In order to examine the performances of the directional coupler, measurements were carried out by using the Rohde & Schwarz ZVB8 Vector Network Analyzer. Amplitude and phase responses of the proposed directional coupler were compared.

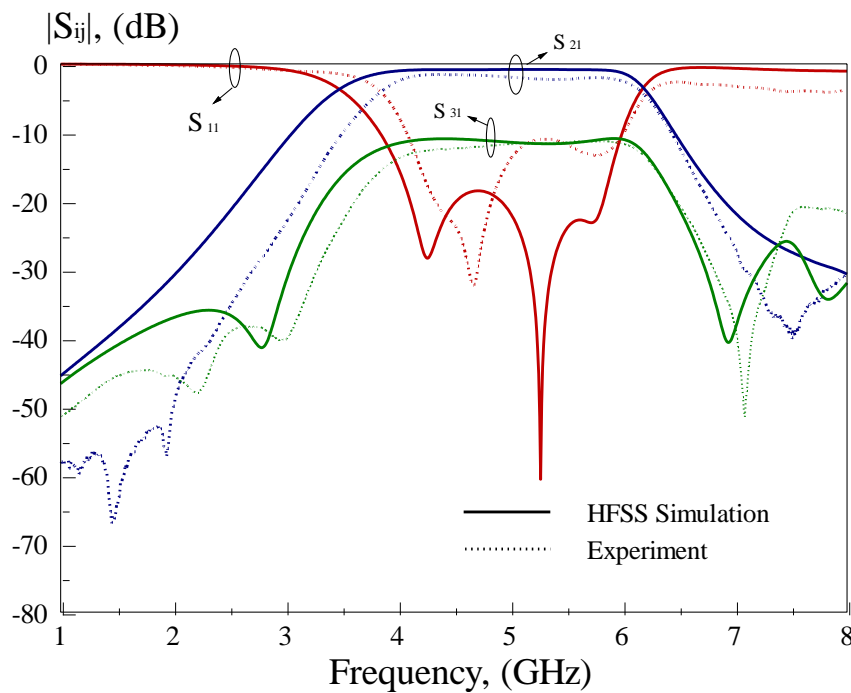


Figure 3.6: Simulated and measured amplitude responses of the filtering directional coupler.

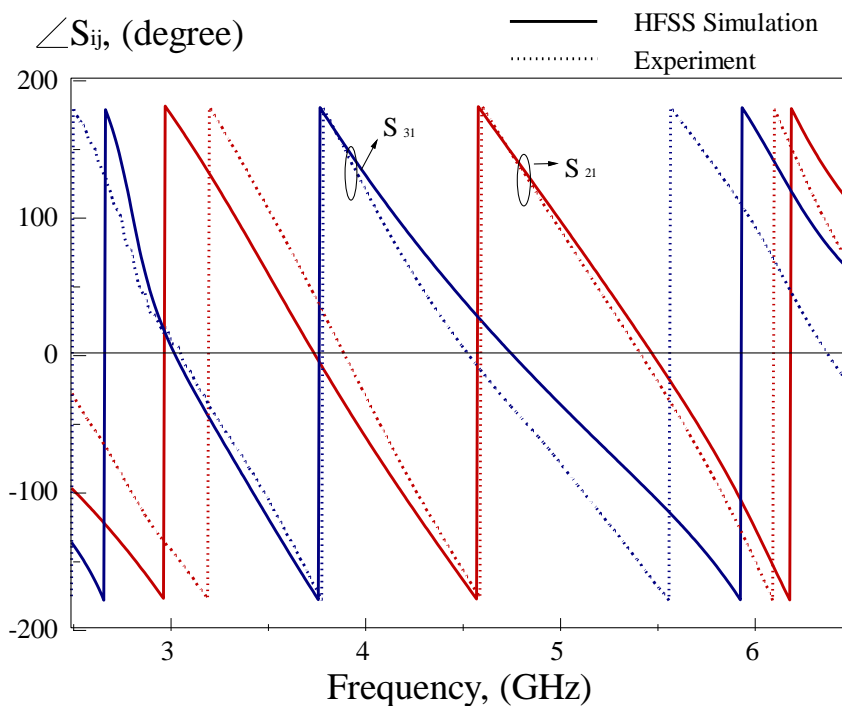


Figure 3.7: Simulated and measured phase responses of the filtering directional coupler.

Based on the results above, it is obvious that a three-mode filtering directional coupler can be realised with the proposed design. The experimental

results agree well with the simulated data. Figure 3.6 shows the amplitude responses of proposed directional coupler. As can be seen from the experimental result, a 10-dB flat coupling directional coupler can be achieved in the frequency range of 4 GHz to 6 GHz, giving a total bandwidth of 2 GHz, which is 93.46% of that in HFSS simulation. Simulation shows that it is capable to operate from 3.86 GHz to 6 GHz, yielding a total bandwidth of 2.14 GHz. Obviously, there are three poles contributing to the wideband performance of the proposed directional coupler. The first pole locates at 4.26 GHz whereas the third pole is at 5.73 GHz, for both simulated and measured results. There is a shift in frequency where the experimental resonance of second pole locates at 4.75 GHz, instead of 5.25 GHz. However, this does not cause any significant effect to the proposed directional coupler as its bandwidth can be maintained. Apart from that, the proposed directional coupler is able to achieve high selectivity. Filtering effect is seen in Figure 3.6 where two significant zeros are observed in the transmission coefficients S_{21} and S_{31} around the out-of-band region.

Apart from using Ansoft HFSS to perform simulation, the same configuration has been simulated using Microwave Office. Figure 3.8 and 3.9 show the comparison of the measured result with that of the transmission line model, showing good agreement. By observing the figure, we can notice there are two significant zeros for both the transmission coefficient S_{21} and insertion loss S_{31} as well.

Table 3.1: Comparison of the experiment, HFSS simulation, and TLM modelling results.

| | Experiment | HFSS Simulation | TLM Modelling |
|---------------------------|-------------|-----------------|---------------|
| f_L (GHz) / f_H (GHz) | 4.00 / 6.00 | 3.86 / 6.00 | 4.25 / 5.55 |
| f_c (GHz) | 5.00 | 4.93 | 4.9 |
| Fractional Bandwidth (%) | 40.0 | 43.4 | 26.5 |

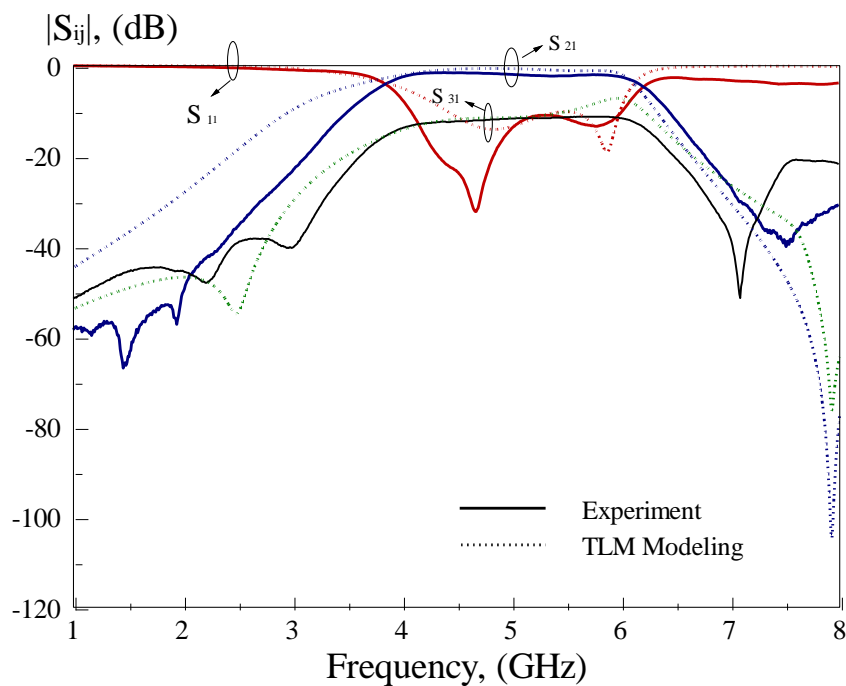


Figure 3.8: Amplitude responses of the experimental and TLM model.

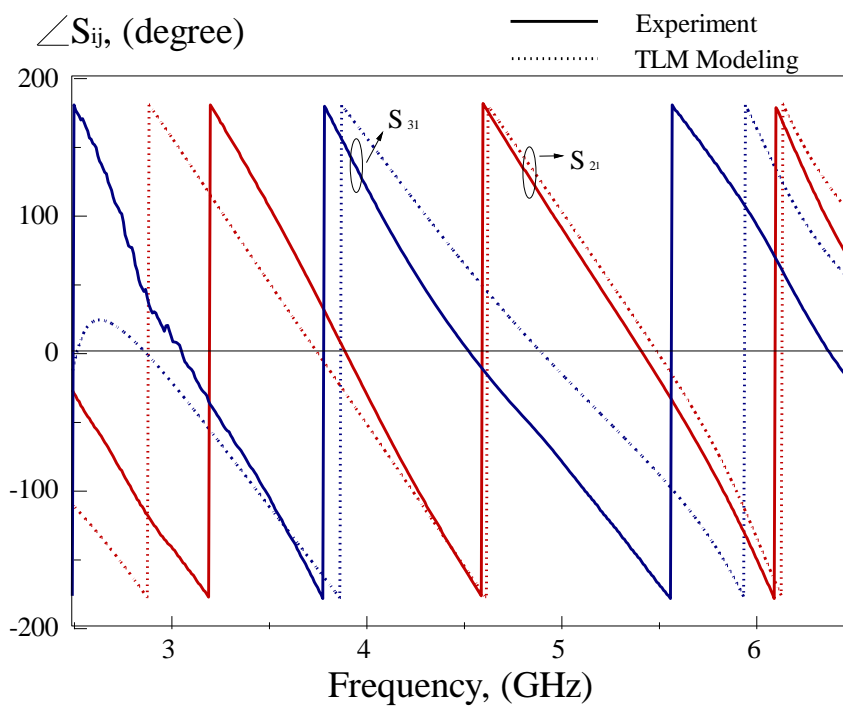


Figure 3.9: Phase responses of the experimental and TLM model.

3.2.4 Parametric Analysis

In order to obtain the optimal configuration of the proposed directional coupler, all the parameters were stepped up and stepped down to analyze the effect of every parameter by using Ansoft HFSS. Overall, the key parameter of the proposed directional coupler is the gap between each coupled lines. However, all the parameters will be discussed in detail, including length and width of the coupled lines according to the configuration in figure 3.3.

Analysis 1

- Parameter : w_1
- Optimum value : 1.4 mm
- Step-down value : 1.2 mm
- Step-up value : 1.6 mm

Results:

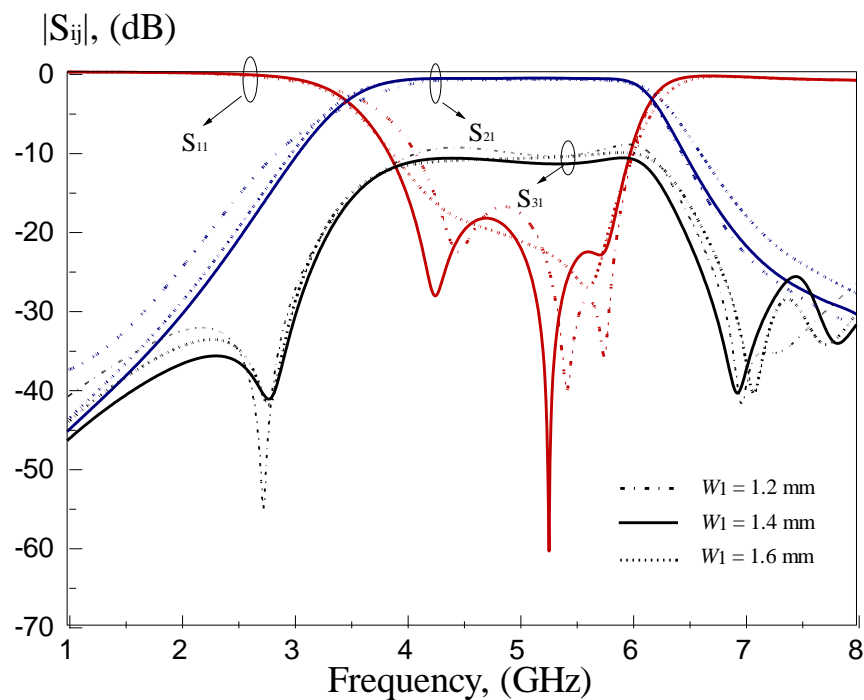


Figure 3.10: Effect of width w_1 on the filtering directional coupler.

Description:

The parameter w_1 does not cause significant effect on the proposed directional coupler. It only slightly affects the positions of poles in the passband of the directional coupler. According to Figure 3.10, the optimal value of w_1 can give the best reflection coefficient S_{11} with a matching level below -20 dB across the operating frequency band. Also, varying width w_1 does not introduce any shift to the zeros located at S_{21} and S_{31} .

Analysis 2

- Parameter : w_2
- Optimum value : 0.3 mm
- Step-down value : 0.2 mm
- Step-up value : 0.4 mm

Results:

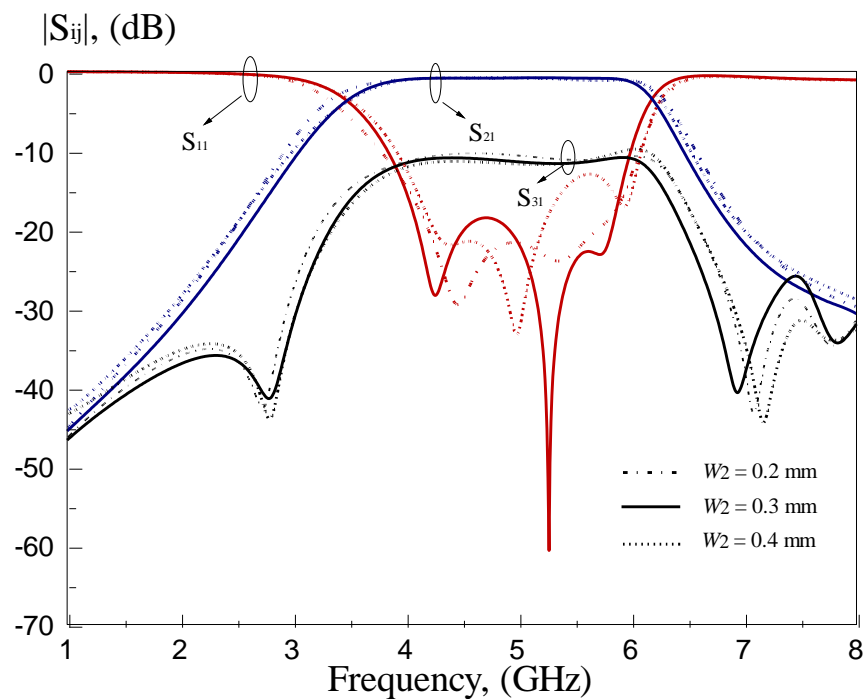


Figure 3.11: Effect of width w_2 on the filtering directional coupler.

Description:

By varying the parameter w_2 , the coupling level of the proposed directional coupler is kept constant at 10 dB across the frequencies in the passband. In this analysis, the positions of the zeros are not affected. But, there is minor change in S_{11} where the positions of poles shift when the width w_2 is altered. The value of w_2 is chosen to be 0.3mm for easier fabrication and better impedance matching. This is because fabrication tolerance would be higher if tiny line widths such as 0.1 mm or 0.2 mm were to be used.

Analysis 3

- Parameter : w_3
- Optimum value : 1.12 mm
- Step-down value : 1.02 mm
- Step-up value : 1.22 mm

Results:

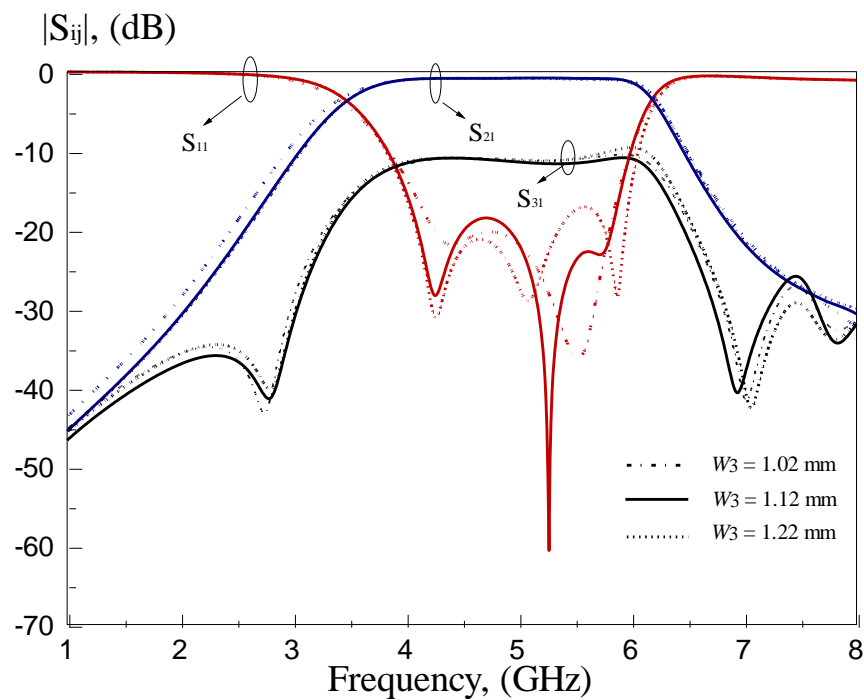


Figure 3.12: Effect of width w_3 on the filtering directional coupler.

Description:

The w_3 value has very slight effect on the positions of the poles, all of which are well below -20 dB. It is chosen to be 1.12mm since the power divider has flat coupling response at 6 GHz. It is important to maximize the operating bandwidth of the proposed directional coupler.

Analysis 4

- Parameter : w_4
- Optimum value : 1.14 mm
- Step-down value : 0.94 mm
- Step-up value : 1.34 mm

Results:

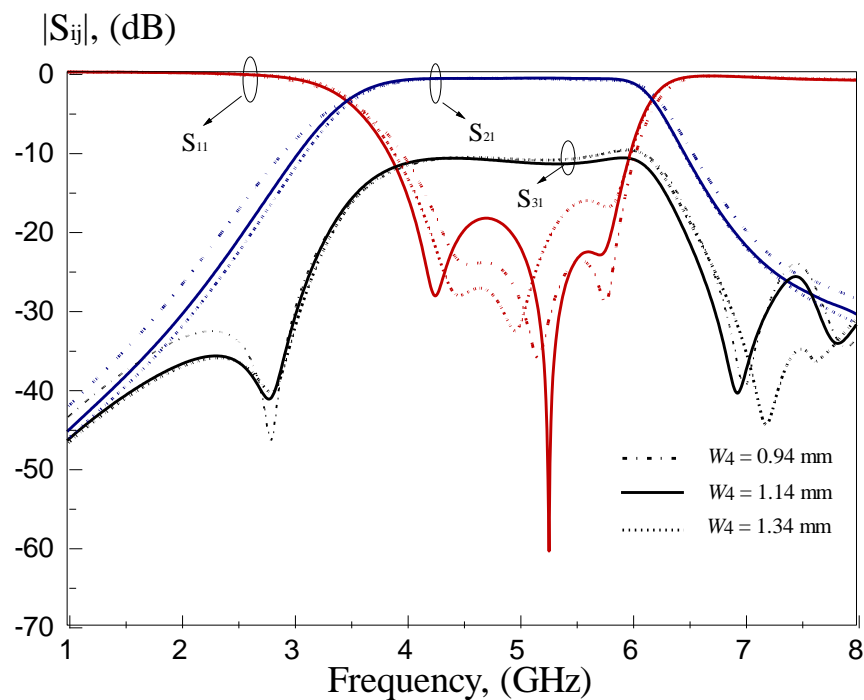


Figure 3.13: Effect of width w_4 on the filtering directional coupler.

Description:

Parameter w_4 affects the performance of S_{21} at the out-of-band frequencies. It does not introduce significant effect to the proposed directional coupler. The matching levels of the poles are well maintained below -20 dB. The width w_4 was chosen to be 1.14mm to obtain maximum bandwidth. It is very difficult to make the coupling level flat at 6 GHz by changing the width w_4 alone.

Analysis 5

- Parameter : w_5
- Optimum value : 1.14 mm
- Step-down value : 0.94 mm
- Step-up value : 1.34 mm

Results:

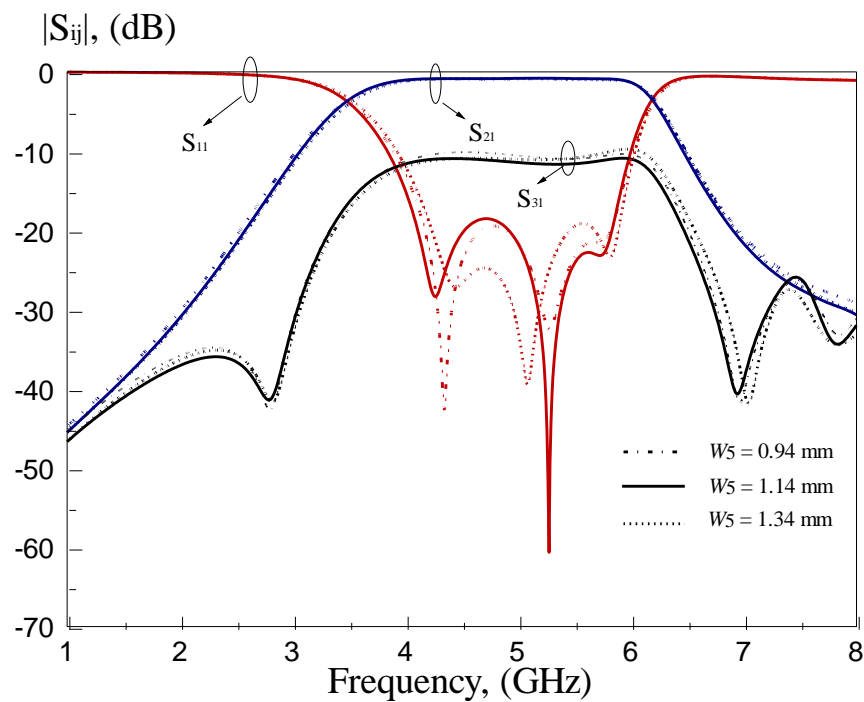


Figure 3.14: Effect of width w_5 on the filtering directional coupler.

Description:

The w_5 value has minor effect on the reflection coefficient S_{11} . Although the matching levels seem to be better for widths 0.94 mm and 1.34 mm, the w_5 value is chosen to be 1.14 mm as it has a more constant coupling level of 10 ± 1 dB. Besides that, there is no major difference in the positions of zeros when width w_5 alters.

Analysis 6

- Parameter : w_6
- Optimum value : 0.3 mm
- Step-down value : 0.2 mm
- Step-up value : 0.4 mm

Results:

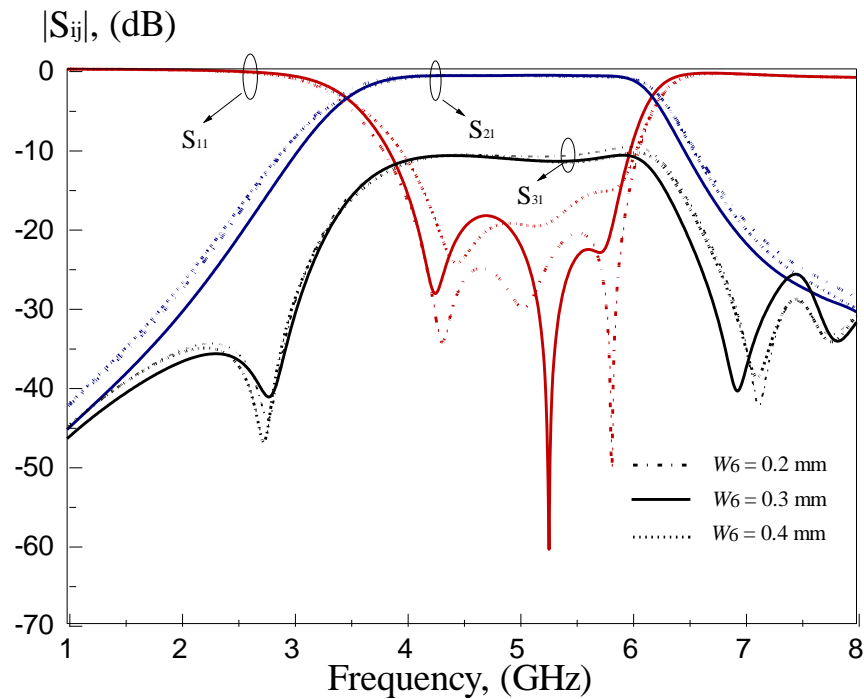


Figure 3.15: Effect of width w_6 on the filtering directional coupler.

Description:

By changing the value of w_6 to 0.4 mm, the operating frequencies are slightly shifted, causing the operating bandwidth to reduce as well. Although the matching level is better for w_6 of 0.2 mm, the coupling level S_{31} shows significant fluctuation in coupling level nearing 6 GHz. As a result, the width w_6 is fixed to be 0.3 mm where it maximizes the operating bandwidth of the proposed directional coupler. No other major effect is observed for this parameter.

Analysis 7

- Parameter : w_7
- Optimum value : 1.0 mm
- Step-down value : 0.8 mm
- Step-up value : 1.2 mm

Results:

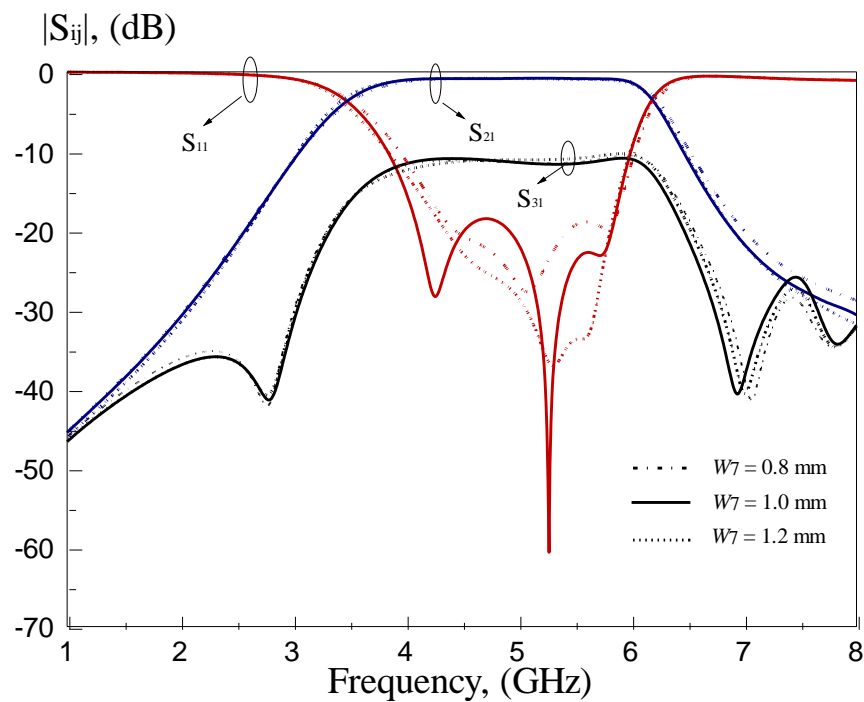


Figure 3.16: Effect of width w_7 on the filtering directional coupler.

Description:

Parameter w_7 does not bring much effect on the proposed directional coupler. It introduces shift in the position of poles of the directional coupler when the width is altered. As can be seen in Figure 3.16, the optimum value of w_7 gives the best reflection coefficient S_{11} . Apart from that, it has no significant effect on positions of zeros.

Analysis 8

- Parameter : g_2
- Optimum value : 0.20 mm
- Step-down value : 0.15 mm
- Step-up value : 0.25 mm

Results:

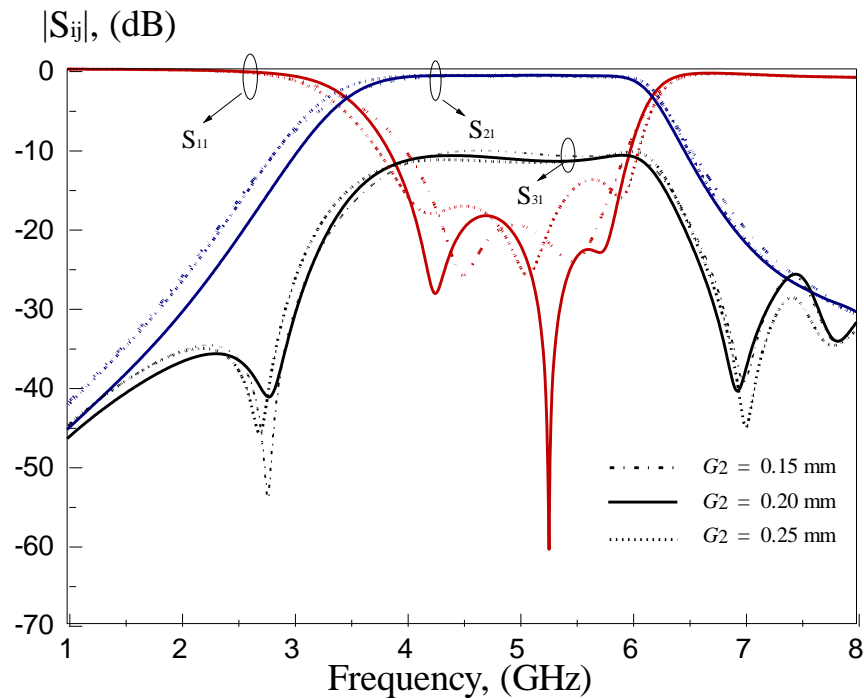


Figure 3.17: Effect of gap g_2 on the filtering directional coupler.

Description:

With reference to the amplitude response shown in Figure 3.17, we can clearly see that the gap g_2 affects the coupling level of the proposed directional coupler. When it is set as 0.15 mm, the difference between the two coupling ports slightly reduces. However, it does not change when g_2 is stepped up to 0.25 mm. The operating bandwidth becomes narrower when the gap is stepped down. In this case, the value of g_2 is chosen to be 0.20 mm.

Analysis 9

- Parameter : g_3
- Optimum value : 0.24 mm
- Step-down value : 0.01 mm
- Step-up value : 1.04 mm

Results:

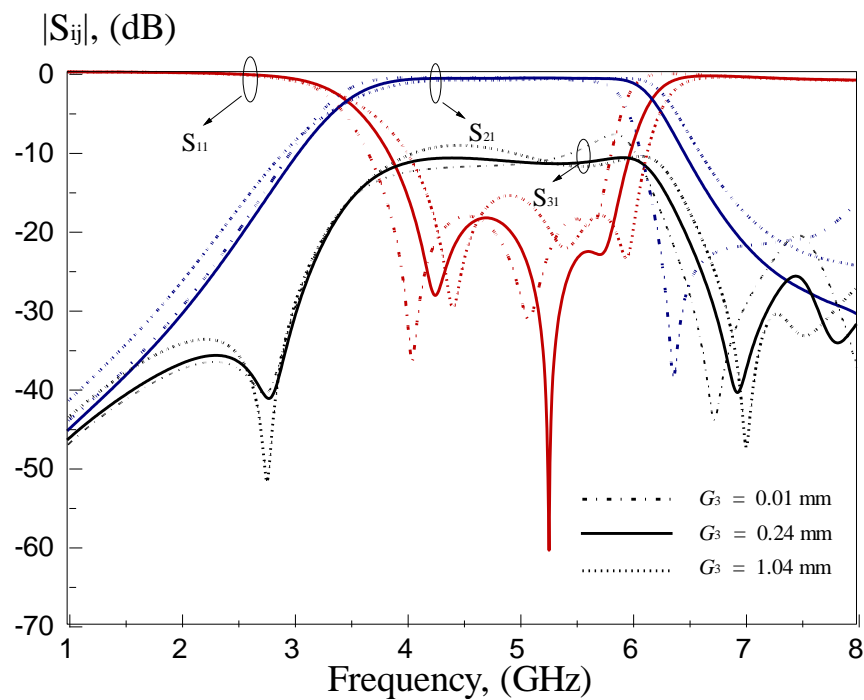


Figure 3.18: Effect of gap g_3 on the filtering directional coupler.

Description:

In this project, the gap g_3 of the proposed directional coupler is designed to be 0.24 mm. By changing the value of g_3 , it introduces significant effect to the rolloff rate of the curve S_{31} . When the gap size is decreased, the slope of S_{31} increases, narrowing down the operating bandwidth of the device. But the passband deteriorates if it's decreased. The optimum gap size is 0.24 mm. The positions of zeros move nearer to the passband when the gap g_3 is stepped down.

Analysis 10

- Parameter : g_4
- Optimum value : 0.30 mm
- Step-down value : 0.05 mm
- Step-up value : 0.50 mm
-

Results:

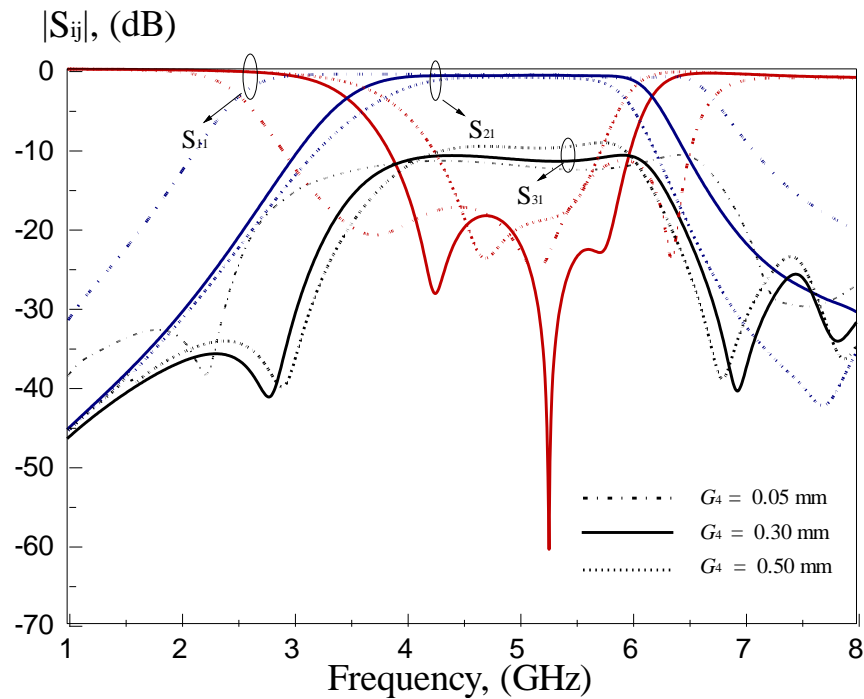


Figure 3.19: Effect of gap g_4 on the filtering directional coupler.

Description:

Gap g_4 plays a big role in the determination of the operating frequencies of the proposed directional coupler. When it is reduced to 0.05 mm, the passband becomes larger but the coupling level deteriorates. The passband is only 1.7 GHz when g_4 is decreased to 0.50mm, but with a flat coupling response. As a compromise, the gap g_4 is fixed at 0.30 mm at which maximum bandwidth (~ 2.14 GHz) and good coupling level (within 10 ± 1 dB) are obtainable, as shown in Figure 3.19.

Analysis 11

- Parameter : g_5
- Optimum value : 0.54 mm
- Step-down value : 0.14 mm
- Step-up value : 1.04 mm

Results:

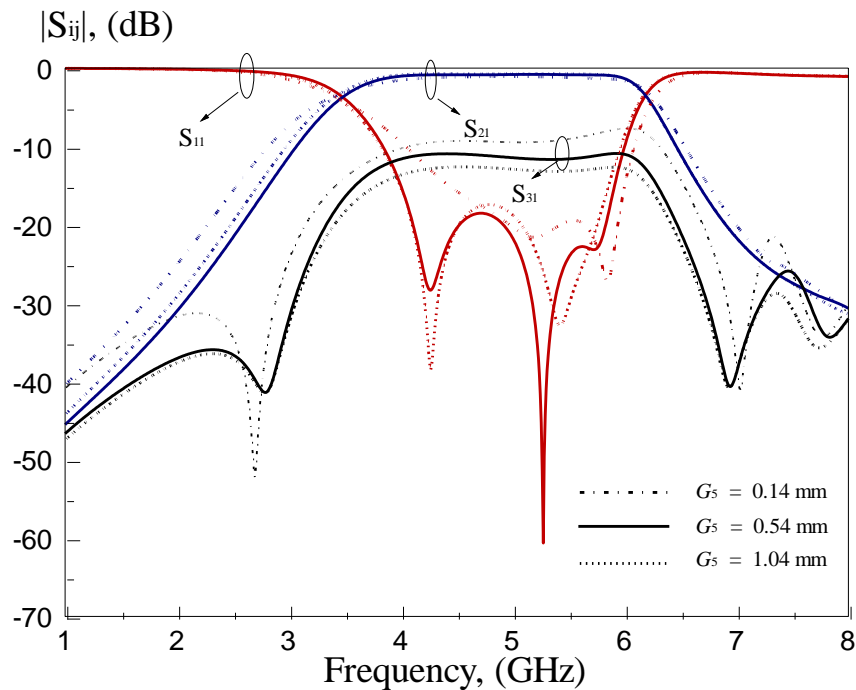


Figure 3.20: Effect of gap g_5 on the filtering directional coupler.

Description:

As for the coupled-line directional coupler, the gap between each pair of coupled lines play an important role in the determination of the desired coupling level of the directional coupler. When the gap g_5 is stepped down to 0.14 mm, the matching level becomes poorer while the insertion loss S_{31} stays at 8 ± 1 dB. Although the matching improves when the gap g_5 is increased to 1.04mm, in this case, the coupling level is only about -12 ± 1 dB, which is not the desired value. The optimum gap size for g_5 is 0.54 mm.

Analysis 12

- Parameter : g_6
- Optimum value : 0.50 mm
- Step-down value : 0.10 mm
- Step-up value : 1.00 mm

Results:

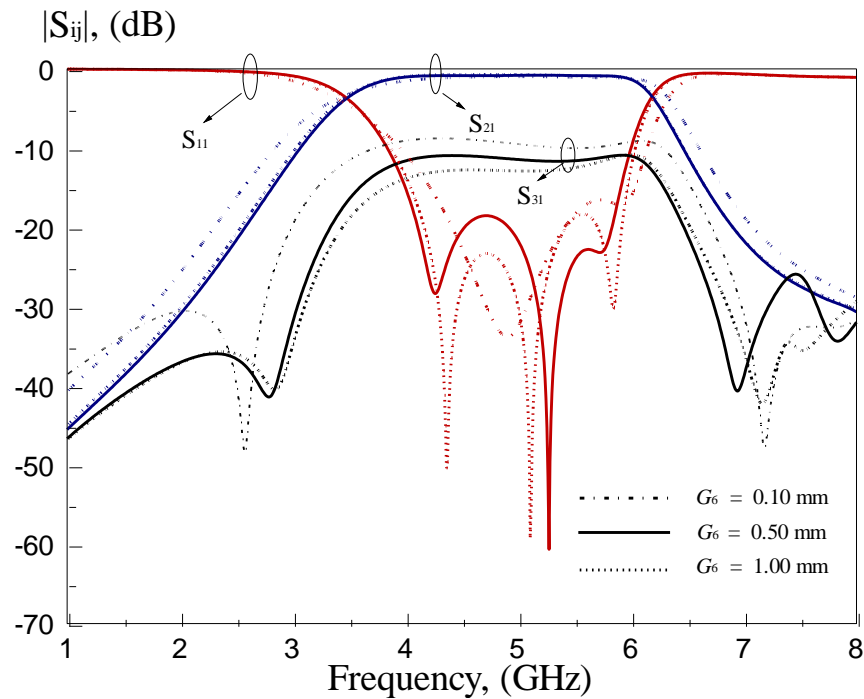


Figure 3.21: Effect of gap g_6 on the filtering directional coupler.

Description:

By controlling the gap g_6 , the coupling level of the proposed directional coupler can be adjusted. When the gap size is 0.10 mm, more signal power is able to pass through the coupled lines. As a result, the received power at port 3 is stronger and the difference between S_{21} and S_{31} falls within range of 8 ± 1 dB. If the gap g_6 increased to 1 mm, lesser signal power is able couple through the coupled lines. The gap g_6 is designed as 0.50 mm to achieve a constant coupling of 10 ± 1 dB at the desired operating frequencies.

Analysis 13

- Parameter : l_1
- Optimum value : 5.40 mm
- Step-down value : 3.40 mm
- Step-up value : 7.40 mm

Results:

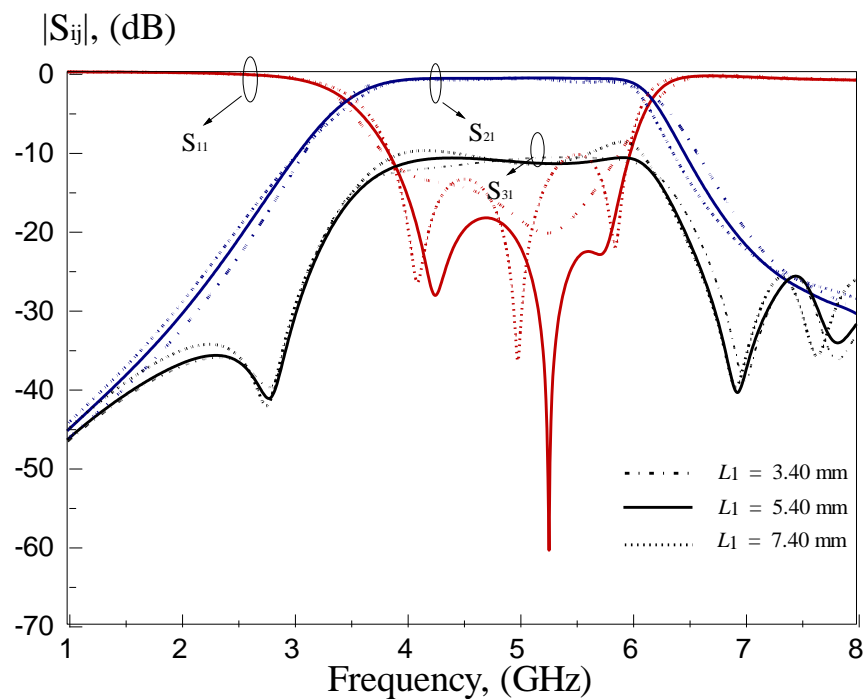


Figure 3.22: Effect of length l_1 on the filtering directional coupler.

Description:

The matching at Port 1 changes when the stub length l_1 is altered. With reference to Figure 3.22, the matching level is maintained below -20 dB at the optimum gap of 5.40 mm. This is important to ensure that the input signal not to get reflected back to the input port. Besides that, the coupling level is also affected when length l_1 changes. Hence, the length of l_1 is designed at 5.40 mm to achieve flat coupling level with maximum bandwidth.

Analysis 14

- Parameter : l_2
- Optimum value : 8.75 mm
- Step-down value : 7.75 mm
- Step-up value : 9.75 mm

Results:

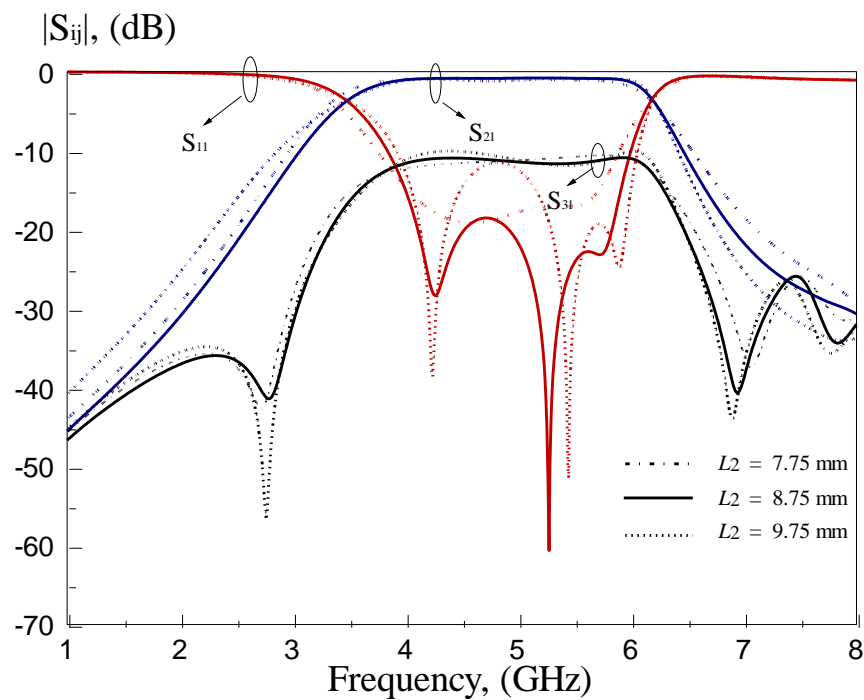


Figure 3.23: Effect of length l_2 on the filtering directional coupler.

Description:

The length l_2 has no significant effect on the positions of zeros and the coupling level. However, it causes the matching to vary. Obviously, it is much better when l_2 is equal to the optimum value. It can be maintained well below -20 dB across the entire operating passband.

Analysis 15

- Parameter : l_3
- Optimum value : 2.93 mm
- Step-down value : 2.43 mm
- Step-up value : 3.43 mm

Results:

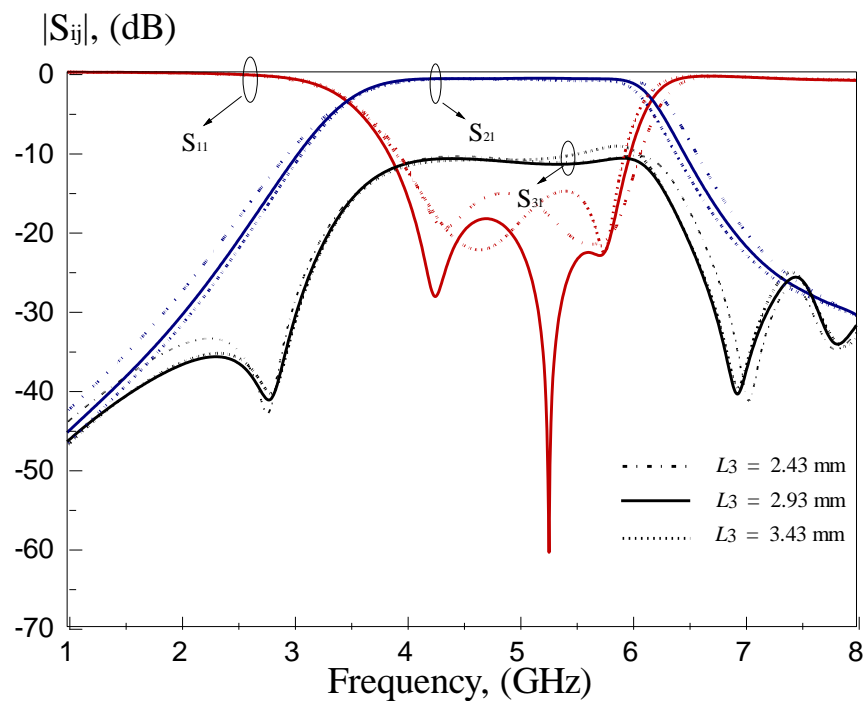


Figure 3.24: Effect of length l_3 on the filtering directional coupler.

Description:

The positions of zeros for both the S_{21} and S_{31} are not affected much when the length l_3 changes. When l_3 is varied to 2.43 mm or 3.43 mm, the impedance matching level becomes poorer, causing the bandwidth of the proposed directional coupler to reduce. Also, the coupling amplitude of the directional coupler fails to maintain at 10 ± 1 dB when l_3 is stepped up.

Analysis 16

- Parameter : l_4
- Optimum value : 3.00 mm
- Step-down value : 2.00 mm
- Step-up value : 4.00 mm

Results:

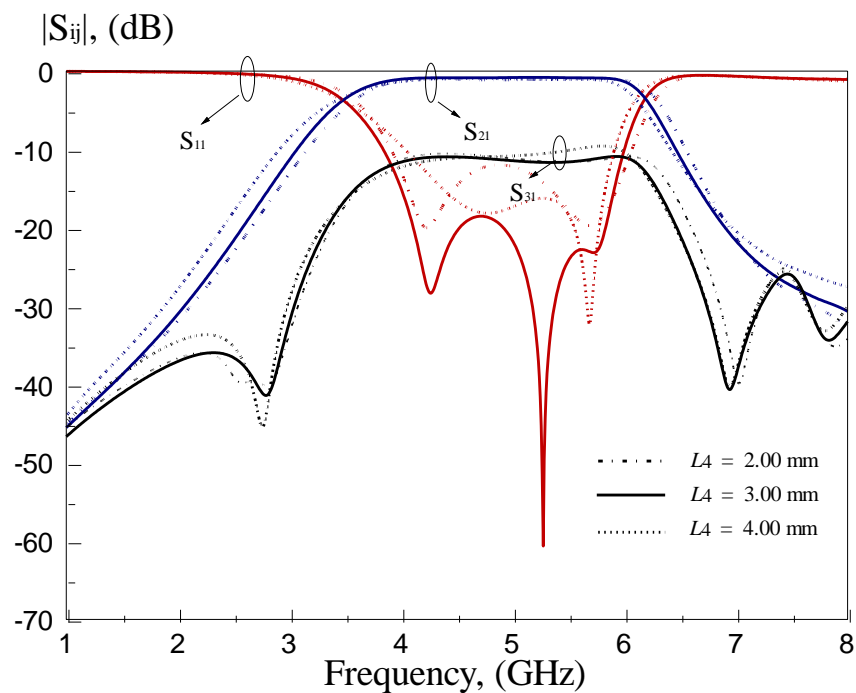


Figure 3.25: Effect of length l_4 on the filtering directional coupler.

Description:

The impedance matching of the proposed directional coupler is affected when the length l_4 changes. When l_4 is increased, the first pole of the directional coupler shifts higher. Also, it moves to combine with the second pole. In addition, the coupling level of the directional coupler fluctuates around 6 GHz. In this case, the length l_4 is designed as 3.00 mm. It has the maximum operating bandwidth with a coupling level of 10 ± 1 dB across the passband.

Analysis 17

- Parameter : l_5
- Optimum value : 6.88 mm
- Step-down value : 4.88 mm
- Step-up value : 8.88 mm

Results:

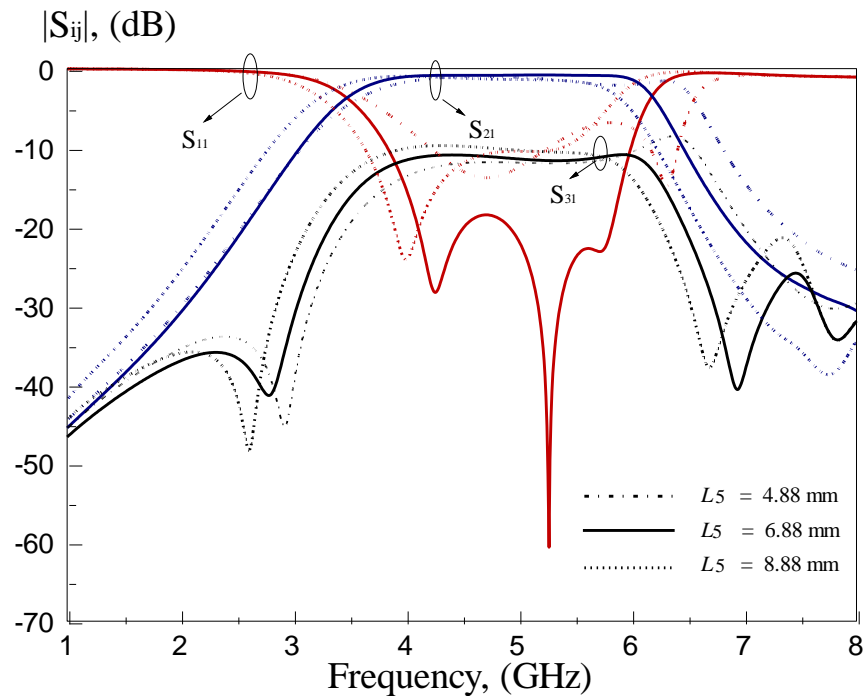


Figure 3.26: Effect of length l_5 on the filtering directional coupler.

Description:

The parameter l_5 has significant impact on the resonances of the proposed directional coupler. The pole frequencies become higher when l_5 is decreased and vice versa. This can be explained by $c = f\lambda$ - resonance at higher frequency has a shorter wavelength. For this design, the length $l_5 = 6.88$ mm gives the best performances in terms of bandwidth and coupling level.

Analysis 18

- Parameter : l_9
- Optimum value : 6.88 mm
- Step-down value : 4.88 mm
- Step-up value : 8.88 mm

Results:

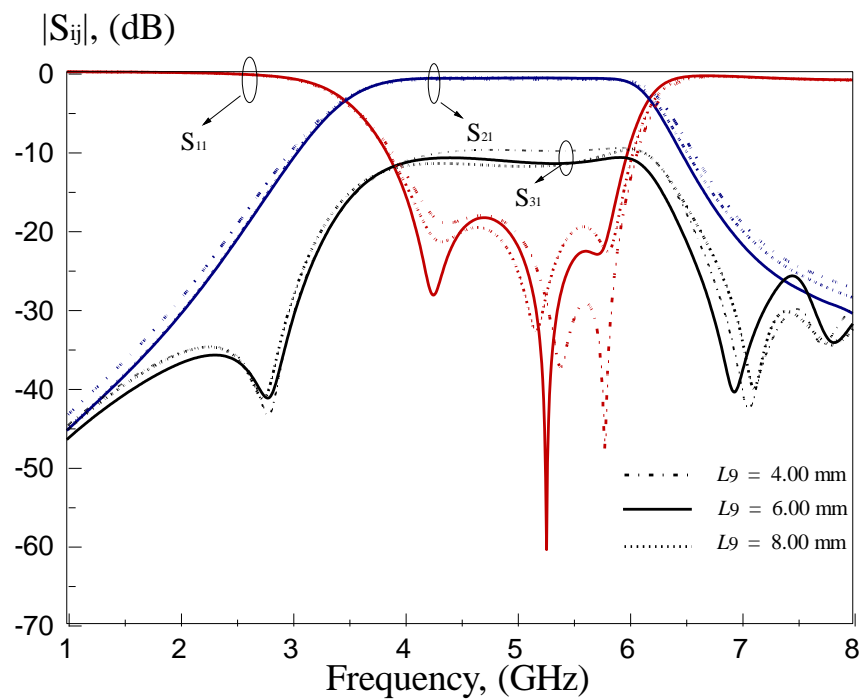


Figure 3.27: Effect of length l_9 on the filtering directional coupler.

Description:

Figure 3.27 shows the effect of l_9 on the amplitude response. It can be seen that flat coupling fails to maintain at 10 ± 1 dB if the value of l_9 changes. Apart from that, it has no significant effect on the positions of zeros.

3.3 Five-mode Filtering Directional Coupler

The proposed design in Section 3.2 can be improved to have a wider bandwidth by increasing the number of modes of the directional coupler. In the previous section, a bandpass-filtering directional coupler was designed operating in three modes. In this section, the design of the five-mode filtering directional coupler will be shown.

3.3.1 Configuration

Using the same concept discussed in section 3.2.1, a higher-order directional coupler with five resonance mode will be designed by adding in two additional microstrip coupled lines in the middle of the configuration. The newly proposed configuration is shown in Figure 3.28.

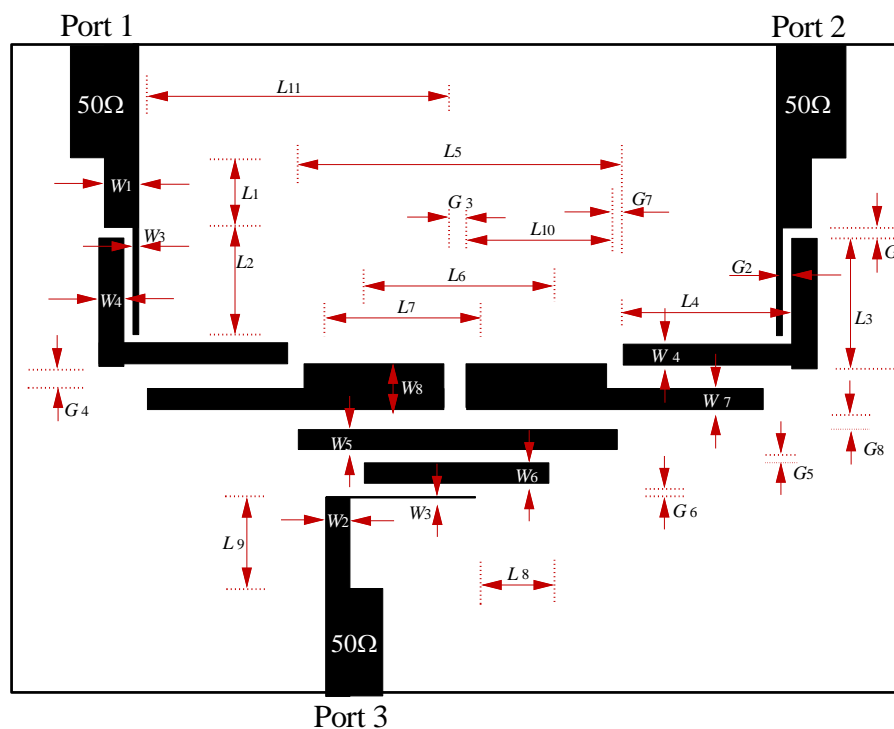


Figure 3.28: Top-down view of the five-mode filtering directional coupler

The detailed design parameters are given by: $w_1 = 1.4$ mm, $w_2 = 1.0$ mm, $w_3 = 0.3$ mm, $w_4 = 1.12$ mm, $w_5 = 1.14$ mm, $w_6 = 0.3$ mm, $w_7 = 1.14$ mm, $w_8 = 2.14$ mm, $l_1 = 4.06$ mm, $l_2 = 9.75$ mm, $l_3 = 14.0$ mm, $l_4 = 9.88$ mm, $l_5 = 21.0$ mm, $l_6 = 14.0$ mm, $l_7 = 10.0$ mm, $l_8 = 4.90$ mm, $l_9 = 5.68$ mm, $l_{10} = 12.0$ mm, $l_{11} = 21.5$ mm, $g_1 = 0.20$ mm, $g_2 = 0.20$ mm, $g_3 = 0.26$ mm, $g_4 = 0.30$ mm, $g_5 = 0.54$ mm, $g_6 = 0.4$ mm, $g_7 = 0.27$ mm, and $g_8 = 0.30$ mm.

The characteristic impedance of the center coupled-lines was slightly decreased by increasing the line width from w_7 (1.14 mm) to w_8 (2.14 mm) to enable higher coupling.

3.3.2 Results

The configuration was simulated using Ansoft HFSS. With reference to Figure 3.29, five resonances are observed with the first mode at 3.8 GHz. As can be seen from the simulation, the five-mode filtering directional coupler has the second pole combined with the third one at the frequency of 4.58 GHz. The fourth pole locates at the frequency of 5.5 GHz while the fifth one is at 5.7 GHz. With five poles combined, the operating frequency of this directional coupler stretches from 3.59 GHz to 5.83 GHz, covering a total bandwidth of 2.24 GHz. Again, the coupling level of the directional coupler is maintained at 10 ± 1 dB within the passband. The fractional bandwidth of the five-mode directional coupler can be calculated as follows:

Center Frequency

$$\begin{aligned}
 &= \frac{\text{LowerFrequency} + \text{HighFrequency}}{2} \\
 &= \frac{3.59 \text{ GHz} + 5.83 \text{ GHz}}{2} \\
 &= 4.71 \text{ GHz}
 \end{aligned}$$

Fractional Bandwidth

$$\begin{aligned}
 &= \frac{\text{HighFrequency} - \text{LowerFrequency}}{\text{CenterFrequency}} \times 100\% \\
 &= \frac{5.83 \text{ GHz} - 3.59 \text{ GHz}}{4.71 \text{ GHz}} \times 100\% \\
 &= 47.56\%
 \end{aligned}$$

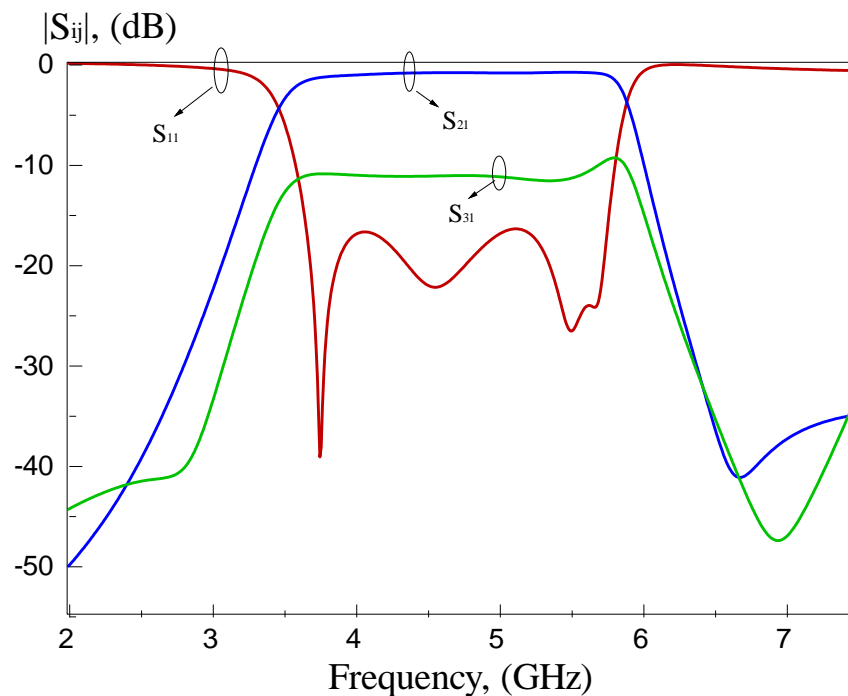


Figure 3.29: Amplitude responses of five-mode filtering directional coupler.

3.4 Discussion

In general, a highly selective directional coupler has high roll-off skirts. It contains zeros at the transition frequencies. This helps to filter out the undesired signals. In the past, this can be done by cascading a multimode bandpass filter next to a directional coupler, as shown in figure 3.30. However, a multimode filtering directional coupler has been proposed in this chapter as shown in figure 3.31 where the directional coupler has both high selectivity and wide bandwidth. The combination of the bandpass filter and the directional coupler helps to reduce the

complexity of the network. The bandwidth of the five-mode filtering directional coupler increases by 104.7% comparing with that of the three-mode one.

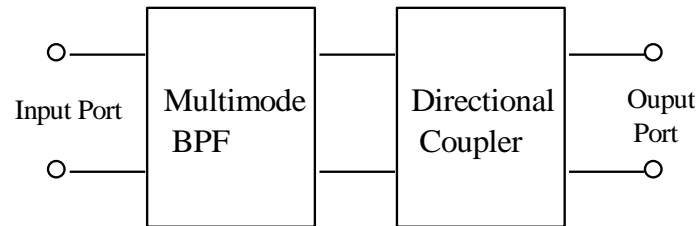


Figure 3.30: Cascading a multimode bandpass filter with a directional coupler.

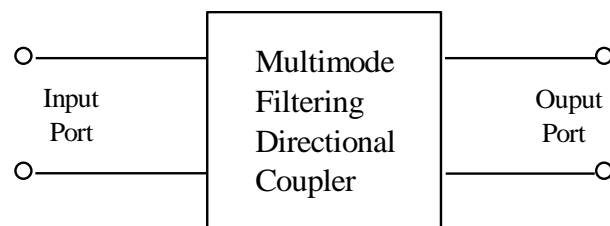


Figure 3.31: The proposed idea of the multimode filtering directional coupler.

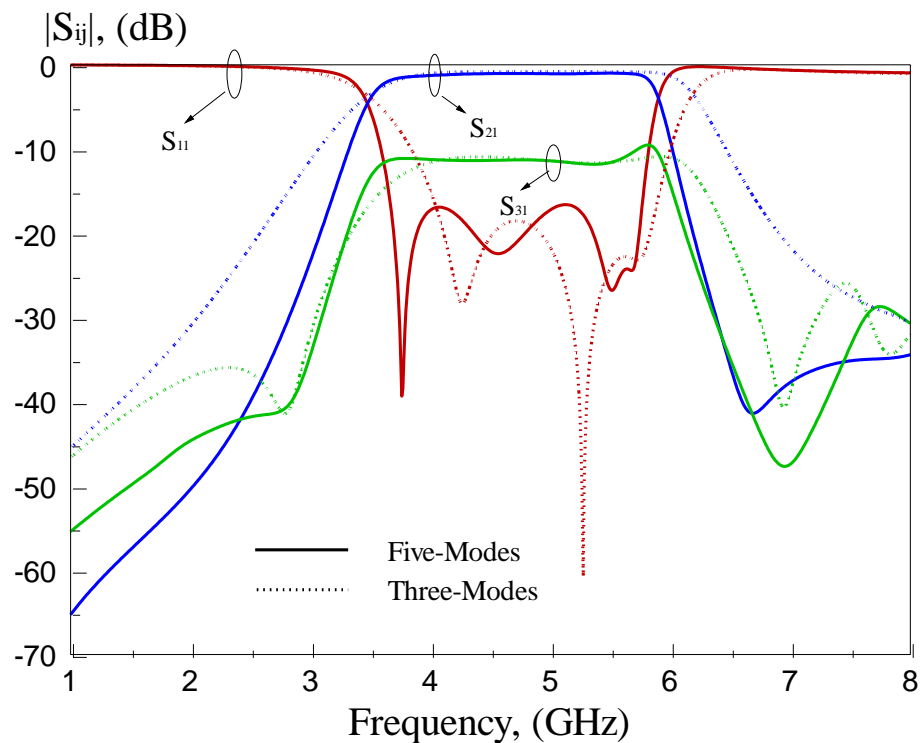


Figure 3.32: Amplitude responses of the three- and five-mode filtering directional couplers.

Based on the parametric analysis in Section 3.2.4, several parameters are found to be important for the performances of the directional couplers. Parameters such as g_3 , g_4 , and l_5 are crucial for the determination of the operating frequencies of the directional coupler. The coupling level is mainly affected by the gaps g_5 and g_6 . As a rule of thumb, the closer the coupled lines are placed, the more the signal couples through the lines. By knowing the characteristics and effects of all the design parameters, the proposed multimode filtering directional couplers can be easily optimized.

CHAPTER 4

MULTI-PORT DIRECTIONAL COUPLER

4.1 Background

In the beginning part of this chapter, a conventional directional coupler with four-port is simulated and analyzed. Next, a new six-port directional coupler will be designed and discussed. With this multi-port directional coupler, power splitting and network combining can be done easily. (Ferdinando Alessandri, Marco Giordano, Marco Guglielmi, Giacomo Martirano, Francesco Vitulli, May 2003).

4.2 Four-port Directional Coupler

Conventional coupled-line directional coupler is also known as four-port directional coupler where it consists of port 1 (input port), port 2 (direct port), port 3 (coupled port), and port 4 (isolation port). Based on the design theory that was discussed in Section 2.2, a four-port directional coupler with 10 dB coupling factor is simulated and investigated here.

4.2.1 Configuration

A directional coupler that operates across the ISM bands with a center frequency of 2.4 GHz was designed. Substrate RT Duroid 5870 (with dielectric constants of $\epsilon_r = 2.33$ and thickness of 1.57mm) was used in this simulation. By using theory of directional coupler, the quarter wavelength of this directional coupler is about 22 mm. Besides that, all the four ports of the directional coupler are designed with the characteristic impedance of 50Ω for ease of interconnection with other microwave systems. However, the coupled-line sections of the proposed configuration are designed at 90Ω to control the electrical signals flows in the directional coupler. The edge of the coupled-lines was cut to minimize power leakage to the surrounding.

With the design requirements stated above, a conventional directional coupler was drawn using the Ansoft HFSS. The top-down view of the directional coupler is shown in the figure below. The detailed design parameters are given by: $w_1 = 1.4$ mm, $w_2 = 2.0$ mm, $w_3 = 1.34$ mm, $l_1 = 8.83$ mm, $l_2 = 36.00$ mm, $l_3 = 13.74$ mm, and $g_1 = 0.60$ mm.

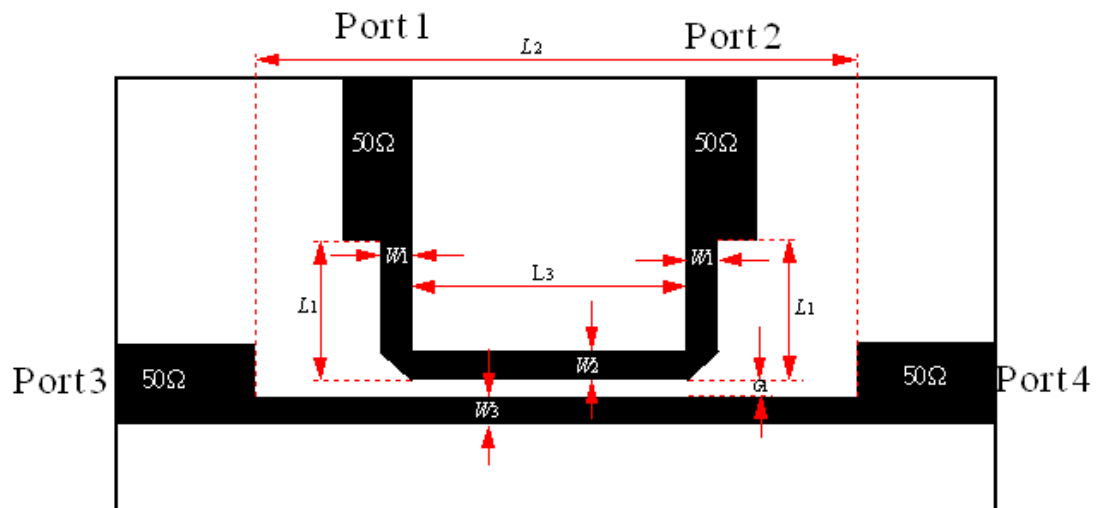


Figure 4.1: Top-down view of the four-port directional coupler.

4.2.2 Transmission Line Model

By using Microwave Office, an equivalent circuit that represents the four-port coupled-line directional coupler is built and analyzed. Ideally, the amplitude and phase responses obtained from this transmission line model (TLM) will match with the results obtained from Ansoft HFSS simulation. Figure 4.2 shows the TLM model of the four-port directional coupler. The detailed design parameters are given by: $w_1 = 4.00$ mm, $w_2 = 1.40$ mm, $w_3 = 2.00$ mm, $w_4 = 1.34$ mm, $w_5 = 1.34$ mm, $w_6 = 4.00$ mm, $l_1 = 10.00$ mm, $l_2 = 6.83$ mm, $l_3 = 13.74$ mm, $l_4 = 13.74$ mm, $l_5 = 11.30$ mm, $l_6 = 10.00$ mm, and $g_1 = 0.60$ mm.

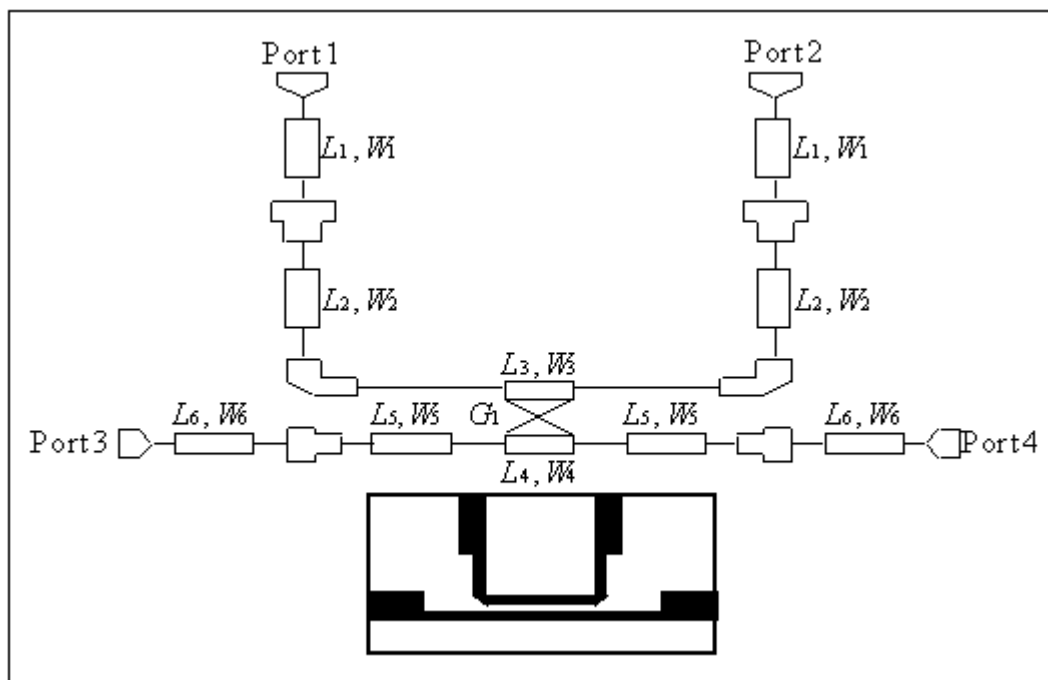


Figure 4.2: Transmission line model of the four-port directional coupler.

4.2.3 Results

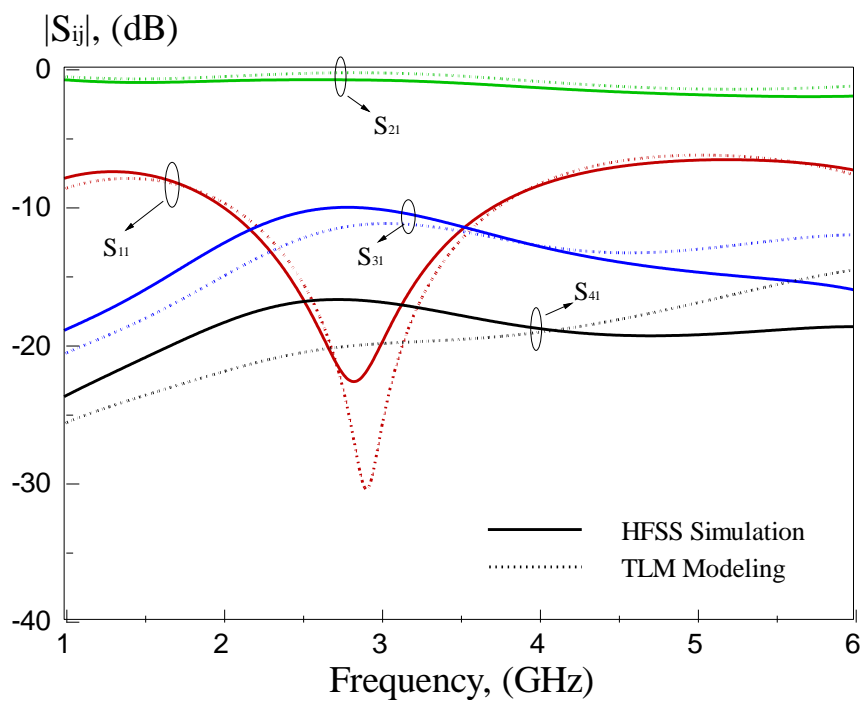


Figure 4.3: S-parameters of the four-port directional coupler.

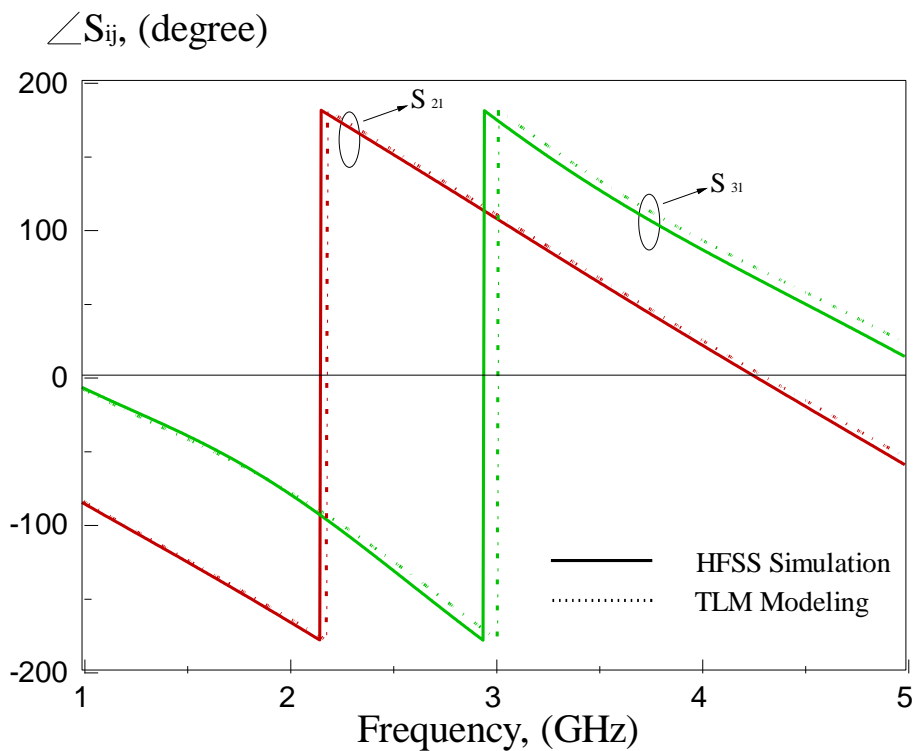


Figure 4.4: Phase response of the four-port directional coupler.

Table 4.1: Comparison of HFSS simulation and TLM modelling.

| | HFSS Simulation | TLM Modeling |
|---------------------------|-----------------|--------------|
| f_L (GHz) / f_H (GHz) | 2.41 / 3.25 | 2.50 / 3.34 |
| f_c (GHz) | 2.83 | 2.92 |
| Fractional Bandwidth (%) | 29.68 | 28.77 |

The amplitude and phase responses of the TLM model and HFSS simulation are compared in this section. With reference to Figure 4.3, we observe that the operating frequency band for HFSS simulation is from 2.41 GHz to 3.25 GHz with a total bandwidth of 843 MHz. The reflection coefficient S_{11} is slightly offset and it operates from 2.5 GHz to 3.34 GHz, giving a total bandwidth of 843 MHz as well. This can be caused by the 90° bends that make the proposed design compact. Besides that, the signal at the isolation port is kept well below -15 dB. With gap g_1 of 0.60 mm between the microstrip coupled-lines, only 10% of the input power can be transmitted to port 3. In this case, the insertion loss S_{31} of the directional coupler is designed at -10 dB across the operating frequencies.

By the way, the phase responses of the HFSS simulation and transmission line model agree well. Hence, it can be concluded that the TLM model is the equivalence of the HFSS simulation.

4.3 Six-port Directional Coupler

Based on the design methodology of the four-port directional coupler, a novel six-port directional coupler was proposed and designed. The main idea of this project is to combine two independent directional couplers into one. A directional coupler with two output coupling ports can then be obtained. In this design, it is very crucial to minimize the interaction of the two individual parts.

In this experiment, a six-port directional coupler with the coupling factors of 10 dB and 20 dB were designed. It has a total of six ports in this newly proposed directional coupler. Port 1 functions as an input port and Port 2 as a direct port. For this design, Port 3 and 4 are the coupled ports to provide coupling levels of 10 dB and 20 dB, respectively. Port 5 and 6 are the isolation ports.

4.3.1 Configuration

A six-port directional coupler has been proposed and analyzed successfully in this research project. The top-down view of the proposed directional coupler is shown in Figure 4.5. It was fabricated on a substrate RT Duroid 5870 substrate (with dielectric constants of $\epsilon_r = 2.33$ and thickness of 1.57mm), with the prototype shown in Figure 4.6.

The corners of the coupled-lines were trimmed to minimize the radiation loss. As mentioned earlier, this new directional coupler is composed by two independent ones that are combined and merged. It can be obtained from calculations that a gap of 0.60 mm in between two coupled lines yields a coupling level of 10 dB. Also, separation of 1.25 mm introduces coupling amplitude of 20 dB. Both of the coupled lines (with gap sizes 0.60 and 1.25 mm) sections are then combined to become a dual-channel directional coupler to give coupling outputs of 10 dB and 20 dB simultaneously. The gaps between the coupled lines play an important role in the determination of the coupling factors of the proposed multi-port directional coupler. Besides that, the transmission line w_2 (2.0 mm) that is used to connect with another w_1 (1.4 mm) is designed to be broader for a better impedance matching. The proposed directional coupler is symmetrical with high isolation and good matching.

The detailed design parameters are given by: $w_1 = 1.4$ mm, $w_2 = 2.0$ mm, $w_3 = 1.34$ mm, $l_1 = 8.83$ mm, $l_2 = 8.58$ mm, $l_3 = 13.74$ mm, $l_4 = 22.74$ mm, $l_5 = 36.0$ mm,

$g_1 = 0.60$ mm and $g_2 = 0.65$ mm. The proposed six-port directional coupler is implemented on microstrip.

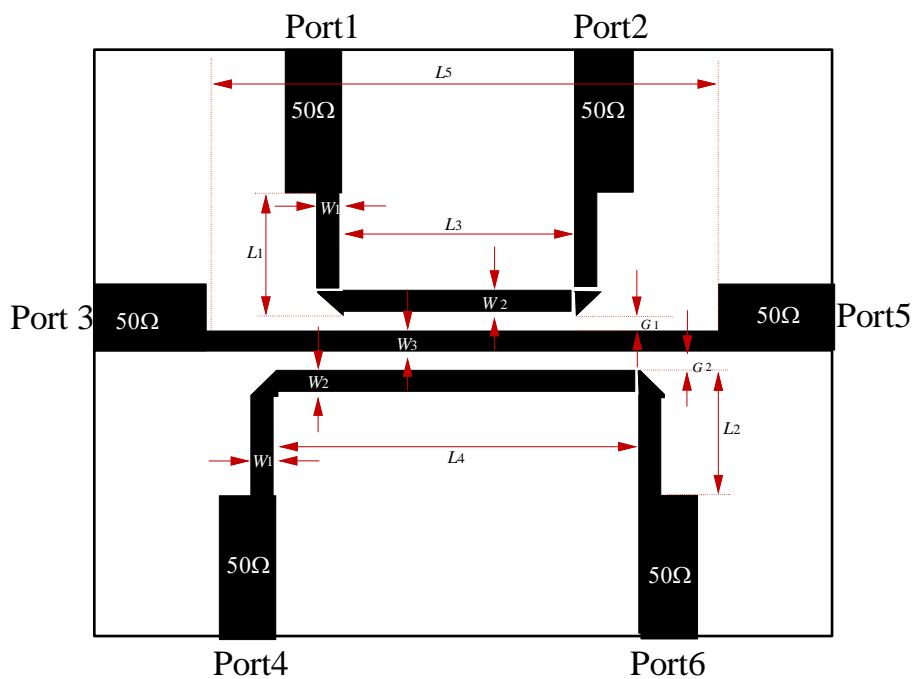


Figure 4.5: Top-down view of the proposed six-port directional coupler.

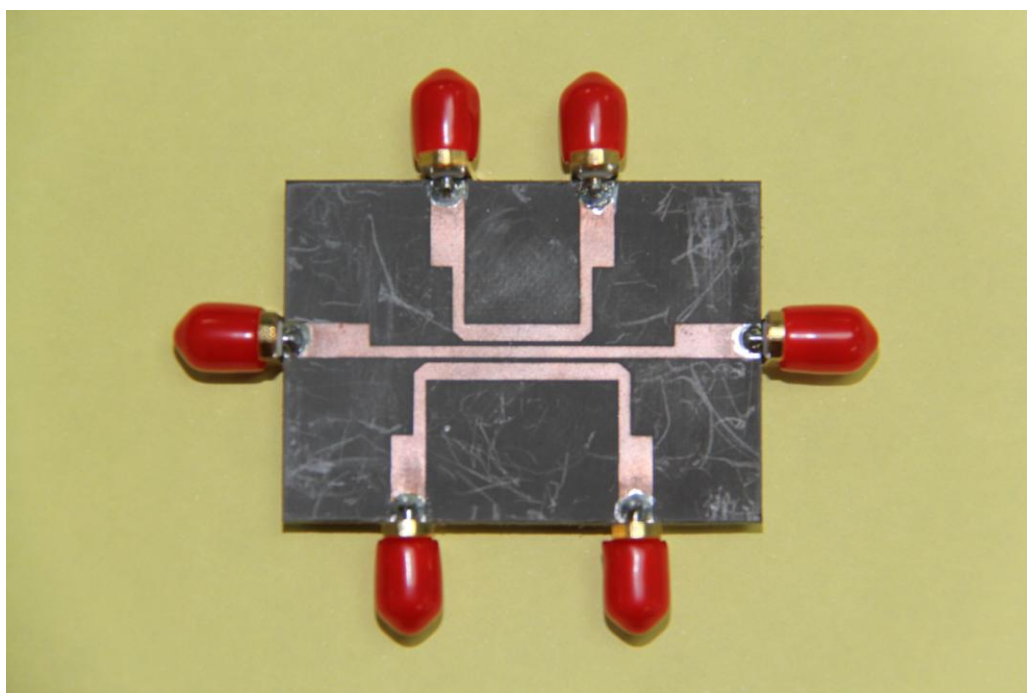


Figure 4.6: Prototype of the proposed six-port directional coupler.

4.3.2 Transmission Line Model

By converting the directional coupler into its TLM equivalent model, I would like to show that a dual-channel directional coupler can be realised. Figure below shows the corresponding equivalent circuit of the proposed directional coupler, which was simulated using Microwave Office. A M3CLIN (3 edge coupled microstrip lines) model was used to represent the coupling effect of the physical circuit.

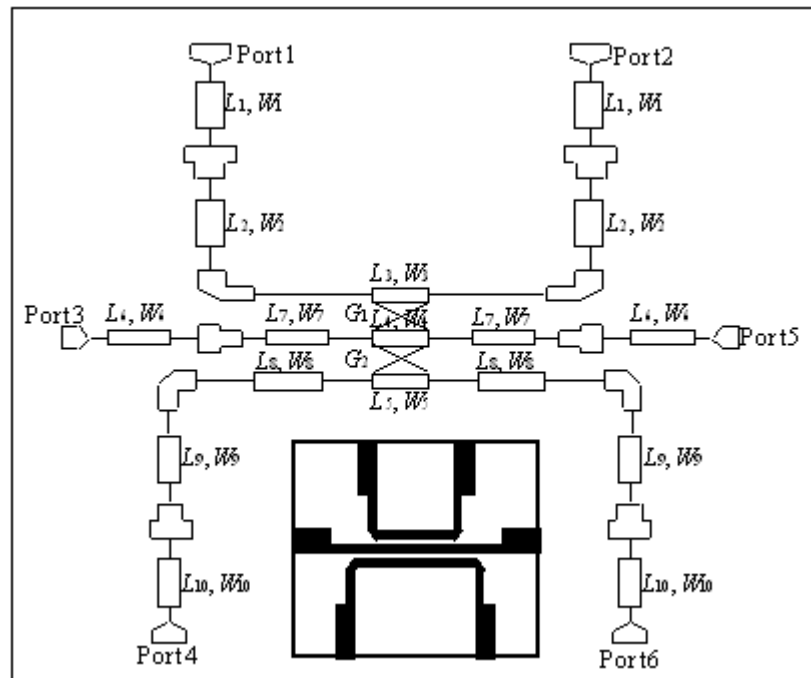


Figure 4.7: Transmission line model of the six-port directional coupler.

The detailed design parameters are given by: $w_1 = 4.00$ mm, $w_2 = 1.40$ mm, $w_3 = 2.00$ mm, $w_4 = 1.34$ mm, $w_5 = 2.00$ mm, $w_6 = 4.00$ mm, $w_7 = 1.34$ mm, $w_8 = 2.00$ mm, $w_9 = 1.40$ mm, $w_{10} = 4.00$ mm, $l_1 = 10.00$ mm, $l_2 = 6.83$ mm, $l_3 = 13.74$ mm, $l_4 = 13.74$ mm, $l_5 = 13.74$ mm, $l_6 = 10.00$ mm, $l_7 = 11.13$ mm, $l_8 = 4.50$ mm, $l_9 = 6.58$ mm, $l_{10} = 10.00$ mm, $g_1 = 0.60$ mm, and $g_2 = 0.65$ mm.

4.3.3 Results

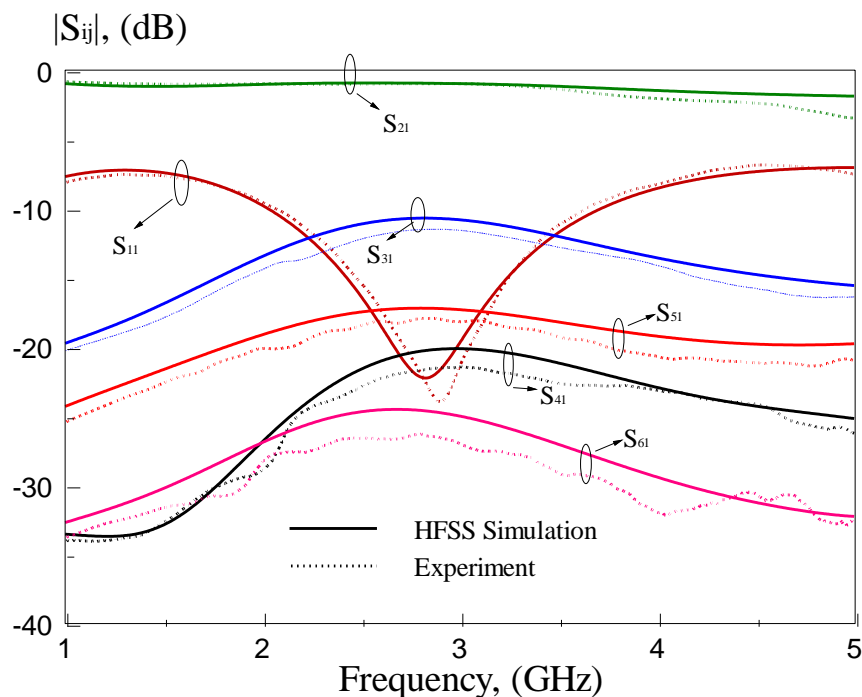


Figure 4.8: Amplitude responses of the HFSS simulation and experiment for the proposed six-port directional coupler.

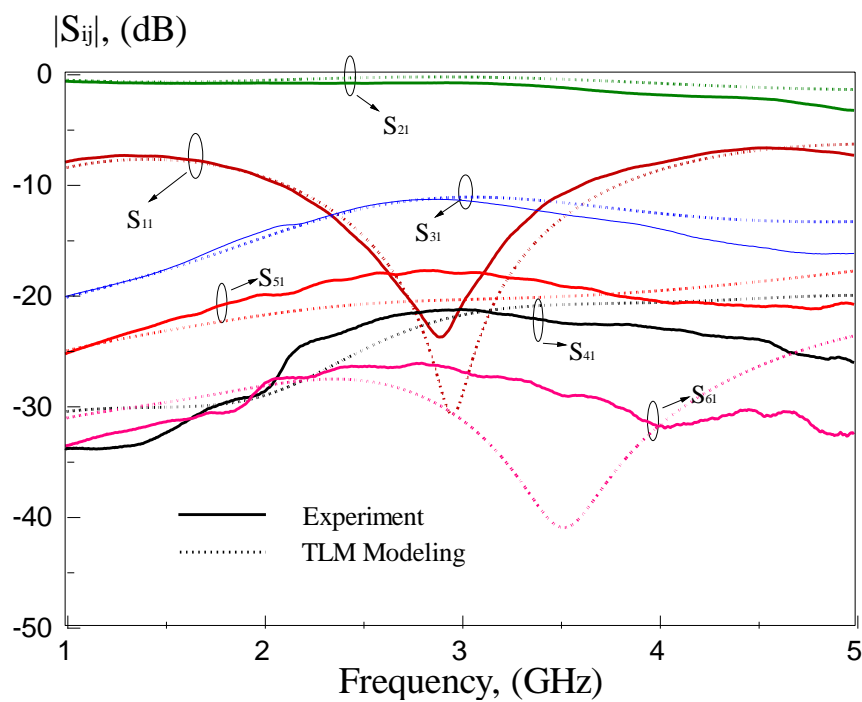


Figure 4.9: Amplitude responses of the experiment and TLM model for the proposed six-port directional coupler.

Before carrying out this experiment, the proposed six-port directional coupler was drawn and simulated by using Ansoft HFSS. A Vector Network Analyzer was used to measure the performance of the directional coupler. Amplitude and phase responses of the six-port directional coupler were analyzed.

In this project, the reflection coefficient is assumed to achieve -15 dB in the frequency passband. A lower reflection can help to improve the isolation level and impedance matching of the proposed directional coupler.

Table 4.2: Comparison of the experiment, HFSS simulation, and TLM modelling.

| | Experiment | HFSS Simulation | TLM Modeling |
|---------------------------|-------------|-----------------|--------------|
| f_L (GHz) / f_H (GHz) | 2.66 / 3.25 | 2.54 / 3.27 | 2.65 / 3.65 |
| f_c (GHz) | 2.955 | 2.905 | 3.15 |
| Fractional Bandwidth (%) | 19.97 | 25.13 | 31.75 |

From the HFSS simulation, the operating frequencies of the directional coupler are found ranging from 2.54 GHz to 3.27 GHz with a total bandwidth of 730 MHz. The measured frequency range is from 2.66 GHz to 3.25 GHz, giving a total bandwidth of 590 MHz. The measured bandwidth is 80.82% of that for simulation. Here, the coupling levels must be 10 dB at Port 3 and 20 dB Port 4 simultaneously. For the transmission line model, a 1 GHz of operating bandwidth can be achieved, with a fractional bandwidth of 31.75%. The signals at the isolation ports (Port 5 and 6) are maintained well below -18dB. This is important as signal is not supposed to transmit to the isolation ports.

Figures 4.10 and figure 4.11 show the phase responses of the proposed six-port directional coupler. As can be seen from the figures, we can confirm that the TLM model is the equivalence of the six-port directional coupler as good agreement is found at all frequencies.

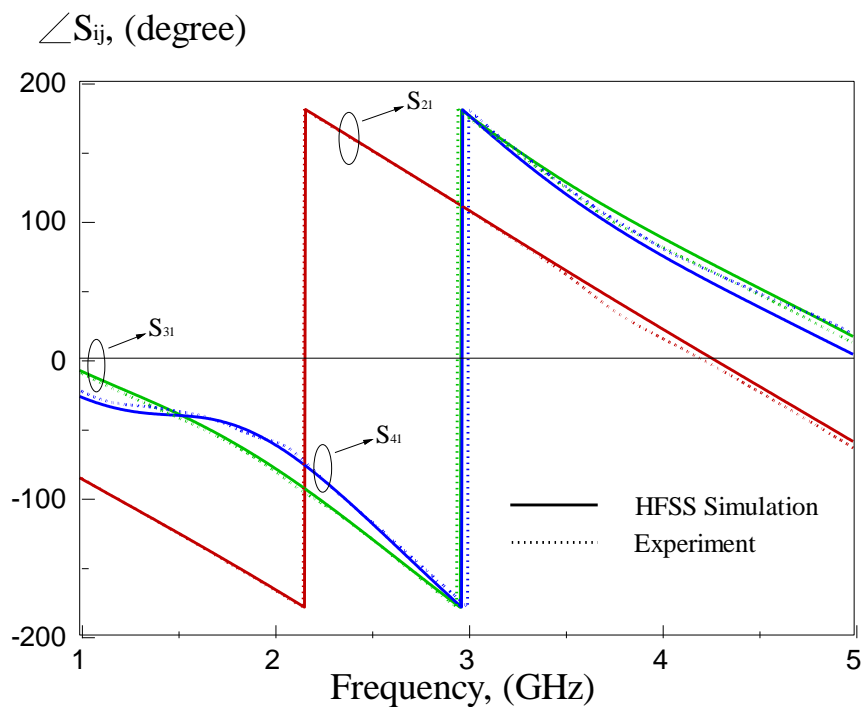


Figure 4.10: Phase responses of the HFSS simulation and experiment for the six-port directional coupler.

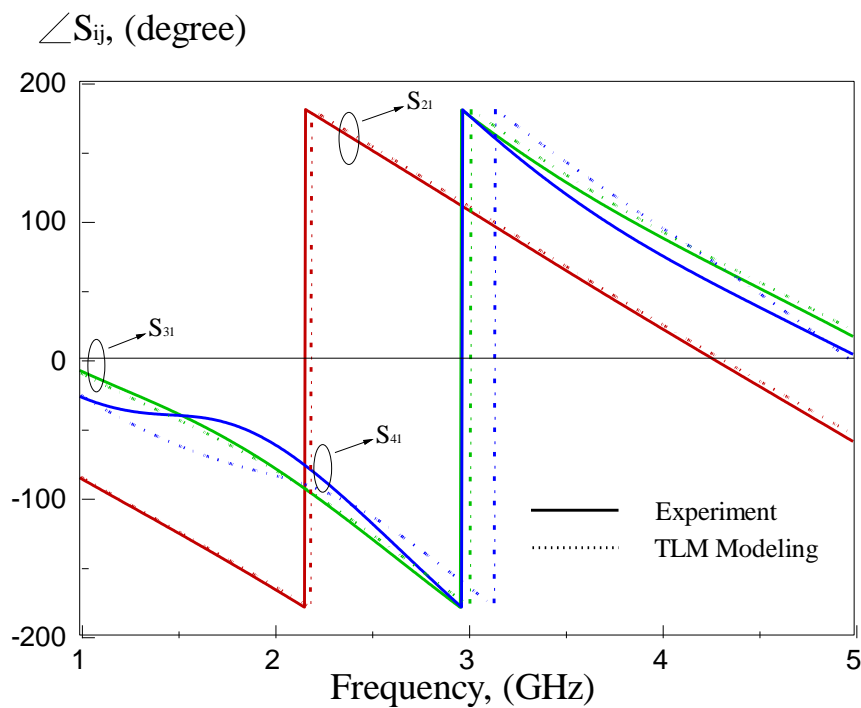


Figure 4.11: Phase responses of the experiment and TLM model for the six-port directional coupler.

4.3.4 Parametric Analysis

All the design parameters were analyzed using HFSS to study the effects. The design considerations and issues of each parameter will be discussed here.

Analysis 1

- Parameter : w_1
- Optimum value : 1.4 mm
- Step-down value : 1.0 mm
- Step-up value : 1.8 mm

Results:

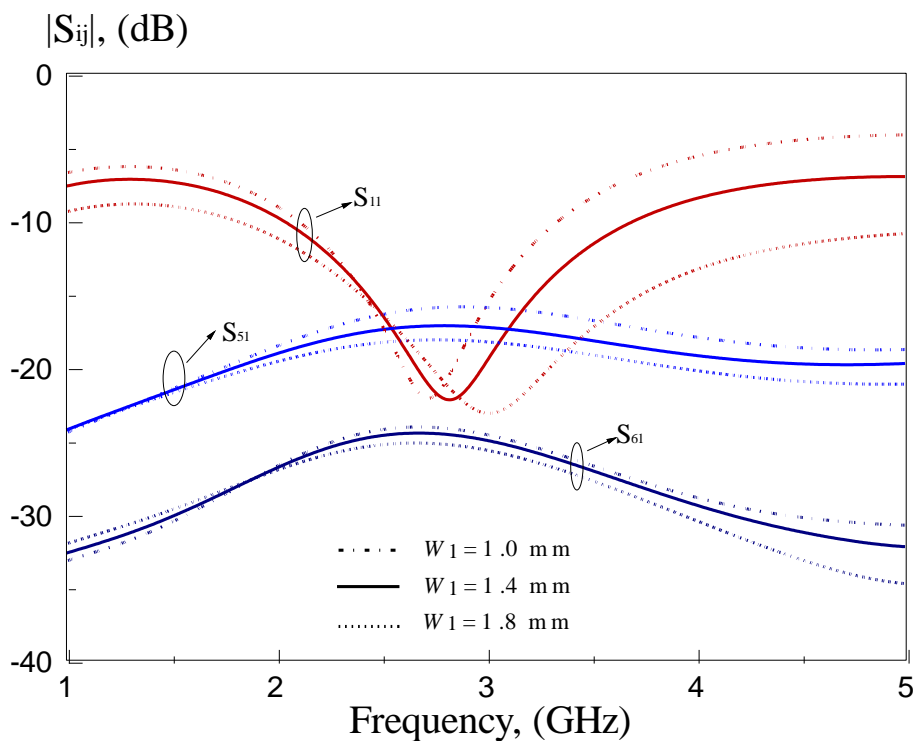


Figure 4.12: Effects of width w_1 on the reflection coefficient and isolation.

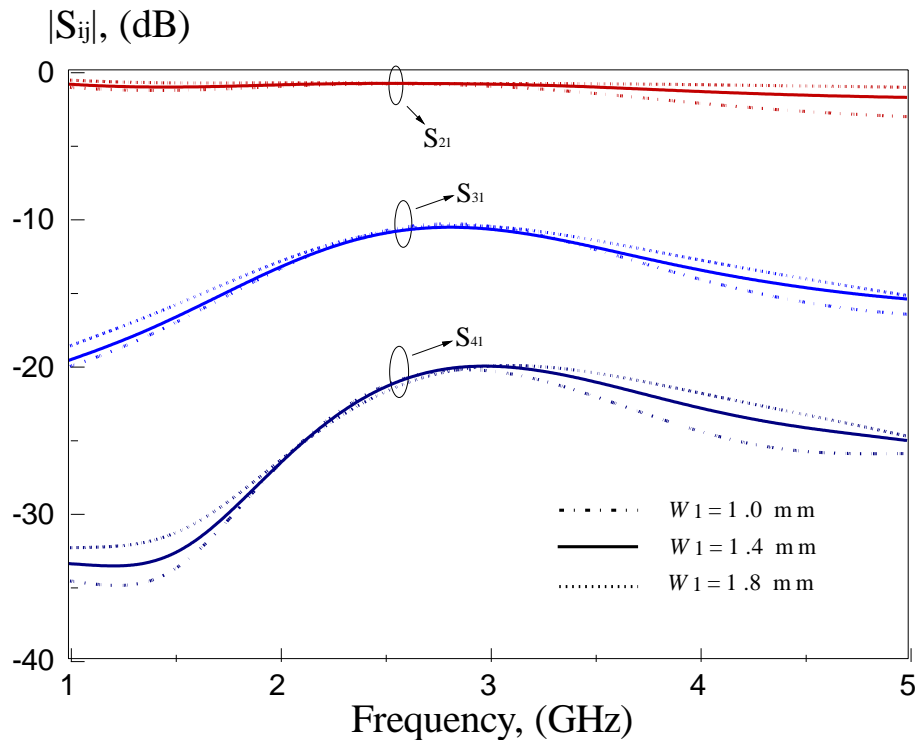


Figure 4.13: Effects of width w_1 on the insertion loss and coupling.

Description:

By observing the amplitude responses when varying parameter w_1 , we can clearly see that the resonance frequency of the directional coupler is affected. When line width w_1 is stepped down, the bandwidth of the proposed directional coupler becomes narrower. In this case, the resonance frequency of the proposed directional coupler increases. Minor effect is seen on the isolation port. However, the parameter w_1 does not cause significant effect on the direct and couple ports.

Analysis 2

- Parameter : w_2
- Optimum value : 2.0 mm
- Step-down value : 1.5 mm
- Step-up value : 2.5 mm

Results:

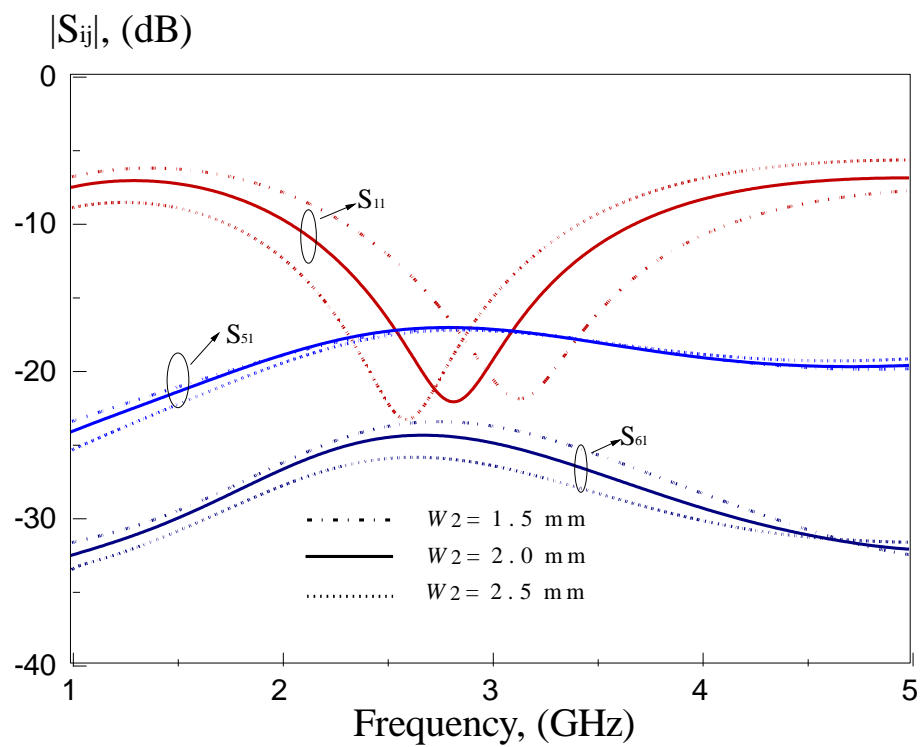


Figure 4.14: Effects of width w_2 on the reflection coefficient and isolation.

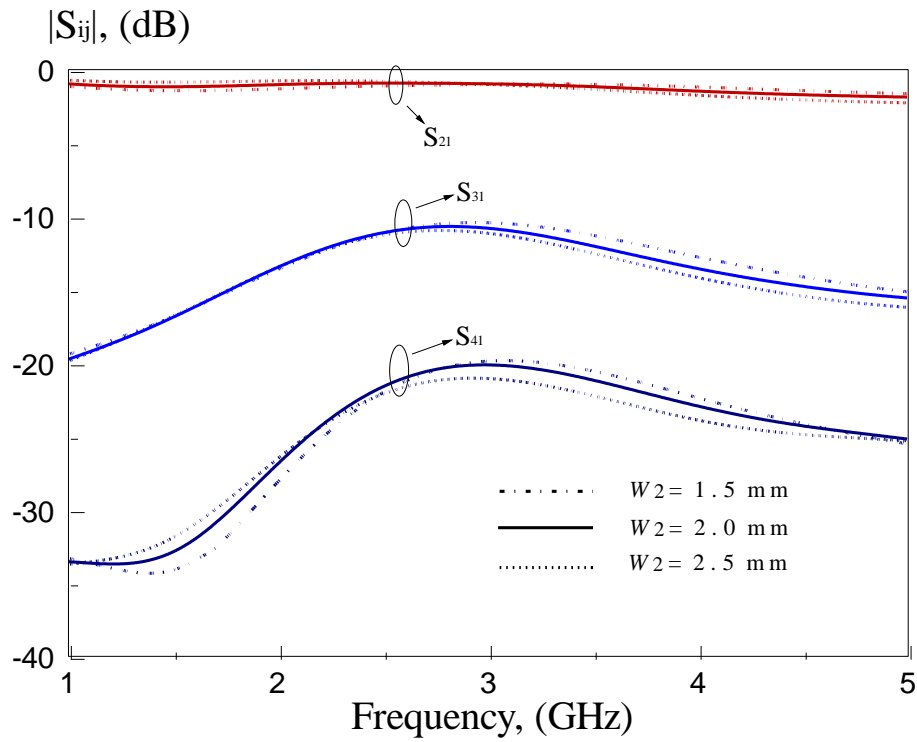


Figure 4.15: Effects of width w_2 on the insertion loss and coupling.

Description:

The parameter w_2 affects the operating frequency of the proposed directional coupler. It becomes higher when width w_2 is decreased. It has no significant effect on the transmission coefficients (S_{21} , S_{31} , and S_{41}). The second isolation port (Port 6) has improved when parameter w_3 is stepped up.

Analysis 3

- Parameter : w_3
- Optimum value : 1.34 mm
- Step-down value : 1.04 mm
- Step-up value : 1.64 mm
-

Results:

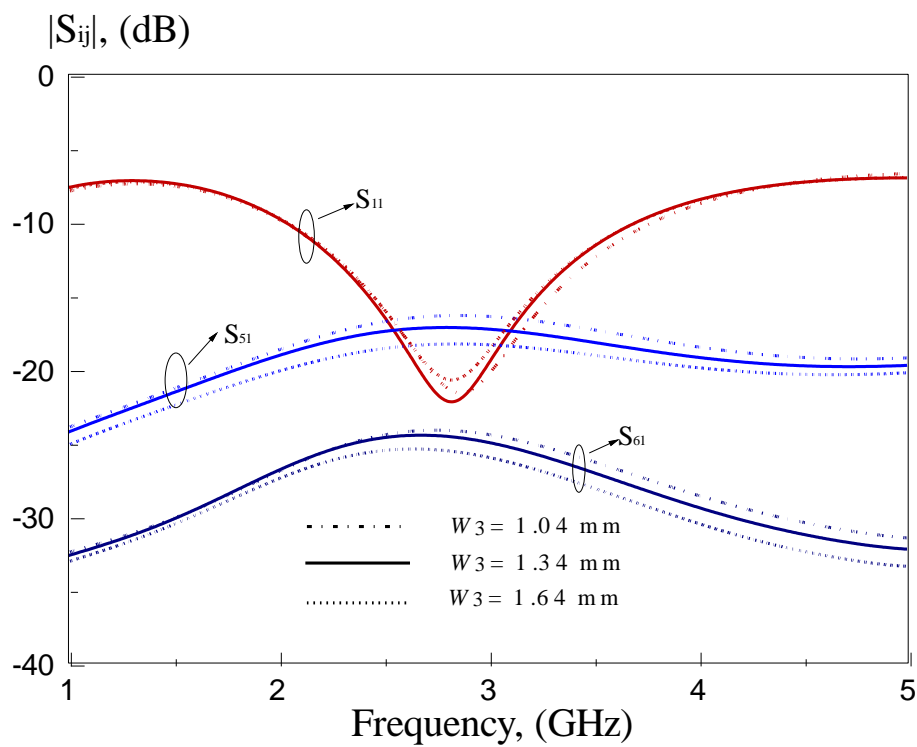


Figure 4.16: Effects of width w_3 on the reflection coefficient and isolation.

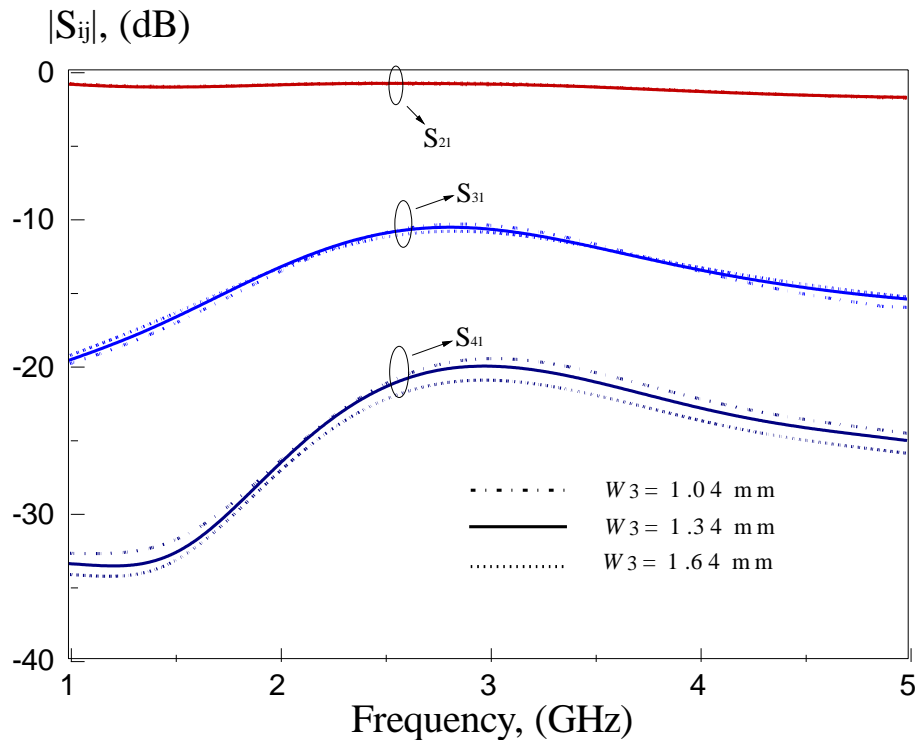


Figure 4.17: Effects of width w_3 on the insertion loss and coupling.

Description:

Firstly, the resonance frequency of the proposed directional coupler is not affected when the width w_3 changes. Also, S_{21} and S_{31} remain unchanged as well. The second coupled port (S_{41}) receives weaker signal for a larger w_3 . It can be caused by impedance mismatch.

Analysis 4

- Parameter : g_1
- Optimum value : 0.60 mm
- Step-down value : 0.35 mm
- Step-up value : 0.80 mm

Results:

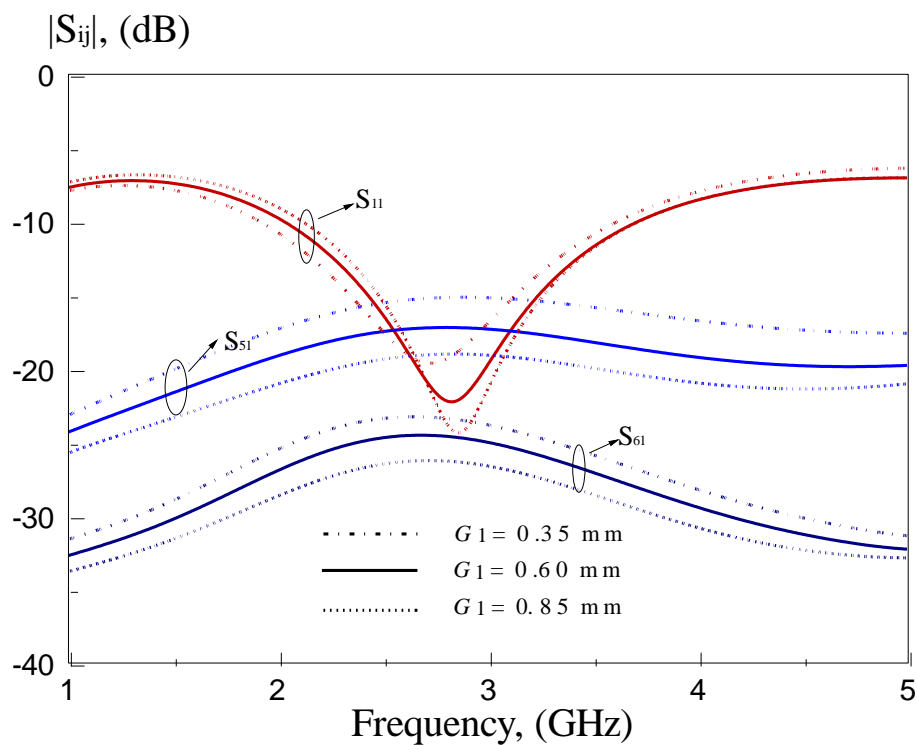


Figure 4.18: Effects of gap g_1 on the reflection coefficient and isolation.

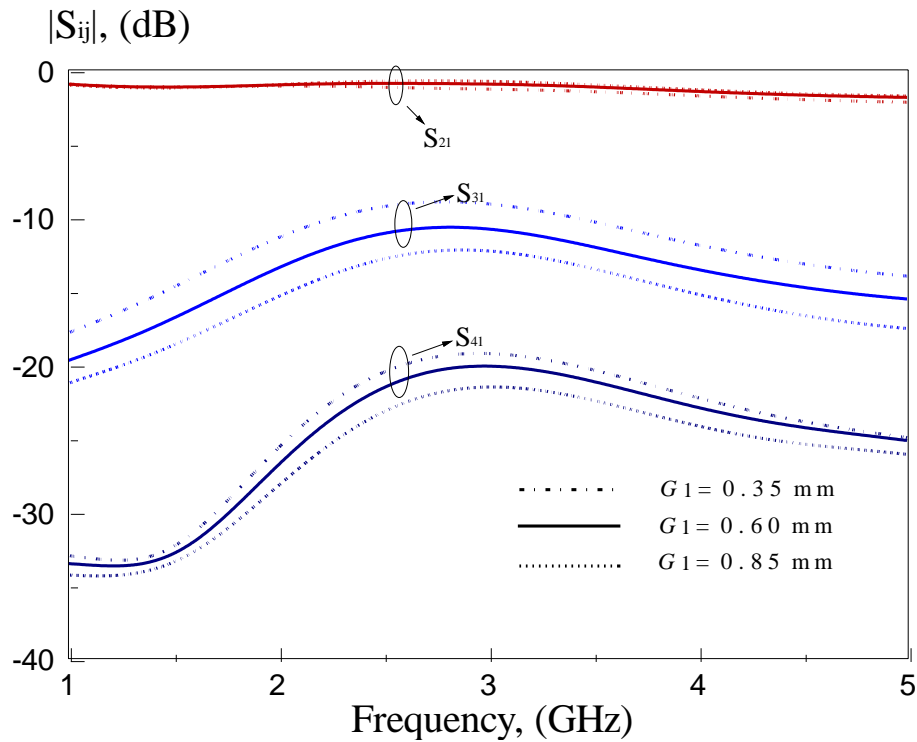


Figure 4.19: Effects of gap g_1 on the insertion loss and coupling.

Description:

As can be seen in the figures, we can clearly see that the gap g_1 plays an important role in deciding how much is signal coupled through the directional coupler. More signal power is received at the coupled ports when the gap between coupled-lines is closer. Here, the gap g_1 is chosen to be 0.60 mm so that it can contribute a total coupling level of 10 dB at Port 3 and 20 dB at Port 4. It has no major effect on the reflection coefficient S_{11} .

Analysis 5

- Parameter : g_2
- Optimum value : 0.65 mm
- Step-down value : 0.40 mm
- Step-up value : 0.90 mm

Results:

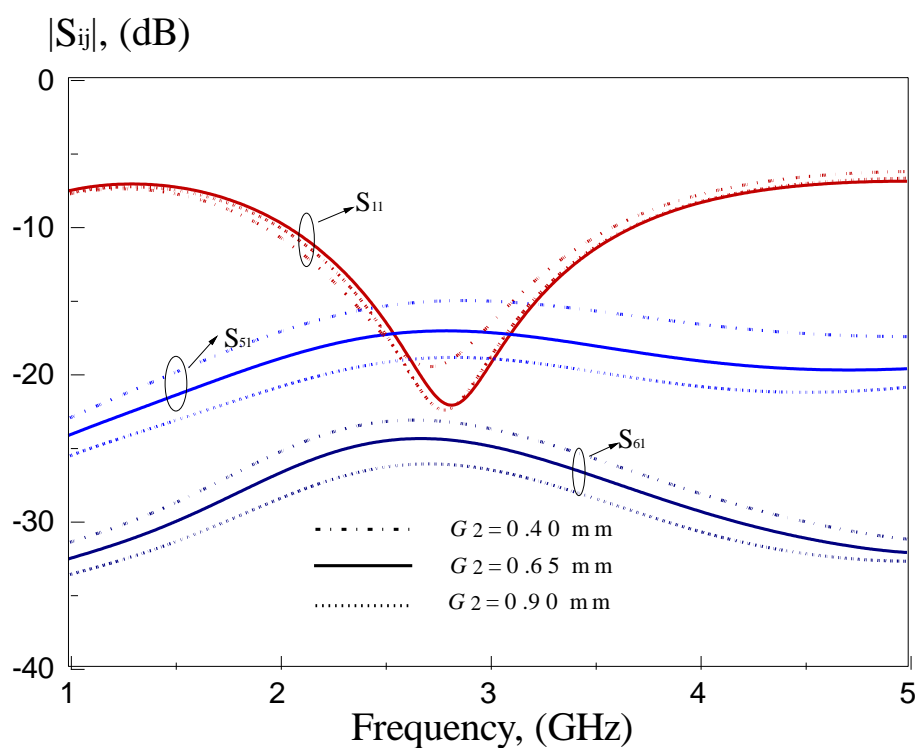


Figure 4.20: Effects of gap g_2 on the reflection coefficient and isolation.

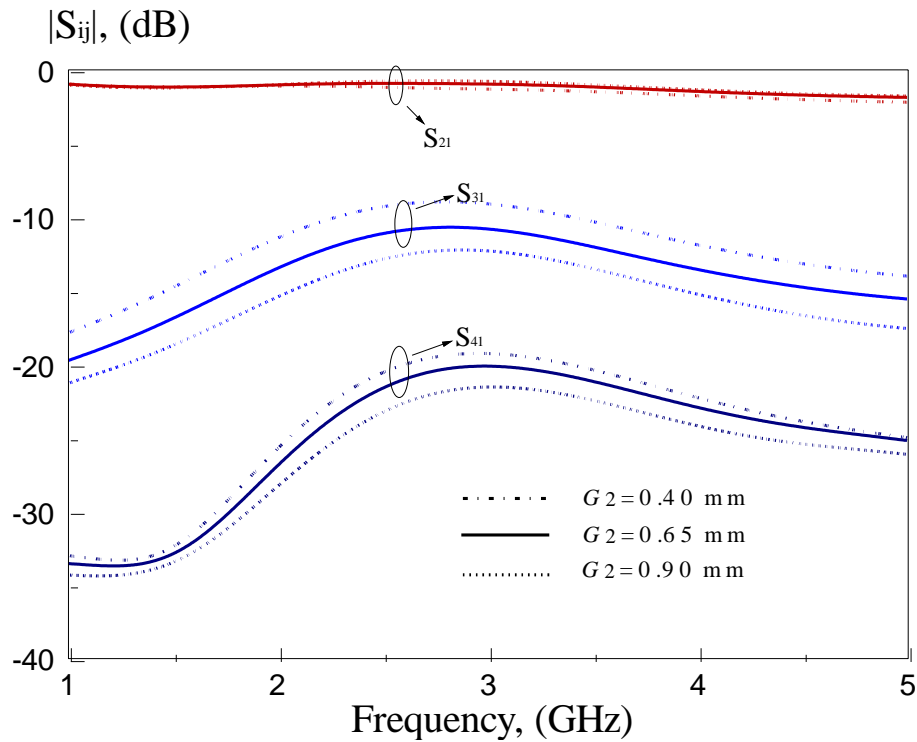


Figure 4.21: Effects of gap g_2 on the insertion loss and coupling.

Description:

Parameter g_2 has the same effect as that for g_1 . Gap g_2 is the gap between second and third coupled lines shown in Figure 4.5. The received signals S_{21} and S_{31} of the directional coupler are stronger when the gap g_2 is stepped down but weaker when it is stepped up. The same effect goes for the isolation ports. A difference of 10 dB in between S_{31} and S_{21} as well as another difference of 20 dB in between S_{41} and S_{21} can concurrently be achieved by using the gap g_2 of 0.65 mm.

Analysis 6

- Parameter : l_1
- Optimum value : 8.83 mm
- Step-down value : 7.83 mm
- Step-up value : 9.83 mm

Results:

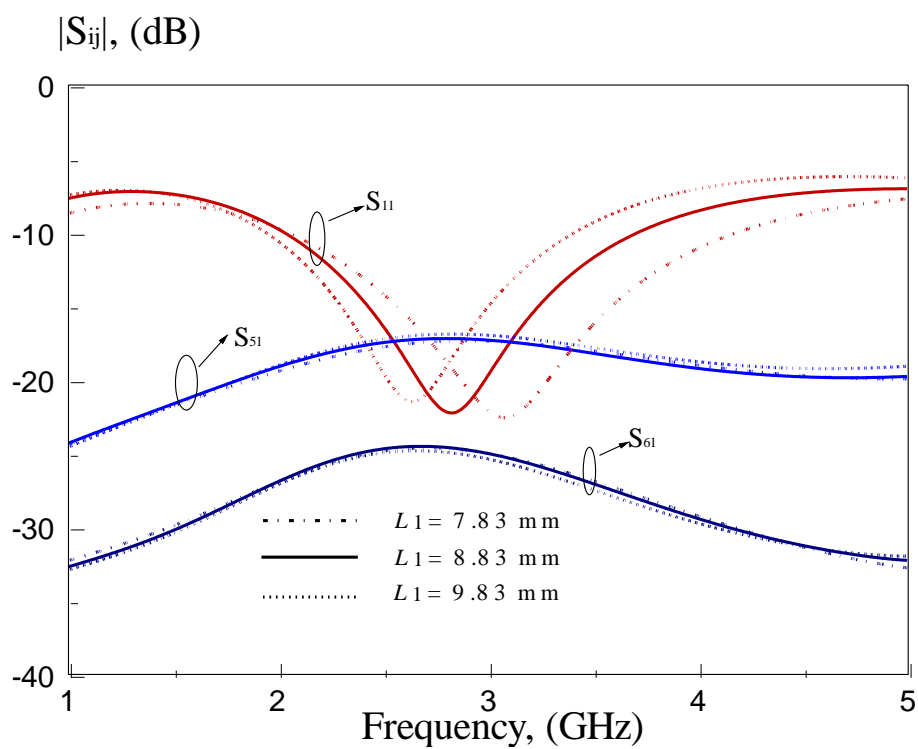


Figure 4.22: Effects of length l_1 on the reflection coefficient and isolation.

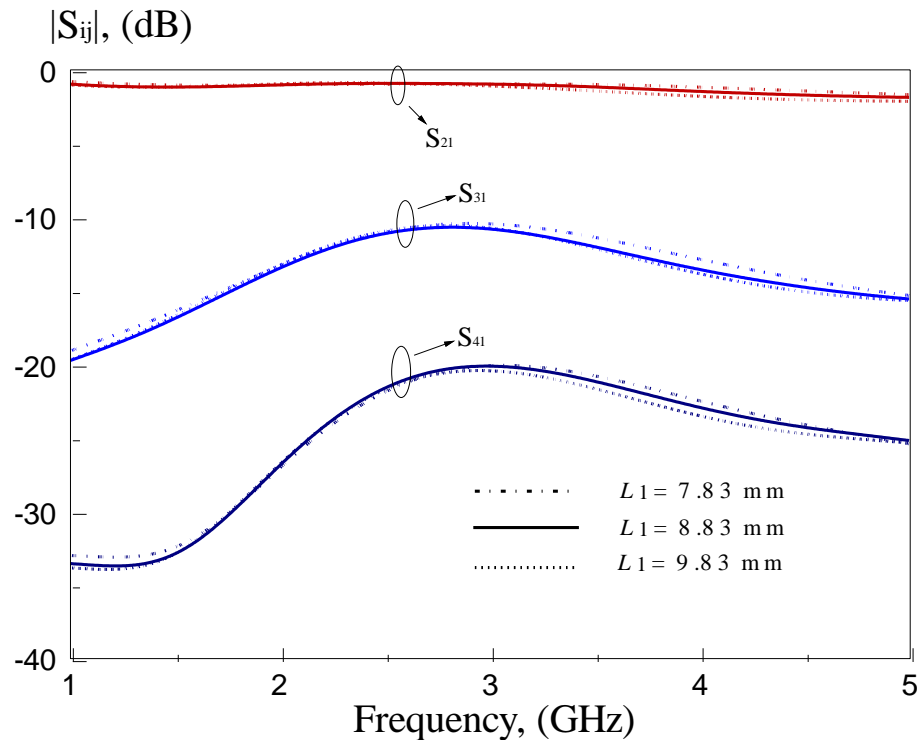


Figure 4.23: Effects of length l_1 on the insertion loss and coupling.

Description:

The parameter l_1 has no significant effect on the direct, coupled, and isolation ports. By changing this parameter, S_{21} , S_{31} , S_{41} , S_{51} , and S_{61} mostly remain unchanged in the frequency range of 2.54 GHz - 3.27 GHz. The resonance frequency moves lower when l_1 is stepped up to 9.83 mm. When the length l_1 is stepped down to 7.83 mm, the resonance frequency shifts from 2.71 GHz to 3.54 GHz.

Analysis 7

- Parameter : l_2
- Optimum value : 8.58 mm
- Step-down value : 7.58 mm
- Step-up value : 9.58 mm

Results:

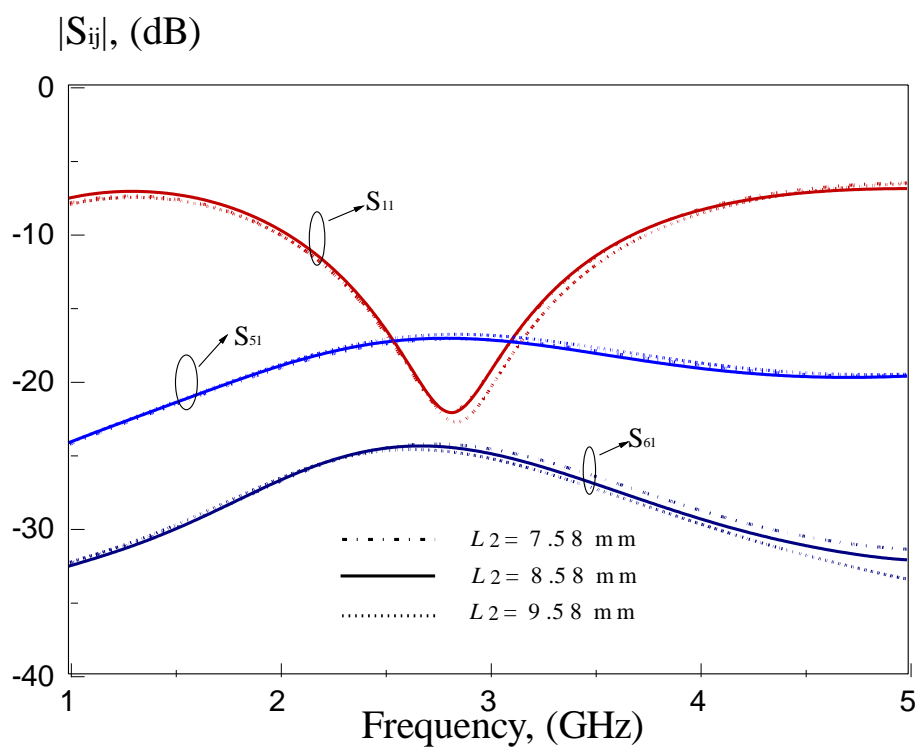


Figure 4.24: Effects of length l_2 on the reflection coefficient and isolation.

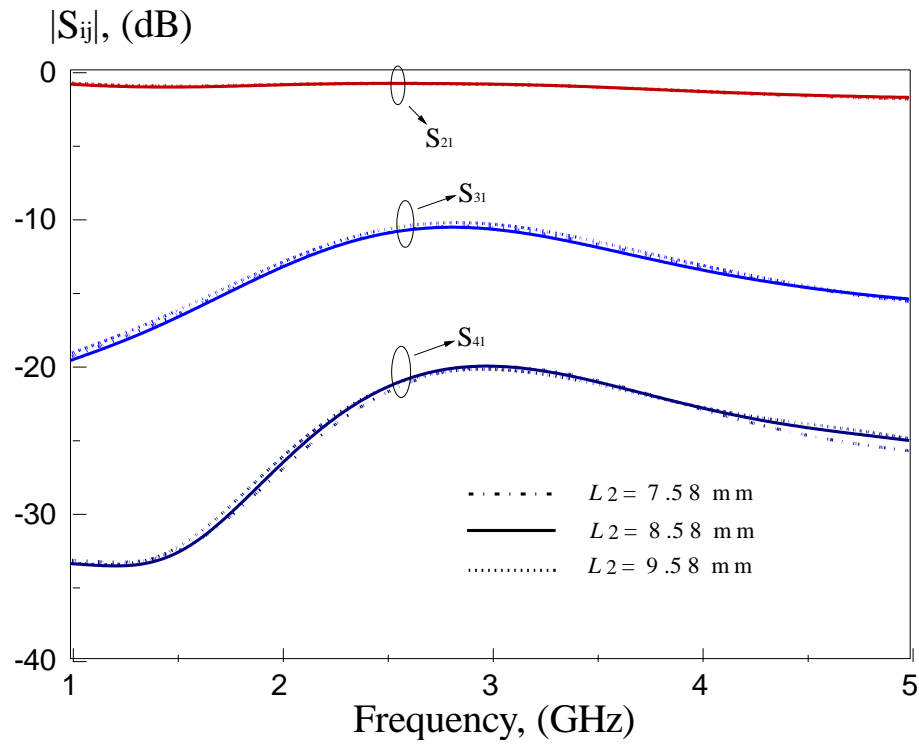


Figure 4.25: Effects of length l_2 on the insertion loss and coupling.

Description:

Analysis was done for the parameter l_2 and no major effect was found. Both the reflection coefficient and isolation maintain on the same level, with a constant insertion loss. The bandwidth of the proposed six-port directional coupler covers the frequency range of 2.54 GHz - 3.27 GHz.

Analysis 8

- Parameter : l_3
- Optimum value : 13.74 mm
- Step-down value : 11.74 mm
- Step-up value : 15.74 mm

Results:

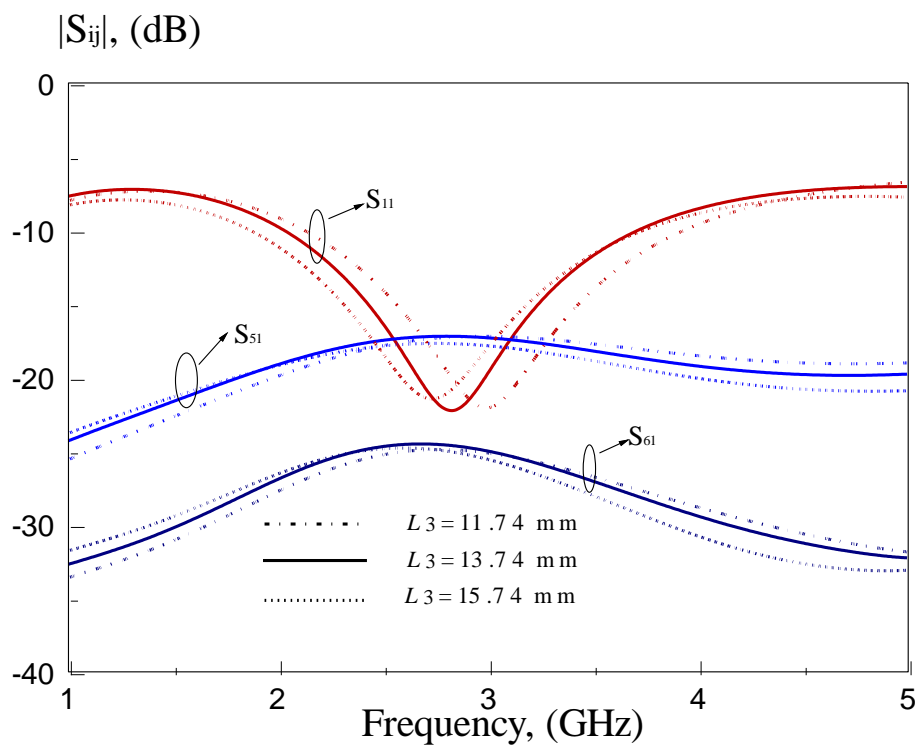


Figure 4.26: Effects of length l_3 on the reflection coefficient and isolation.

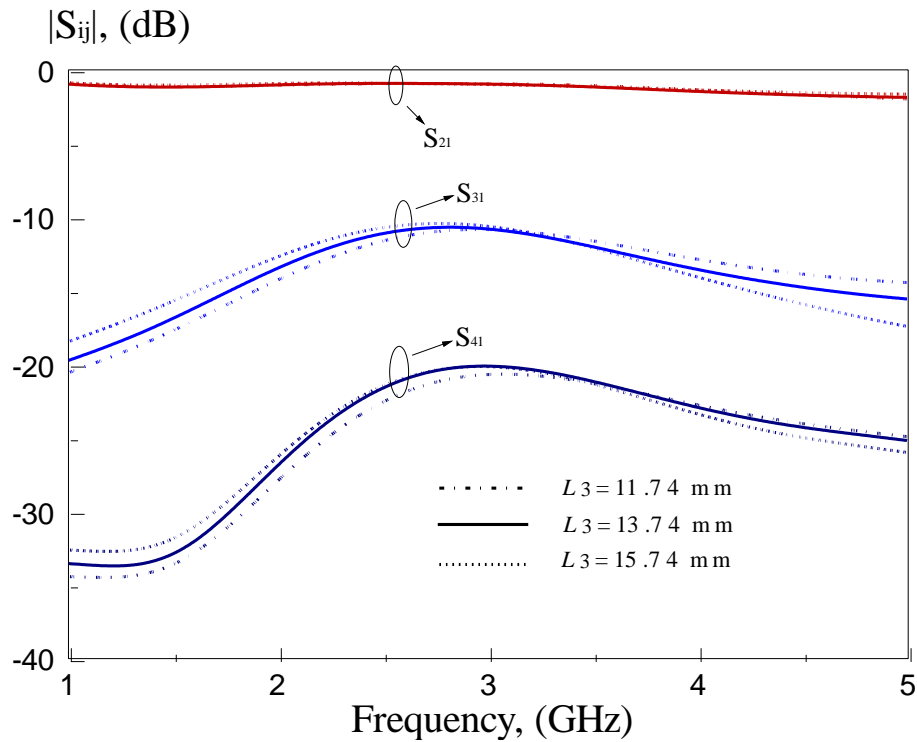


Figure 4.27: Effects of length l_3 on the insertion loss and coupling.

Description:

The parameter l_3 plays an important role when designing this directional coupler. It decides the resonance frequency of the device. When l_3 is increased to 15.74 mm, the resonance frequency goes higher. On the other hand, it moves lower for $l_3 = 11.74$ mm. The line length l_3 is important as it affects the resonance frequency of the coupled lines. Here, the length l_3 is designed to be 13.74 mm to make the directional coupler working at the desired operating frequency.

Analysis 9

- Parameter : l_4
- Optimum value : 22.74 mm
- Step-down value : 20.74 mm
- Step-up value : 24.74 mm

Results:

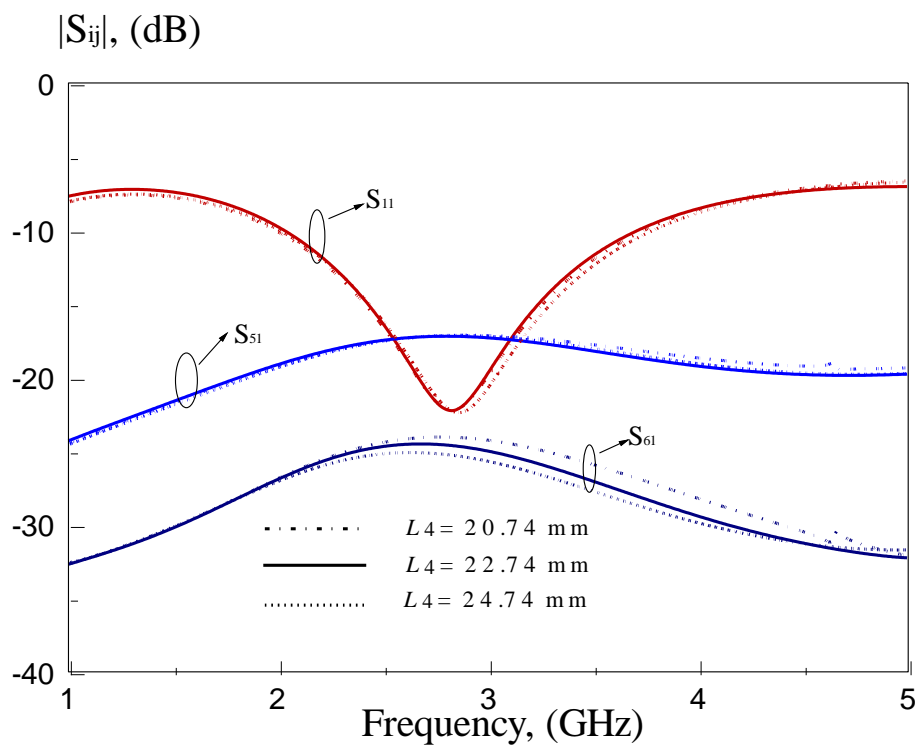


Figure 4.28: Effects of length l_4 on the reflection coefficient and isolation.

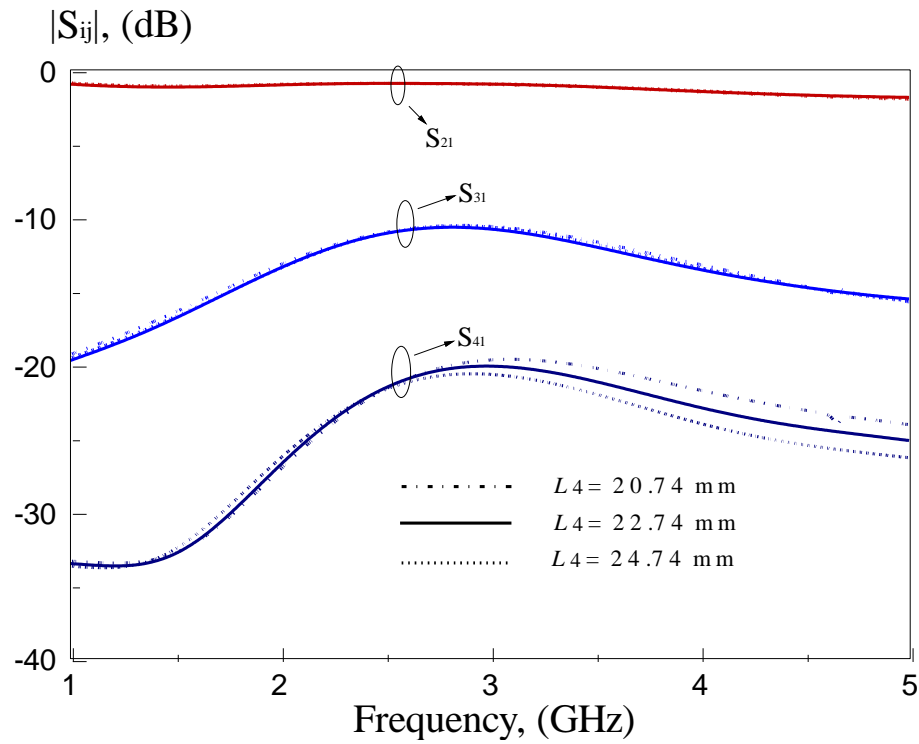


Figure 4.29: Effects of length l_4 on the insertion loss and coupling.

Description:

No major effect is found in the performance of the directional coupler when l_4 changes. The reflection coefficient S_{11} and transmission coefficients S_{21} and S_{31} remain unchanged when length l_4 is modified. Apart from that, the isolation port (Port 6) receives a stronger signal when length l_4 is stepped down. Another isolation port (Port 5) remains unchanged at all frequencies.

Analysis 10

- Parameter : l_5
- Optimum value : 36.00 mm
- Step-down value : 34.00 mm
- Step-up value : 38.00 mm

Results:

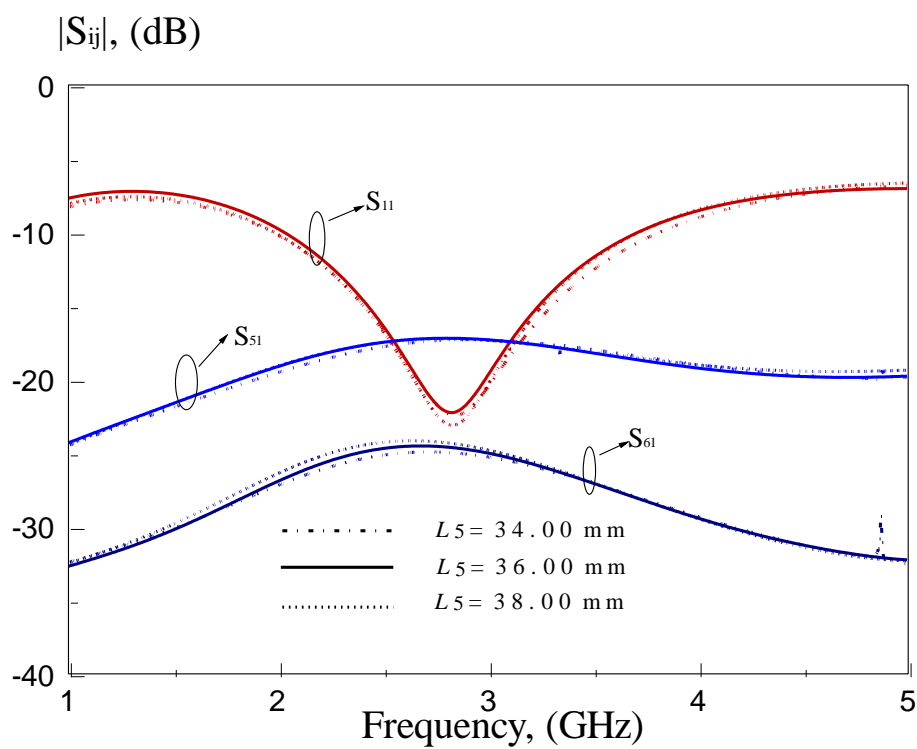


Figure 4.30: Effects of length l_5 on the reflection coefficient and isolation.

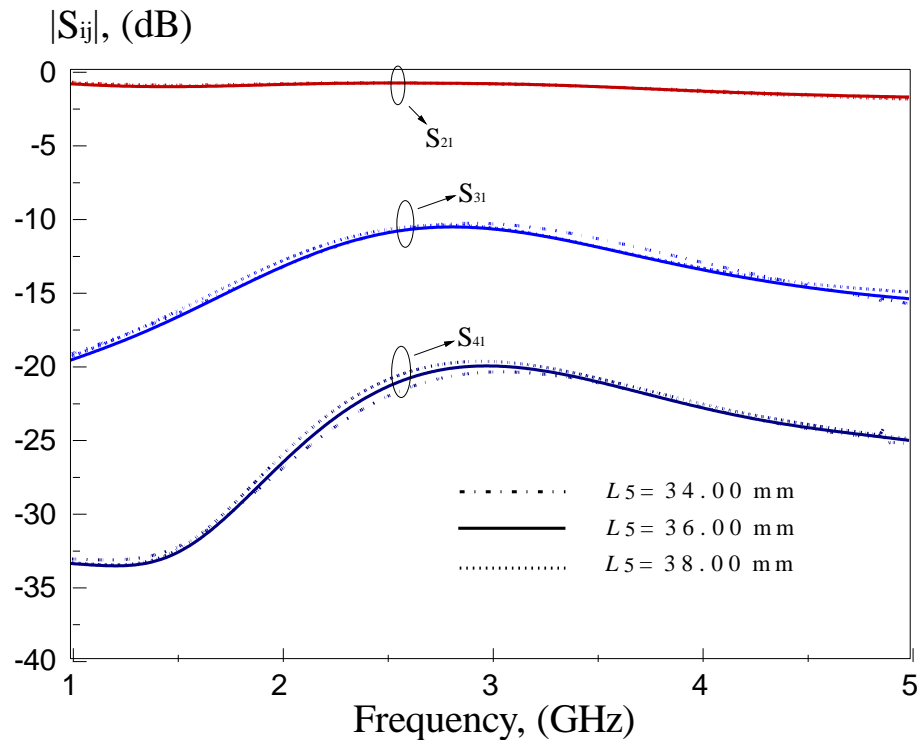


Figure 4.31: Effects of length l_5 on the insertion loss and coupling.

Description:

Similarly, the length l_5 does not have significant effect on the S parameters. The received signals at both Ports 5 and 6 are stronger when l_5 is increased to 38.00 mm but weaker when l_5 is reduced to 36.00 mm. In all cases, the signals at the isolation ports are well kept below -15 dB.

4.4 Discussion

In the past, two independent directional couplers were usually needed when two coupling levels were required at the same time, as shown in Figure 4.32. For example, the end users can ask for the coupling levels of 10 dB and 20 dB to perform a certain power monitoring in microwave measurements.

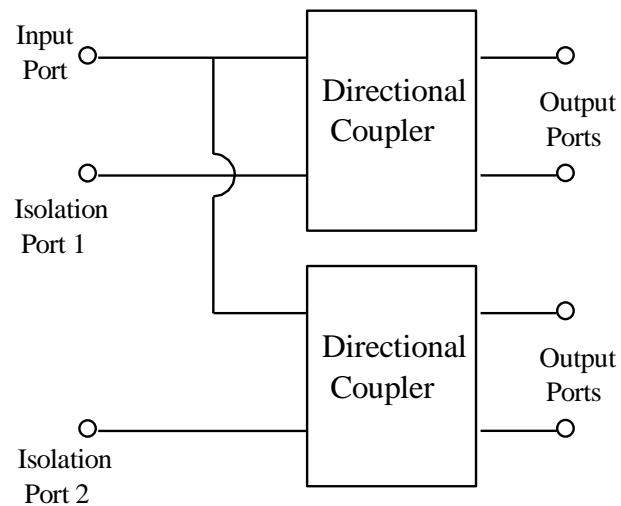


Figure 4.32: Two independent conventional directional couplers.

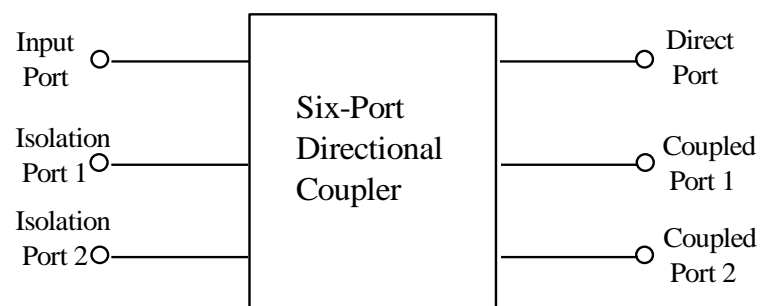


Figure 4.33: The proposed six-port directional coupler.

A dual-channel six-port directional coupler with two different coupling factors has been proposed and studied. It can be useful for power splitting in the complex networks. For the proposed configuration in Figure 4.5, the coupling levels at both the coupled ports (Ports 3 and 4) can be determined by the gap g_1 and g_2 , as discussed in Analysis 4 and Analysis 5 in Section 4.3.4. The gaps are important as they control the amount of power coupling through the coupled lines. Theoretically, the more input signal can couple through the lines when the gap is smaller. The resonance frequency of the directional coupler is mainly dependent on the parameters l_1 , l_3 , and w_2 . These are the key parameters to design the newly proposed six-port directional coupler.

CHAPTER 5

FUTURE WORK AND RECOMMENDATIONS

5.1 Achievements

In this project, the multimode filtering directional coupler has been proposed and investigated in the Chapter 3. By using the proposed wideband bandpass filter shown in Figure 3.1, a three-mode filtering directional coupler can be designed. The proposed idea was demonstrated on the RT Duroid 5870 substrate. The measured data are compared with the simulation and modelling (TLM) results. To further enhance the bandwidth performance, two additional coupled lines are introduced to obtain a five-mode filtering directional coupler. In this case, there are five poles that help to improve the operating bandwidth by 104.7%. Besides that, this multimode filtering directional coupler has wideband performance, with high rolloff near to the cutoff frequencies. It has two zeros in S_{21} and S_{31} .

A multi-port directional coupler has been proposed and discussed in Chapter 4. The design idea was further demonstrated on substrate RT Duroid 5870. Measurement, simulation and transmission line model were discussed and compared. In this new design, a total bandwidth of 590 MHz was obtained. It has been confirmed that an input signal can be coupled into two different channels with different coupling levels.

5.2 Future Work

As for the proposed multimode filtering directional coupler, the circuit size increases if more resonances are to be included. This is because more resonators are required by the parallel-coupled filter. Therefore, as for future improvement, the coupled lines can be designed into U-shaped to make the circuit compact. The same idea applies to the configuration of the six-port directional coupler. Besides that, filtering techniques such as those discussed in Chapter 3 can also be added to the six-port directional coupler to achieve better out-of-band rejection. For example, the $\lambda/4$ open-circuited coupled lines can be added to the output ports to obtain better performance as the method being reviewed in Section 2.3.2.

5.3 Conclusion

Both the multimode filtering directional couplers and multi-port directional coupler have been designed and demonstrated in this project. The measured results agree well with those of the HFSS simulation and TLM models. In this thesis, the design considerations and issues of the proposed directional couplers have also been studied. The objectives of this project have been met. It is worth mentioned that the results generated by this project enable paper submission to the *IEEE Transaction on Microwave Theory and Techniques* and *IEEE Microwave and Wireless Components Letters*.

REFERENCES

Amin M. Abbosh and Marek E. Bialkowski. (February 2007). Design of Compact Directional Couplers for UWB Applications. *IEEE Transaction on Microwave Theory and Techniques* , Vol. 55, No. 2.

Chang, K. *RF and Microwave Wireless System*. New York/ Chichester/ Weinheim/ Brisbane/ Singapore/ Toronto: John Wiley & Sons, Inc.

Directional Couplers. (n.d.). Retrieved March 5, 2012, from Microwave Encyclopedia: www.microwaves101.com/encyclopedia/directionalcouplers.cfm

Dydyk, M. (1999). Microstrip Directional Couplers with Ideal Performance via Single-Element Compensation. *IEEE Transaction on Microwave Theory and Techniques* , vol 47, No.6.

Ferdinando Alessandri, Marco Giordano, Marco Guglielmi, Giacomo Martirano and Francesco Vitulli. (May 2003). A new multiple-tuned six-port riblet-type directional coupler in rectangular waveguide. *IEEE Transaction on Microwave Theory and Techniques* , Vol. 51, No.5.

Ferdinando Alesssandri, Marco Giordano, Marco Guglielmi, Giacomo Martirano, Francesco Vitulli. (May 2003). A New Multiple-Tuned Six-Port Riblet-Type Directional Coupler in Rectangular Waveguide. *IEEE Transactions on Microwave Theory and Techniques* , Vol. 51, No.5.

Han, L. (Dec 2011). A design method of microstrip directional coupler with multi-element compensation. *IEEE International Symposium on Radio Frequency Integration Technology* .

Hong J. S. & M.J. Lancaster. . (2001). *Microstrip Filter for RF/Microwave Applications*. New York/ Chichester/ Weinheim/ Brisbane/ Singapore/ Toronto: John Wiley & Sons, Inc.

Hyde, G. (Dec 1998). Historical Perspectives on Commercial and Nonmilitary Government Space Applications of Microwave System in the Baltimore/ Washington Area. *IEEE Transaction on Microwave Theory and Techniques* , Vol. 46, No. 12.

J. Y. Shao, S. C. Huang and Y. H. Pang. (November 2011). Wilkinson power divider incorporating quasi-elliptic filters for improved out of band rejection. *Electronics Letters* , Vol.47 , No. 23.

J.K. Shimizu, E. M. T. Jones. (1958). Coupled-Transmission-Line Directional Coupler. *IEEE Transactions on Microwave Theory and Techniques* , 404.

J-L. Li, S.-W Qu and Q. Xue. (February 2007). Microstrip directional coupler with flat coupling and high isolation. *Electronic Letters* , Vol. 43, No. 4.

Johannes Muller, Minh N. Pham and Arne F. Jacob. (n.d.). Directional Coupler Compensation with Optimally Positioned Capacitances. *IEEE transaction on Microwave Theory and Techniques* .

Juan Enrique Page, Jaime Esteban and Carlos Camacho-Penalosa. (n.d.). Lattice Equivalent Circuits of Transmission-Line and Coupled-Line Section. *IEEE Transaction on Microwave Theory and Techniques* .

Kaixue Ma, Keith Chock Boon Liang, Rajanik Mark Jayasuriya, Kiat Seng Yeo. (Jan 2009). A wideband and high rejection multimode bandpass filter using stub perturbation. *IEEE on Microwave and Wireless Components Letter* , vol 19, no.1, pages 24-26.

Leo Young, M.A., Dr. Eng. (1963). The analytical equivalence of TEM-mode directional couplers and transmission-line stepped-impedance filters. *Proceeding I.E.E.* , vol 110, No.2.

M.Chudzik, I. Arnedo, A. Lujambio, I. Arregui, F. Teberio, M.A.G. Laso and T.Lopetegi. (November 2011). Microstrip coupled-line directional coupler with enhanced coupling based on EBG concept. *Electronic Letters* , Vol 47, No. 23.

Pozar, D. M. (Jan 1985). Microstrip antenna aperture-coupled to a microstripline. *Electronic Letter* , vol. 21, no. 2, pp. 49 - 50.

Pozar, D. M. (1998). *Microwave Engineering* . Canada: John Wiley & Sons, Inc.

Pu-Hua Deng and Li-Chi Dai. (2011). Unequal Wilkinson power dividers with favourable selectivity and high isolation using coupled-line filter transformer. *IEEE transaction of Microwave Theory and Techniques* .

Ravee Phromloungsri, Mitchai Chongcheawchamnan, Ian D. Robertson. (2006). Inductively compensated parallel coupled microstrip lines and their applications. *IEEE transaction on Microwave Theory and Techniques* , Vol. 54, No.9.

Seungku Lee, Yongshik Lee. (April 2010). A Design Method for Microstrip Directional Couplers Loaded With Shunt Inductors for Directivity Enhancement. *IEEE Transactions on Microwave Theory and Techniques* , Vol. 58, No.4.

T. Jensen, V. Zhurbenko, V. Krozer, and P. Meincke. (Dec. 2007). Coupled transmission lines as impedance transformer. *IEEE transaction on Microwave Theory and Techniques* , vol 55, no. 12, pages 2957-2965.

Werner A. Arriola, Jae Young Lee, and Ihn Seok Kim. (2011). Wideband 3 dB Branch Line Coupler Based on $\lambda/4$ Open Circuited Coupled-lines. *IEEE Microwave and Wireless Components Letters* .

Xi Wang, Wen-Yan Yin and Ke-Li Wu. (2011). A Dual Band Coupled-Line Coupler with an Arbitrary Coupling Coefficient. *IEEE transacton on Microwave Theory and Techniques* .

Yuk Shing Wong, Shao Yong Zheng and Wing Shing Chan. (2011). Quasi-Arbitrary Phase Difference Hybrid Coupler. *IEEE transaction on Microwave Theory and Techniques* .